[redacted] UNCLASSIFIED

8632-0001-RC-V02

EVALUATION OF THE JPL PROPOSAL FOR A LARGE FOUR STAGE SOLID ROCKET NOVA VEHICLE FOR MANNED LUNAR LANDING

VOLUME II -- Technical Addendum

September 15, 1961

Contract 950162

RECEIVED
OCT 2
OFFICE OF
A. K. THIEL

CLASSIFICATION CHANGED TO
UNCLASSIFIED
By Authority of Automatic Downgrade System
By JEBlome Date 12-05-80

Approved: A. Fiul
A. Fiul

Approved: P. Dergarabedian
P. Dergarabedian

Approved: Geo E Solomon
G. E. Solomon

~~DOWNGRADED AT 3 YEAR INTERVALS;~~
~~DECLASSIFIED AFTER 12 YEARS.~~
~~DOD DIR 5200.10~~

SPACE TECHNOLOGY LABORATORIES, INC.
P. O. Box 95001
Los Angeles 45, California

RECEIVED
SEP 27
OFFICE OF
A. K. THIEL

UNCLASSIFIED [redacted]

~~This document contains information affecting the national defense of the United States within the meaning of the Espionage Laws, Title 18, U.S.C., Section 793 and 794, the transmission or revelation of which in any manner to an unauthorized person is prohibited by law.~~

CONTENTS

ILLUSTRATIONS

ILLUSTRATIONS (Continued)

ILLUSTRATIONS (Continued)

PREFACE

The Jet Propulsion Laboratory of the California Institute of Technology has proposed the development of a large, all-solid propellant NOVA launch vehicle for early manned lunar landing operations.* An evaluation of this proposal was requested by the Large Launching Vehicle Planning Group (Golovin Committee) of the NASA and was contracted to Space Technology Laboratories, Inc., by JPL who acted as agents for the Golovin Committee.

The contract work statement required "....an objective and independent critique which will discuss the following questions:

a. Is the vehicle system concept technically feasible and valid?

b. Is the program time schedule realistic?

c. Is the cost estimate reasonably accurate as presented in the report?"

Volume I of this report summarizes the results of the initial study which was defined by the requirement that the launch vehicle system should be capable of injecting 130,000 pounds into a lunar transfer trajectory. Volume II presents the details of the analysis. Volume III (to be published shortly in response to a supplement of the basic contract) will extend the results of the study to include the determination of:

a. the effect on the vehicle system, program and cost of increasing the required lunar payload from 130,000 pounds to 156,000 pounds.

b. the performance capability of launch vehicles utilizing the upper three stages of the proposed four stage all solid propellant NOVA vehicle.

c. the effect of substituting a non-cryogenic liquid fourth stage for the presently proposed solid propellant fourth stage.

d. launch vehicle configurations capable of injecting 30,000 and 45,000 pound payloads into a lunar transfer trajectory.

e. the relative reliability of the proposed all solid NOVA launch vehicle and an all liquid NOVA vehicle which utilizes specified combinations of F-1 and J-2 engines.

---

*Part II of the Jet Propulsion Laboratory Report, Technical Memorandum 33-52, "System Considerations for the Manned Lunar Landing Program" and its Addendum A, "A Solid Propellant NOVA Injection Vehicle System".

1.0 INTRODUCTION

An independent evaluation has been made by STL of an all solid NOVA launch vehicle system and program proposed by JPL to provide early manned lunar operations (References 1 and 2). The validity of specific technical solutions, performance data, program philosophy, schedules, and costs proposed in the JPL reports was assessed. However, primary attention was focused on the evaluation of the feasibility of the basic idea of using an all solid propellant system and, to this end, independently derived data, designs, programs, and costs were generated. The study was, moreover, restricted to a consideration of the all solid NOVA vehicle and no attempt was made to compare the system, program, and costs to alternative concepts such as all liquid systems, hybrid systems, rendezvous modes, etc.

As a result of limiting the scope of the STL study to one basic system, it was possible to probe to a considerable depth into underlying problem areas. The study did not attempt, however, to find the optimum vehicle size or subsystem design requirements or to trade-off airborne versus ground system and subsystem problems. A basic system was synthesized which appeared to represent "reasonable" compromises. This system was analysed and changes to the system design were made during the course of the study as problems and solutions evolved.

The examination of program schedule and cost was undertaken simultaneously. Experience with the large weapon systems (Atlas, Titan and Minuteman) was utilized to assist in defining the magnitude of the development work and the schedule relationships for the present system. The resulting development program and cost estimates may therefore have a certain realism, validity, and applicability to NOVA programs in general.

This volume presents in some detail the results of an evaluation of the concept of an all solid propellant launch vehicle. The discussion is primarily restricted to development and fabrication feasibility. Cost and schedule feasibility is discussed in Volume I and will be further amplified in Volume III of this report.

2.0 LAUNCH VEHICLE SYSTEM

The launch vehicle system proposed by JPL has been examined in some depth and found to be feasible in concept. The STL investigation did, however, uncover a number of problem areas. These were investigated as fully as time permitted and where possible, an estimate of the problem difficulty was made. A discussion of the results of the investigation of technical problems is presented in the following sections. Program and cost considerations are treated in Volume I of this report.

2.1 LAUNCH VEHICLE SYSTEM DESCRIPTION

The general arrangement of the four stage solid propellant NOVA launch vehicle proposed by JPL is shown in Figure 2.1-1. (From Figure 14, Reference 1). This vehicle was estimated to weigh twenty-five million pounds. An independent analysis and design study resulted in a very similar configuration shown in Figure 2.1-2. The estimated vehicle weight is 31.5 million pounds. Table 2.1-I presents a summary comparison of the JPL and STL vehicle weight estimates. The vehicle step-stage definition used by JPL (Reference 2) is shown below.

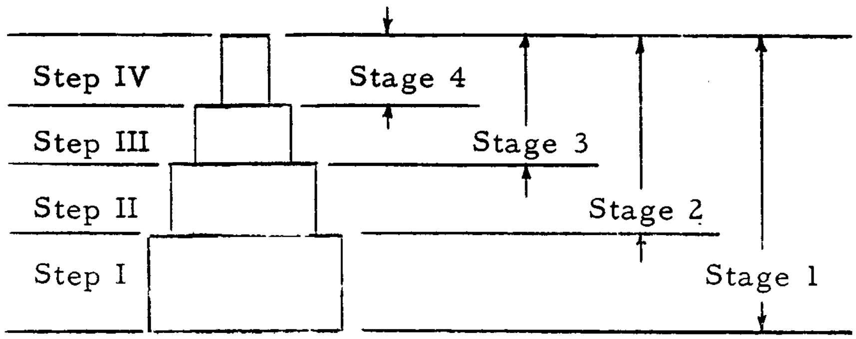

Since it was not the purpose of either the JPL or the STL studies to optimize the vehicle, but rather to determine the feasibility of the concept, the optimum weight of the vehicle was not determined. It is very probable, however, that a four stage, solid propellant NOVA launch vehicle capable of injecting a payload of 130,000 pounds into a lunar transfer trajectory will weigh between 25 and 35 million pounds.

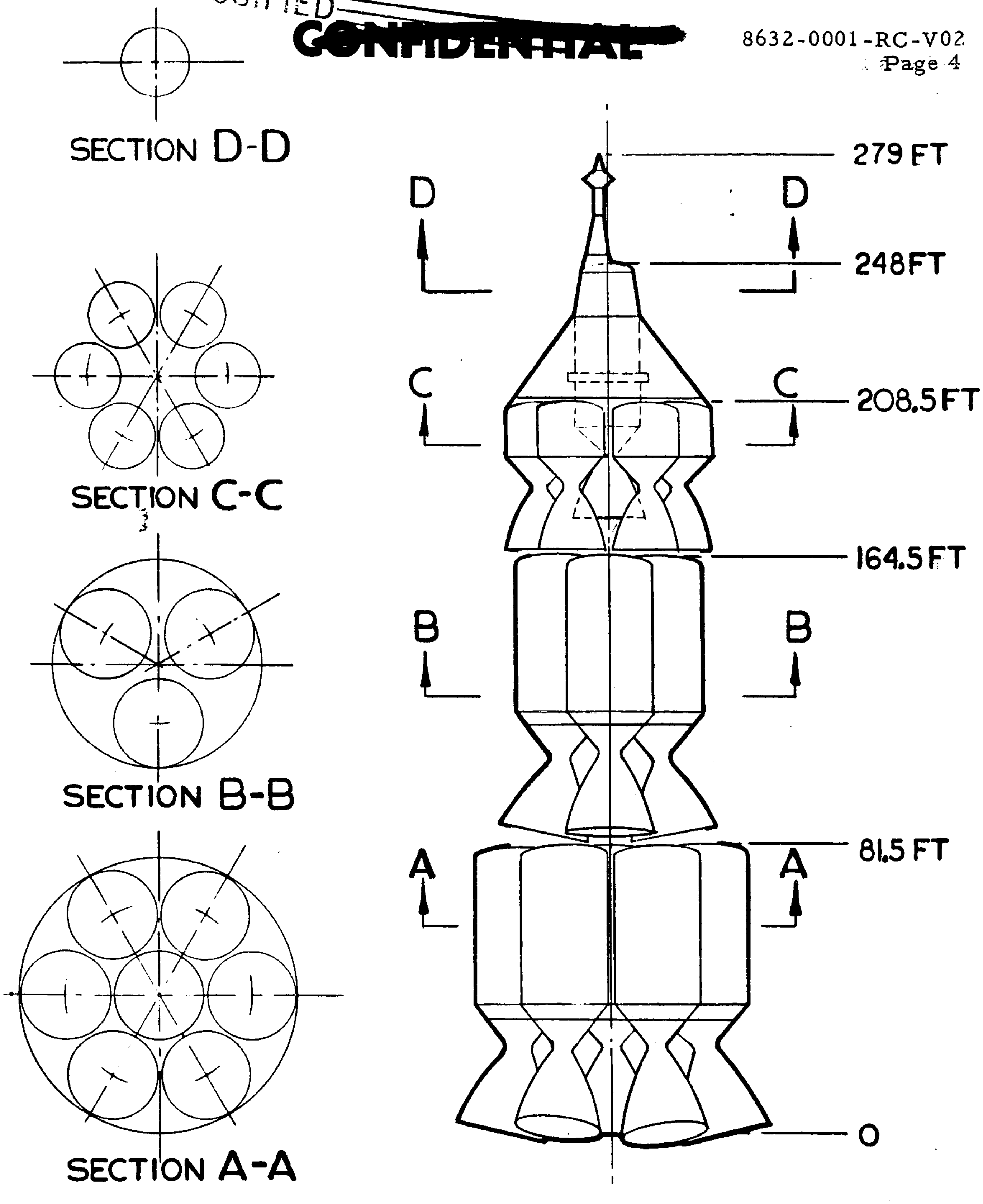

Figure 2.1-1. General Arrangement, JPL Solid Propellant NOVA Vehicle.

~~CONFIDENTIAL~~ UNCLASSIFIED

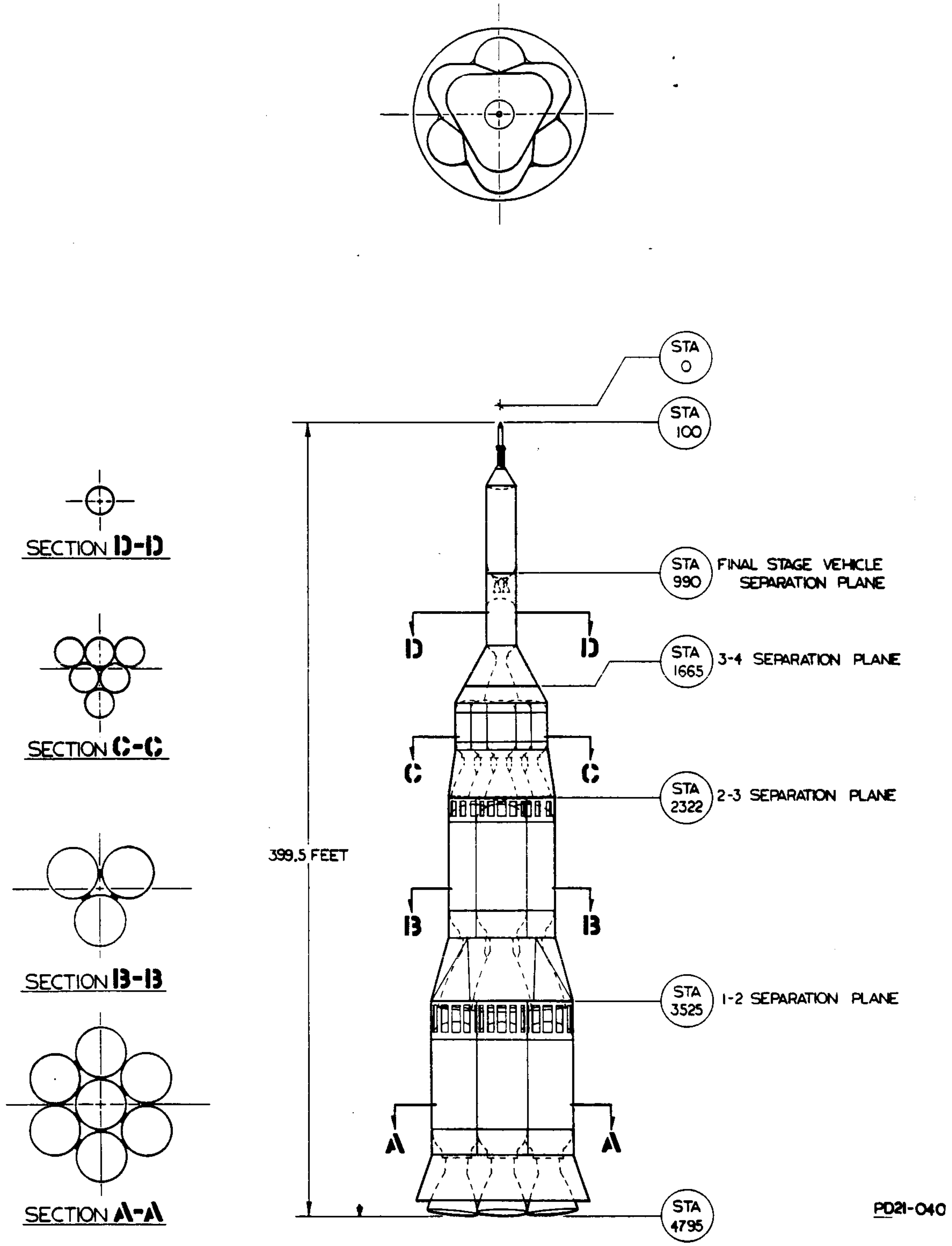

Figure 2.1-2. General Arrangement, STL Solid Propellant NOVA Vehicle.

Table 2. 1-I. Summary Comparison JPL and STL Vehicle Weight Estimates

Condition	Weight --(pounds) JPL	STL
Vehicle at Stage 1 Start	25, 217, 100	31, 463, 934
Step 1 Main Propellant	-13, 533, 100	-17, 325, 000
Step 1 Injectant Available	-579, 000	-744, 975
Step 1 Liner Expended	-	-57, 173
Vehicle at Stage 1 Burnout	11, 105, 000	13, 336, 786
Jettison Step 1	-1, 582, 420	-2, 049, 072
Vehicle at Stage 2 Start	9, 522, 580	11, 287, 714
Step 2 Main Propellant	-5, 799, 900	-7, 425, 000
Step 2 Injectant Available	-124, 000	-155, 925
Step 2 Liner Expended	-	-24, 500
Vehicle at Stage 2 Burnout	3, 598, 680	3, 682, 289
Jettison Step 2	-677, 340	-824, 186
Vehicle at Stage 3 Start	2, 921, 340	2, 858, 103
Step 3 Main Propellant	-2, 100, 000	-2, 022, 000
Step 3 Injectant Available	-109, 000	-105, 144
Step 3 Liner Expended	-	-19, 715
Vehicle at Stage 3 Burnout	712, 340	711, 244
Jettison Step 3	-186, 020	-177, 228
Vehicle at Stage 4 Start	526, 320	534, 016
Step 4 Main Propellant	-350, 000	-337, 000
Step 4 Injectant Available	-7, 600	-7, 313
Step 4 Liner Expended	-	-3, 286
Vehicle at Stage 4 Burnout	164, 720	166, 596
Jettison Step 4	-34, 720	-36, 596
Payload	130, 000	130, 000

Table 2.1-II. Comparison of JPL and STL Engine Characteristics

Stage	JPL "A" I and II	STL "A" I	STL "A" II	JPL "B" III and IV	STL "B" III	STL "B" IV
Diameter, ft	25.0	25.0	25.0	18.5	13.8	13.8
Length, ft	81.5	93.9	101.5	43.2	44.8	46.9
Total Weight, lbs*	2,087,300	2,711,647	-	373,420	362,634	-
Propellant Weight, lbs*	1,900,000	2,475,000	2,475,000	350,000	337,000	337,000
Average Thrust, lbs (vac)	6,400,000	8,000,000	8,250,000	740,000	760,000	766,000
Burning Time, sec lbf sec/lbs	85	85	85	138	129	129
Specific Impulse, vac	281	274	283	294	291	293
Chamber Pressure, psi	800	800	800	350	590	590
Nozzle Expansion Ratio	10	10	16	33	28	33

*Less Secondary Injection Tanks and Fluid

The vehicle shown on Figure 2.1-2 has an overall length of 400 feet and a base diameter of 85 feet. Steps I, II, and III are used to achieve a circular parking orbit. The fourth step injects the 130,000 pound payload into the lunar transfer trajectory.

The general arrangement of the vehicle shown on Figure 2.1-2 differs somewhat from the arrangement discussed by JPL. In particular, the STL arrangement of the clustered engines of step III, eliminates some of the base heating problems, minimizes attitude control problems at staging step III, and permits a better interstage structure.

The two engine development proposed by JPL has been retained by STL in the present study. Engine A is used in steps I and II while engine B is used in steps III and IV. Alternative engine arrangements (such as replacement of the six B engines of step III by a single A engine) will be discussed in the supplement to this report. A comparison of the characteristics of the engines is presented in Table 2.1-II.

2.1.1.1 Step I

Step I consists of a cluster of seven solid propellant (Type A) engines with cylindrical cases and bell type nozzles of 10 to 1 expansion ratio. The engines are 93.9 feet long overall and the case diameter is 25 feet. The engines are assembled into a cluster with one engine on the longitudinal center line of the vehicle and the other six engines clustered circumferentially around the center engine. The nozzles on the outside engines are canted outward 5 degrees to reduce the effects of thrust asymmetry during tail off. Shear ties at each end of the engine cases, the vehicle support structure, and the step I to II lower interstage structure complete the step I structure. The completely assembled vehicle is supported on the launch pad by a structure which is permanently attached to the extended aft skirts of the step I rocket cases.

2.1.1.2 Step II

Step II consists of three solid propellant rocket engines identical to the step I engines except for the addition of a nozzle extension which provides an expansion ratio of 16 to 1 for improved altitude performance. When viewed from above, the three engines are arranged in a triangular configuration and are connected into a cluster by upper and lower longitudinal shear ties and the interstage structures. The nozzles are canted outward 5 degrees.

2.1.3 Step III

Step III consists of six solid propellant Type B engines with cylindrical cases and bell type nozzles having a 28 to 1 expansion ratio. The engines are 44.8 feet long overall and the case diameter is 13.8 feet. engines are assembled into a cluster which, when viewed from above, forms a triangular pattern. Longitudinal shear ties between cases at both ends and the interstage structures connect the rocket engines into a cluster. The nozzles are all canted outward 5 degrees.

2.1.4 Step IV

Step IV consists of one solid propellant type B rocket engine and a liquid propellant vernier system. The rocket engine is identical to those in step III except that the nozzle expansion ratio is increased to 33 to 1, and the nozzle is not canted. The vernier system consists of three gimballed thrust chambers, propellant tanks, and pressurizing gas bot-bottles.

2.1.5 Thrust Vector Control

Thrust vector control by either gimballed nozzles or fluid injection is believed to be feasible. For purposes of sizing and weighing the vehicle, fluid injection has been assumed in the present study.

2.1.6 Spacecraft

The spacecraft payload assumed in the present study is the Apollo (as defined in Reference 3) three-man command module, launch escape system, service module, and lunar landing module, and is mounted on an interstage structure attached to the step IV rocket engine.

2.1.7 Interstage Structures

The interstage structure between steps and between the spacecraft and step IV serve as structural ties and provide aerodynamic fairing. Injectant tanks, pressure tanks, plumbing, etc. for the liquid injection thrust vector control systems are partially supported by the interstage structures in each step. Explosive devices, located at the separation planes, are used to break the structural ties between steps at staging. In the lower portion of each interstage structure, exhaust ports are provided to reduce nozzle back pressure at ignition. The step IV vernier system thrust chambers, propellant tanks, plumbing, etc. are mounted to the upper portion of the step III-IV interstage structure. Heat shields will be required for the protection of nozzles and equipment located inside the interstage structures. The interstage structure between the spacecraft and step IV provides a guidance compartment which contains electronics, power supply, guidance system, etc.

2.1.8 Guidance and Control

An inertial guidance system is assumed to be mounted in the guidance compartment. An adaptive autopilot, using rate and position gyros, provides control commands to the thrust vector systems, the vernier propulsion system, and the coast attitude control gas jet system.

2.2 PERFORMANCE EVALUATION

2.2.1 JPL Vehicle Performance Evaluation

The performance of the solid propellant NOVA vehicle proposed in References (1) and (2) was evaluated using the weights, performance data, and trajectory simulation described by JPL. In this simplified simulation, the effect of canted nozzles and the contribution of the thrust vector control system on the performance of the first two stages was neglected. No performance margin was assumed to allow for variations in the vehicle weight and performance parameters from their nominal values. The results of this evaluation essentially verified that under the assumptions of References 1 and 2 a 130,000 pound payload could be placed into a 66 hour lunar transfer trajectory.

The vehicle performance was then recomputed using STL revisions to the basic parameters and a more sophisticated simulation which included the variation of mass flow rate and vacuum thrust with time, thrust tailoff, an improved drag curve, canted nozzles, and the thrust vector control. It was found that 354,290 pounds could be put into a 100 nautical mile parking orbit. Since the weight required for the fourth stage (Reference 1) including 130,000 pounds of payload is 524,320 pounds, it is apparent that the vehicle under consideration cannot perform the desired mission.

The principle factor which degraded the performance of the JPL vehicle was a reduction of the estimated specific impulse. This resulted to a large extent from the inclusion of the effects of nozzle cant angle, and, to a much lesser extent from differences in estimates (made at JPL and STL) of basic engine specific impulse performance. It should be noted that the nozzle cant angles used by JPL in their study were very conservatively chosen to minimize an anticipated vehicle attitude control problem during thrust tailoff. STL control system studies (Section 2.7) indicate that canting the nozzle axis so that they pass through the center of gravity of the stage at burnout is not necessary. This was not, however, known at the time that the JPL vehicle was evaluated.

The effective specific impulse used by JPL in their study and by STL in the computations described above are shown in Table 2.2-I. The STL estimates include the effects of nozzle cant, the effect of secondary fluid injection into the nozzle for thrust vector control, the use of $\gamma = 1.18$, and a nozzle scale effect. The scale effect produces a small increase of effective specific impulse and results from the large nozzle sizes which permit the solid particles in the exhaust to accelerate to near equilibrium with the exhaust gas.

Table 2.2-I. Effective Specific Impulse (Seconds), JPL Design

	Step I	Step II	Step III	Step IV Verniers
Vacuum				
JPL	281	281	294	300
STL	257.4	271.3	272.6	300
Sea Level				
JPL	231.0			
STL	230.4			

The trajectory used a 5-second vertical rise followed by a 105 second gravity turn. The gravity turn was restricted to that part of the trajectory where angle of attack losses would be significant. A constant pitch rate was flown from 110 seconds through third stage burnout after which constant attitude was maintained.

Vacuum thrust for each of the first three stages was assumed to attain its maximum value at ignition and decrease to two thirds this value at the end of the nominal burning time. The decay time to zero thrust was assumed to be ten percent of the nominal burning time. A sketch of the thrust-time curve is shown in Figure 2.2-1. Thrust vector control system propellants were expended at a constant rate with an assumed axial specific impulse of 40 seconds. The vehicle was flown from third stage burnout into orbit using the vernier engines on the fourth stage. The performance margin required for the mission was included.

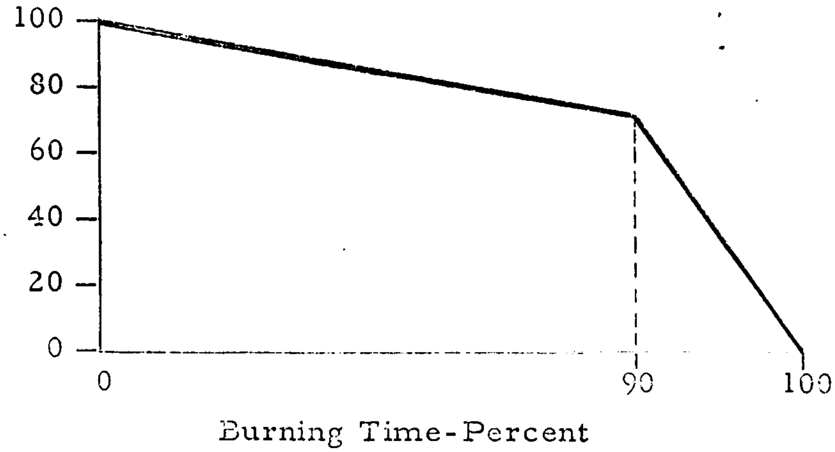

Figure 2.2-1. Typical Thrust-Time History

The weight data used in the trajectory runs are shown in Table 2.2-II and were based on References 1 and 2.

2.2.2 Resized Solid NOVA

Resizing studies were initiated and were rerun several times during the STL evaluation study to incorporate engine performance, weight, and design modifications as these were evolved. The final set of trajectory runs were based on the vehicle design shown in Figure 2.1-2. Rocket nozzle cant angle was reduced to 5 degrees for all peripheral engines and engine burning time was adjusted to satisfy the vehicle attitude control requirements during tailoff. The basic weight data were scaled from the JPL estimates which had been modified to reflect the results of the STL evaluation study (Section 2.3).

Table 2.2-III presents the engine specific impulse estimates which were used. Weight scaling relationships are shown in Section 2.3 of this report. The drag curve used is for a completely shrouded vehicle and is shown in Section 2.5. The flight profile assumed was:

a) vertical rise for 5 seconds,

b) instantaneous rotation of the vehicle centerline and velocity vector to initiate a gravity turn,

Table 2.2-II. JPL Vehicle Weight History

Vehicle at Stage 1 Ignition		25,217,100
Stage 1 Impulse Propellant	-	13,533,100
Stage 1 Liquid Injectant Available	-	579,000
Vehicle at Stage 1 Burnout		11,105,000
Jettison step I (including Nose Shroud)	-	1,582,420
Vehicle at Stage 2 Ignition		9,522,580
Stage 2 Impulse Propellant	-	5,799,900
Stage 2 Liquid Injectant Available	-	124,000
Vehicle at Stage 2 Burnout		3,598,680
Jettison step II	-	677,340
Vehicle at Stage 3 Ignition		2,921,340
Stage 3 Impulse Propellant	-	2,100,000
Stage 3 Liquid Injectant Available	-	109,000
Vehicle at Stage 3 Burnout		712,340
Jettison step III	-	186,020
Vernier Propellant (1/2 of Available)	-	2,000
Vehicle at Stage 4 Ignition		524,320
Stage 4 Impulse Propellant		350,000
Vernier Propellant (1/2 of Available)	-	2,000
Vernier Liquid Injectant Available	-	7,600
Vehicle at Stage 4 Burnout		164,720
Jettison step IV	-	34,720
Net Payload		130,000

c) maintain gravity turn until 110 seconds (approximately 150,000 feet),

d) constant pitch rate resulting in attainment of a specified burnout condition.

This burnout condition was set at 100 nautical mile altitude, horizontal flight path angle, and a velocity 150 feet per second less than required for a circular orbit. This latter criterion reflects an arbitrary solution to the treatment of performance variation in fixed impulse rocket systems. With this choice, all vehicles, except those which produce 3 high performance, are injected into a circular parking orbit by the fourth stage vernier system. The fourth stage then accelerates the vehicle to the velocity required for lunar transfer (35,970 feet/second—66 hour flight) using its single rocket engine and its vernier to remove the final performance dispersion.

Table 2.2-III. Effective Specific Impulse (Seconds), STL Design

Stage	1	1	2	3	4	4
Condition	Sea Level	Vacuum	Vacuum	Vacuum	Vacuum	Verniers
Motor	245.08	273.74	282.81	290.51	293.04	300
Effective	234.09	262.42	275.87	274.52	287.67	300

A sizing study was performed to determine the most desirable distribution of propellant between the several steps of the vehicle. This "optimum" distribution was then approximated by appropriately sizing the "A" engines. The "B" engine size is determined by the lunar transfer velocity increment and the payload weight.

Table 2.2-IV presents an example weight history for an "optimum" vehicle. Table 2.2-V presents a weight history for a point-design vehicle capable of injecting 130,000 pound payload into the lunar transfer trajectory. The deviation from the optimum is seen to be small.

Table 2.2-IV. Weight History - Optimized Solid NOVA

Vehicle at Stage 1 Start	-	31,400,000
Step I Main Propellant	-	18,043,164
Step I Injectant Available	-	771,249
Step I Liner Expended	-	59,180
Vehicle at Stage 1 Burnout		12,526,398
Jettison step I (Including Shroud)	-	2,127,859
Vehicle at Stage 2 Start		10,398,539
Step II Main Propellant	-	6,330,503
Step II Injectant Available	-	145,155
Step II Liner Expended	-	22,808
Vehicle at Stage 2 Burnout		3,900,073
Jettison step II	-	711,966
Vehicle at Stage 3 Start		3,188,107
Step III Main Propellant	-	2,265,259
Step III Injectant Available	-	113,742
Step III Liner Expended	-	20,637
Vehicle at Stage 3 Burnout		788,469
Jettison step III	-	177,226
Vehicle at Stage 4 Start		611,243
Step IV Main Propellant	-	392,130
Step IV Injectant Available	-	7,953
Step IV Liner Expended	-	3,555
Step IV Vernier Propellant Available	-	22,602
Vehicle at Stage 4 Burnout		185,003
Jettison step IV	-	41,333
Payload		143,670

Table 2.2-V. Weight History - Resized 130,000 lb Payload Weight Solid NOVA

Vehicle at Stage 1 Start		31,463,934
Step I Main Propellant	-	17,325,000
Step I Injectant Available	-	744,975
Step I Liner Expended	-	57,173
Vehicle at Stage 1 Burnout		13,336,786
Jettison step I (including Shroud)	-	2,049,072
Vehicle at Stage 2 Start		11,287,714
Step II Main Propellant	-	7,425,000
Step II Injectant Available	-	155,925
Step II Liner Expended	-	24,500
Vehicle at Stage 2 Burnout		3,682,289
Jettison step II	-	824,186
Vehicle at Stage 3 Start		2,858,103
Step III Main Propellant	-	2,022,000
Step III Injectant Available	-	105,144
Step III Liner Expended	-	19,715
Vehicle at Stage 3 Burnout		711,244
Jettison step III	-	177,228
Vehicle at Stage 4 Start		534,016
Step IV Main Propellant	-	337,000
Step IV Injectant Available	-	7,313
Step IV Liner Expended	-	3,286
Step IV Vernier Propellant Available	-	19,821
Vehicle at Stage 4 Burnout		166,596
Jettison step IV	-	36,596
Design Payload		130,000

Typical trajectory parameters as a function of flight time until third stage burnout are shown on Figure 2.2-2 and 2.2-3. The trajectory data indicates a maximum expected dynamic pressure of 1090 lbs/ft^2 and a dynamic pressure, at first stage separation, of 130 lb/ft^2. The total heating indicator $\int qv\,dt$ is 1.06×10^8 lb-ft^{-1} and is of the same order as most liquid propellant vehicles. Therefore, it is reasonably assured that aerodynamic heating insulation would not be required. The maximum accelerations, do not exceed 4.5 g's.

2.2.3 Performance Margin

The fourth stage (step IV) vernier propulsion system is used to remove the trajectory performance dispersions which result from off-nominal vehicle weight and engine performance. The vehicle parameters whose dispersions have significant effects are:

a) propellant specific impulse

b) average thrust level (or burning time)

c) propellant loaded

d) vehicle inert weight.

The residual propellant allowance which contributes heavily to performance dispersion in a liquid-rocket system isessentially zero in a solid rocket vehicle.

A dispersion in propellant specific impulse was assumed to result in a change in flow rate and an increase in burning time (variation at constant thrust). Thrust dispersions were assumed to result in variations both in thrust and in flow rate (at constant specific impulse). Propellant load and inert weight dispersions were assumed to result in variations in available impulse propellant and burnout weights respectively. The assumed values for the 3σ vehicle parameter dispersions used in the performance dispersion computations are presented in Table 2.2-VI and compared with the assumptions made by JPL.

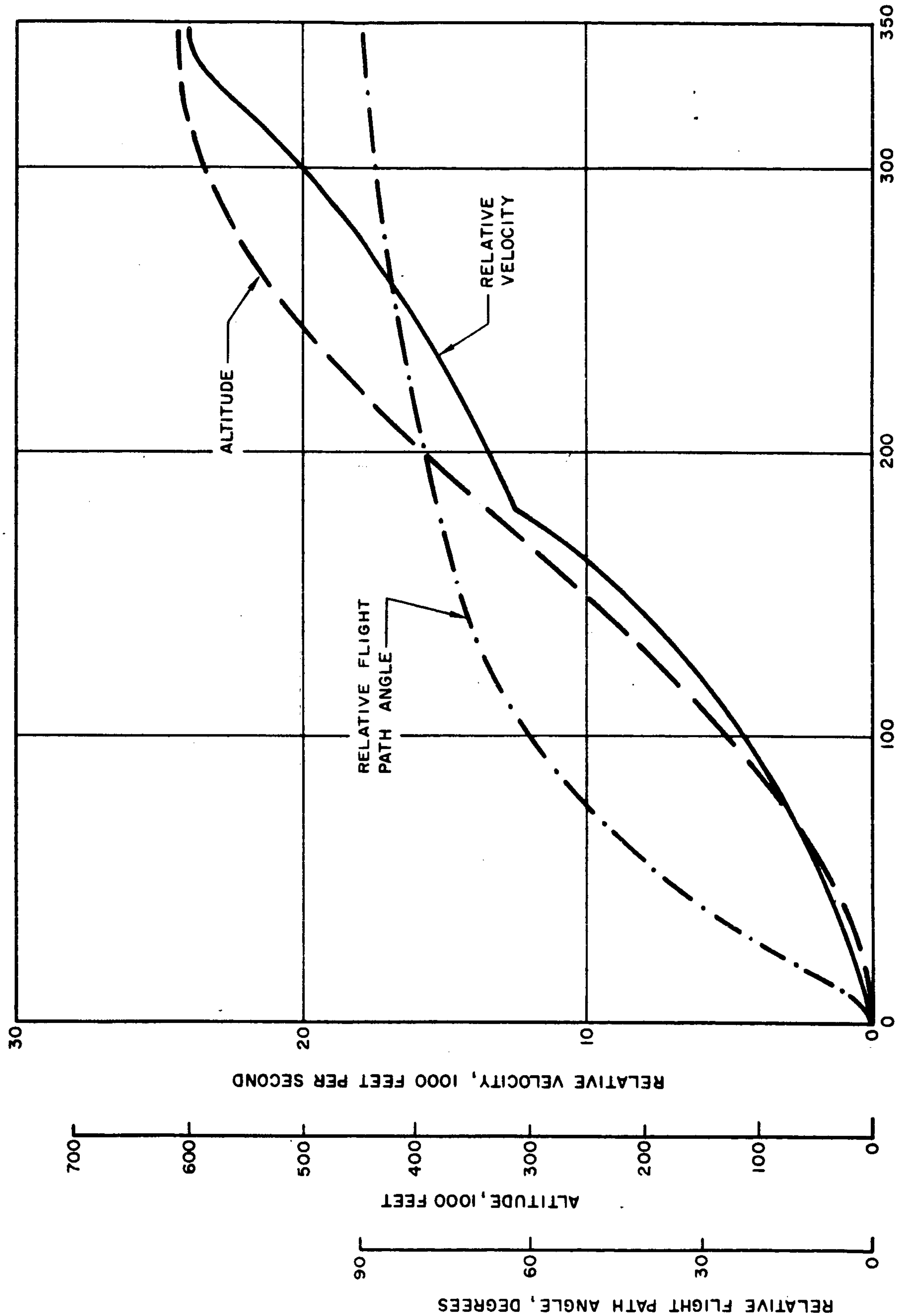

Figure 2.2-2. Trajectory Parameters, STL Solid Propellant NOVA.

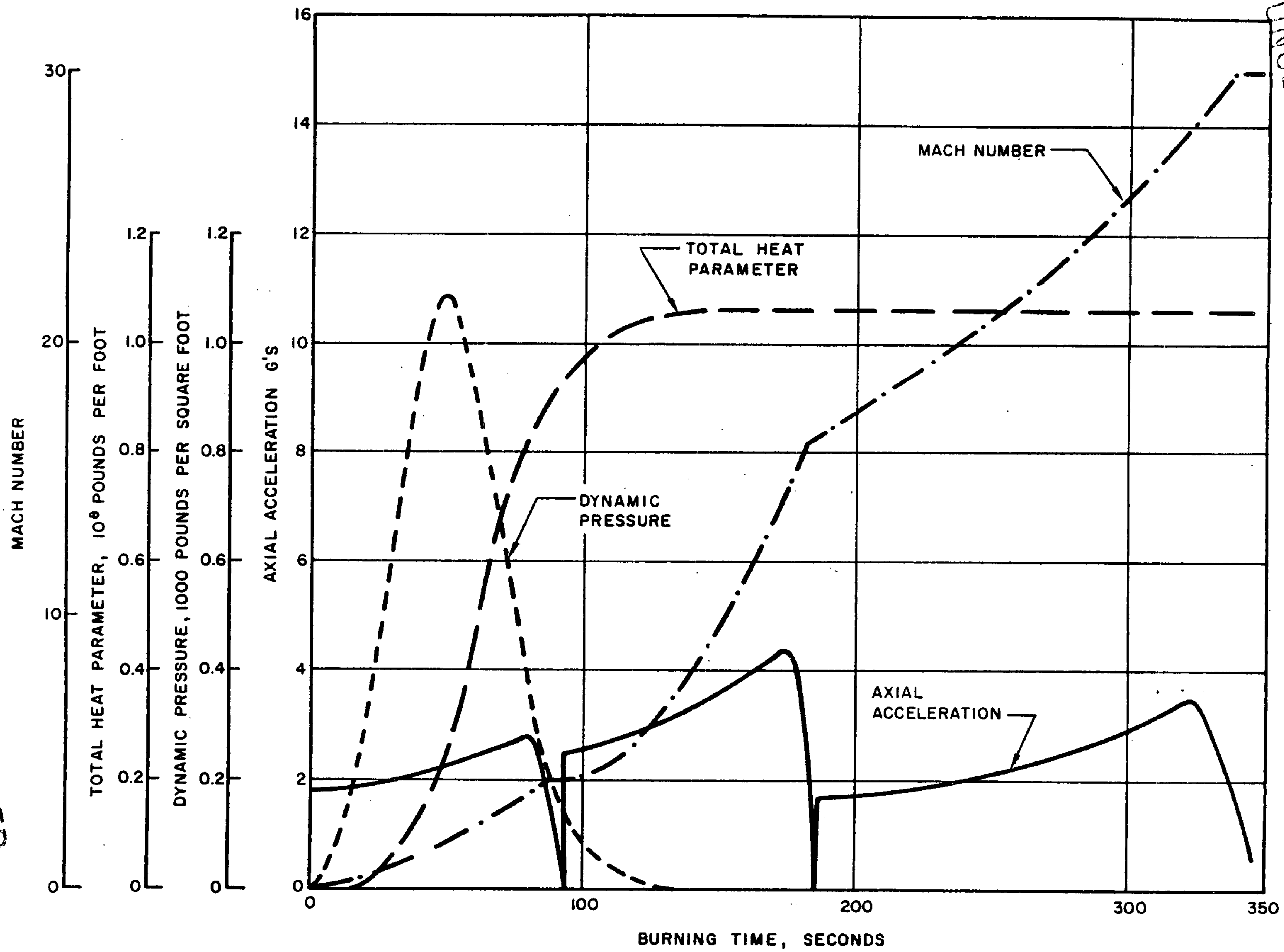

Figure 2.2-3. Trajectory Parameters, STL Solid Propellant NOVA.

Table 2.2-VI. Assumed 3σ Dispersion Parameters

	Assumed Dispersion	
Parameter	STL	JPL
Specific Impulse	0.75 percent/engine	0.48 percent/engine
Average Thrust (burning time)	3.75 percent/engine	0
Propellant Loaded	0.51 percent	0
Inert Weight	3.26 percent	

From the data of Table 2.2-VI the rms of the propulsion parameters were computed taking into account the number of engines in eact step. Similar computations were made for the propellant and structural weight tolerances. Burnout velocity dispersions were then computed using both machine trajectory results and hand computed exchange ratios.

The resulting parking orbit and lunar injection three sigma velocity dispersions were computed to be 140 feet per second and 120 feet per second respectively. These dispersions can be added statistically since only one vernier system is used to make up this velocity. To be conservative, however, the dispersions were divided into two parts; 150 feet per second for first vernier burn and 100 feet per second for the second vernier burn. Since it is undesirable to terminate solid propellant engine thrust, the possibility of a high performance vehicle (above nominal) makes it desirable to force burnout to occur three sigma short of the mission velocity requirements. Therefore, the vernier system has to have the ability of adding 300 feet per second. The contemplated vernier modes are indicated in Figure 2.2-4 below:

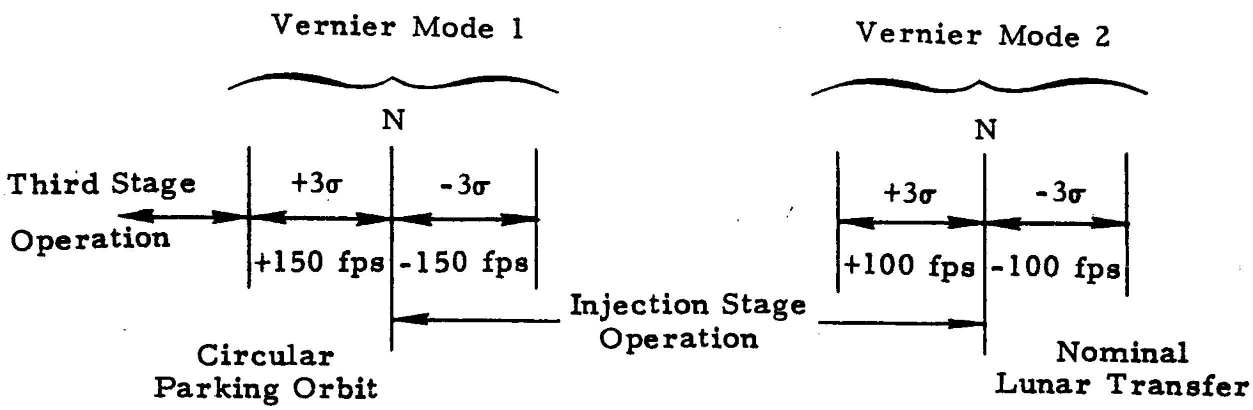

Figure 2.2-4. Vernier Modes

2.2.4 Exchange Ratios

Vehicle exchange ratios provide an indication of the effect of vehicle development perturbations on the performance capability and serve as a basis for trade-off studies. The variations considered in this preliminary study are the effective specific impulse and the structural weight. The sets of exchange ratios are shown in Table 2.2-VII. These indicate:

a) The variation in gross weight for a fixed 130,000 pound lunar injected weight

b) The variation in payload weight for a fixed launch vehicle.

The data were obtained from a compliation of machine trajectory results and hand calculations.

Table 2.2-VII. Exchange Ratios

Design Parameters	Stage 1	2	3	4
	Exchange Ratios			
Ratio of vehicle Gross Weight to Effective Specific Impulse (1000 lbs/sec)	-160	-200	-230	-170
Ratio of Vehicle Gross Weight to Structural Weight (lbs/lbs)	1.8	9.9	56	220
Ratio of Payload Weight to Effective Specific Impulse (1000 lbs/sec)	0.70	0.87	1.0	0.75
Ratio of Payload Weight to Structural Weight (lbs/1000 lbs)	-8.0	- 44	-250	-1000

The effect of multiple design perturbations can be approximated by simply adding the incremental vehicle gross weight due to each perturbation.

2.3 VEHICLE WEIGHT EVALUATION

A vehicle weight evaluation was performed with the following objectives:

a) To check the reasonableness of the JPL assumptions

b) To provide scaling data for vehicle sizing studies

c) To derive weight tolerances for performance analyses

d) To derive moment of inertia and center of gravity estimates for stability and control calculations.

2.3.1 Weight Estimates and Scaling Laws

The weight estimates presented in the JPL reports, References 1 and 2, were analyzed and appear to be reasonable. However, the STL design studies indicated a few changes were desirable to provide a more accurate description of the vehicle system. The changes were made and step weight scaling laws were derived to permit a parametric vehicle performance analysis. These scaling relationships are shown on Figures 2.3-1 through 2.3-4. Table 2.3-I presents the vehicle weight history and estimated tolerances on weight and lateral center of gravity for the STL design point NOVA configuration. A detailed weight breakdown for the STL design point launch vehicle system is presented in Table 2.3-II. The longitudinal center of gravity history of the vehicle is shown in Figures 2.3-5 and 2.3-6. The weight data which have been used are felt to be realistic and possibly a little conservative. A brief discussion is presented below.

2.3.1.1 Structure

Preliminary calculations of interstage structures, based on monocoque design, indicates that the JPL weight estimates are probably reasonable for the 25 million pound vehicle. An additional allowance of 100,000 pound was made in step I to account for launch support structure. Step structure weight (both inter and intrastage) was then scaled as a function of step gross weight.

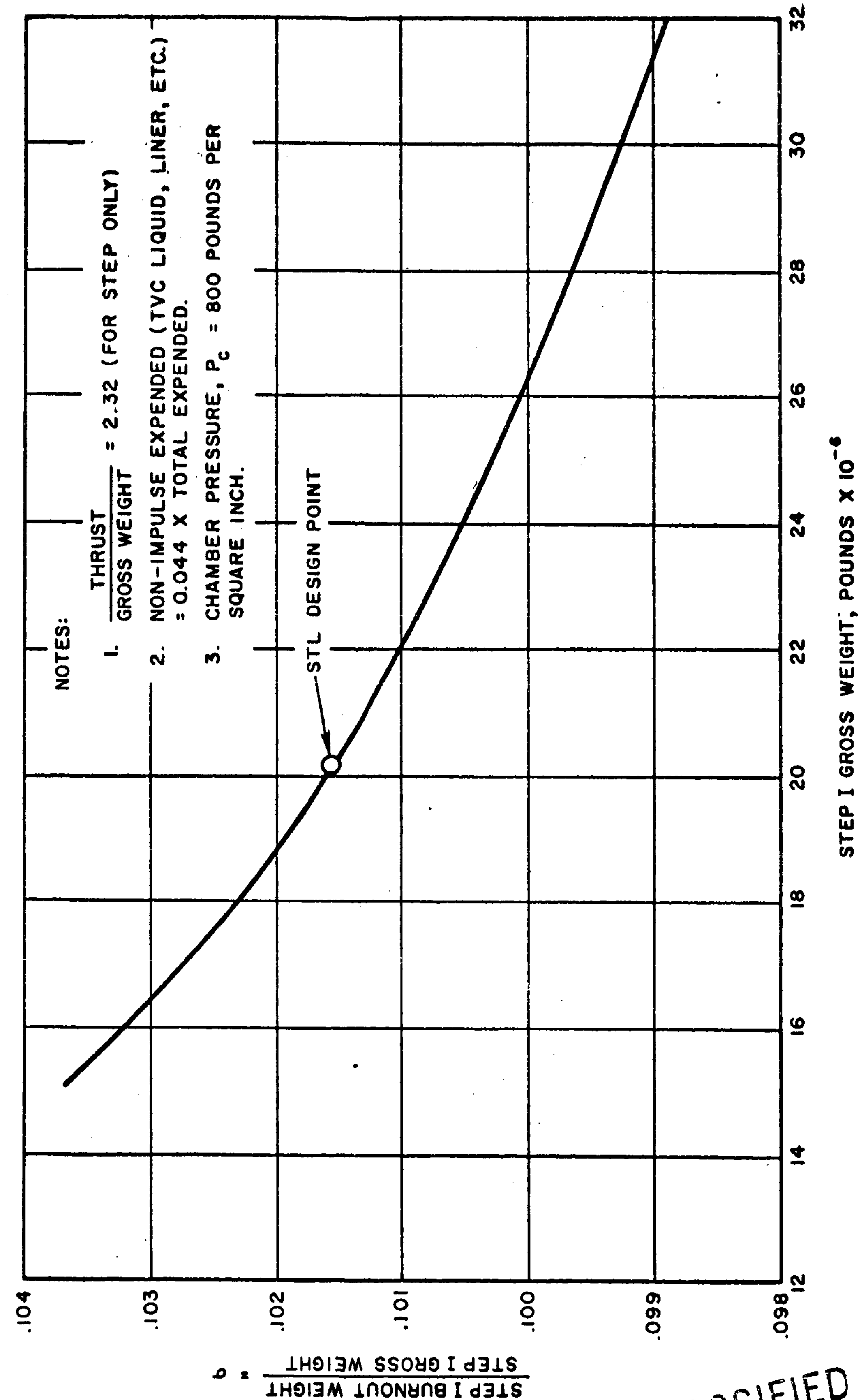

Figure 2.3-1. Step I Structure Factor versus Step I Gross Weight.

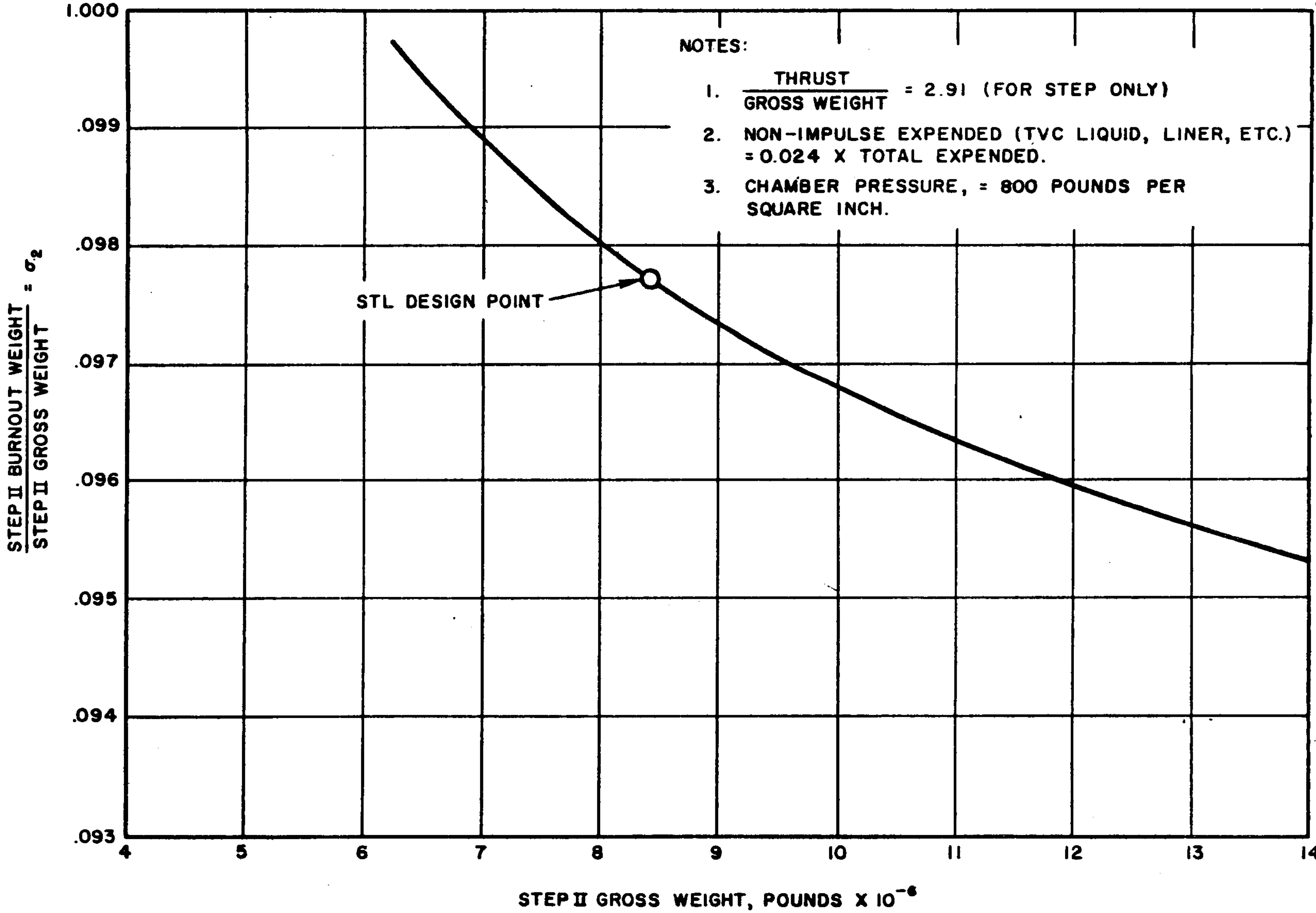

Figure 2.3-2. Step II Structure Factor versus Step II Gross Weight.

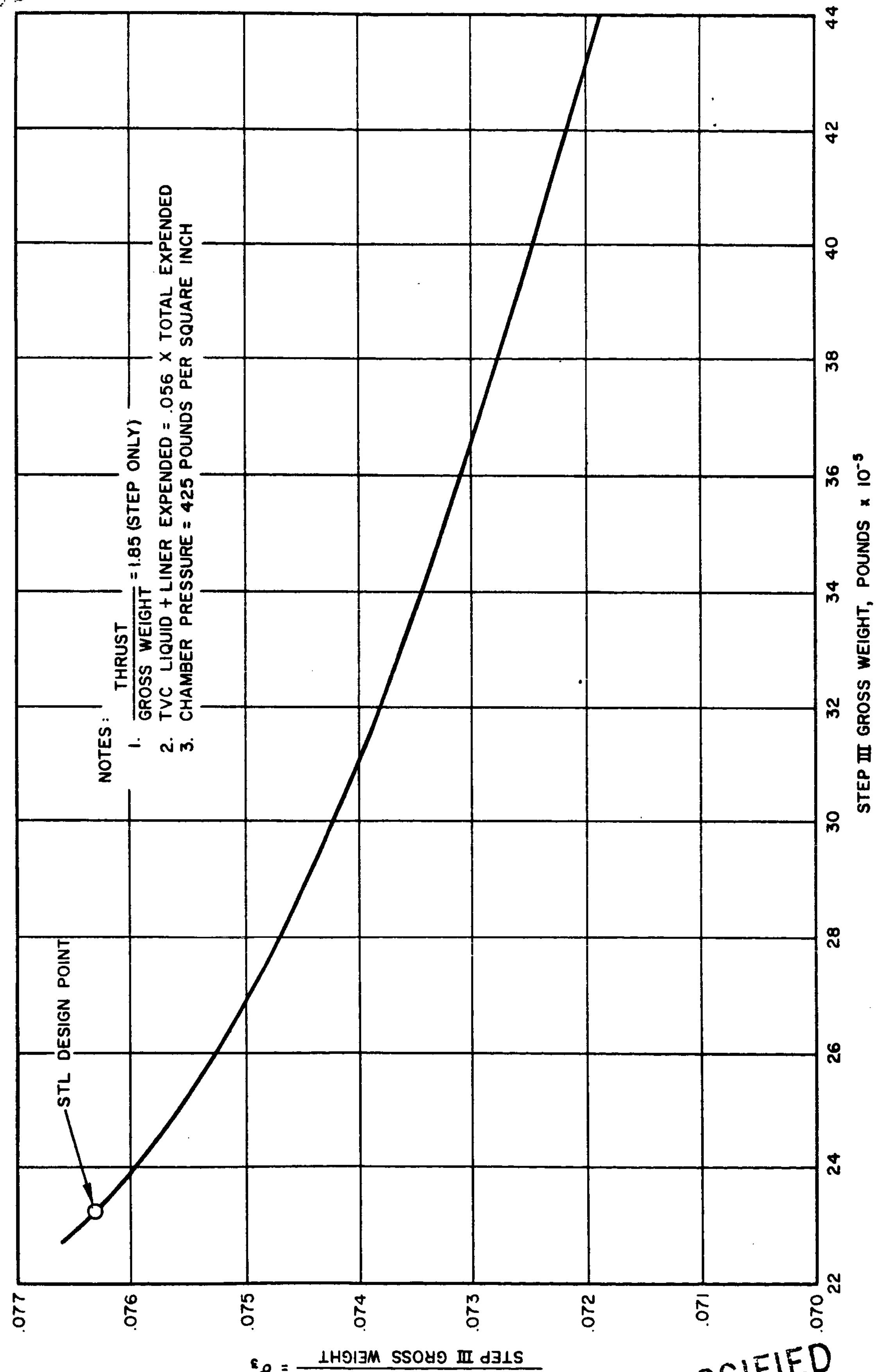

Figure 2.3-3. Step III Structure Factor versus Step III Gross Weight.

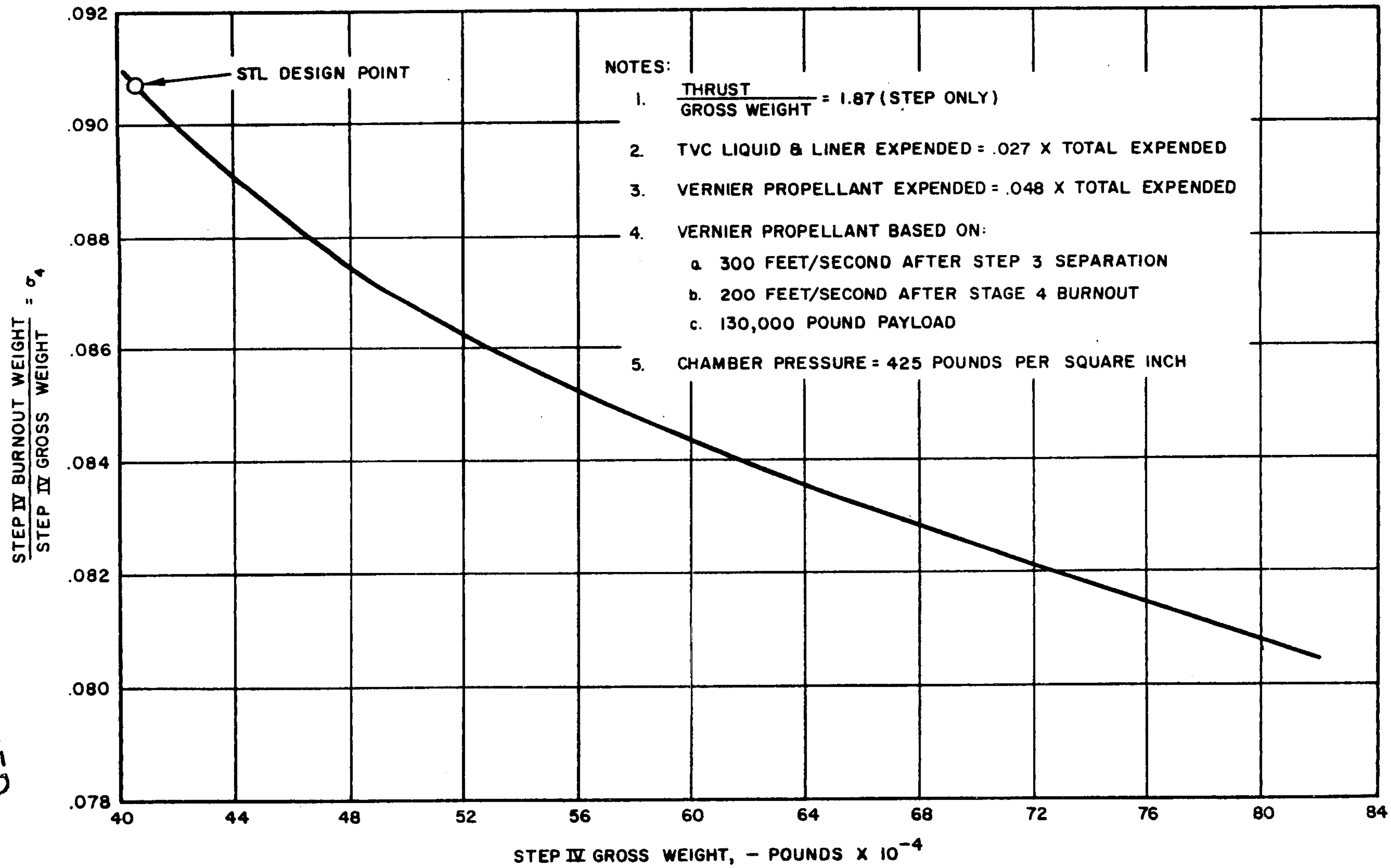

Figure 2.3-4. Step IV Structure Factor versus Step IV Gross Weight.

Table 2.3-I. Weight History and Tolerances - STL Design Point Solid NOVA

Condition	Weight (lbs)	Weight Tolerance (lbs)	Lateral CG Tolerance (inches)
Vehicle At Stage 1 Start	31,463,934		±4.4
Step I Main Propellant	-17,325,000	±33,395	
Step I Injectant Available	-744,975	±3,725	
Step I Liner Expended	-57,173	±7,410	
Vehicle At Stage 1 Burnout	13,336,786		±6.9
Jettison step 1 (Including Shroud)	-2,049,072	±24,730	
Vehicle At Stage 1 Start	11,287,714		±3.2
Step II Main Propellant	-7,425,000	±21,865	
Step II Injectant Available	-155,925	±780	
Step II Liner Expended	-24,500	±4,850	
Vehicle At Stage II Burnout	3,682,289		±5.4
Jettison Step II	-824,186	±14,740	
Vehicle At Stage III Start	2,858,103		±2.8
Step III Main Propellant	-2,022,000	±4,210	
Step III Injectant Available	-105,144	±526	
Step III Liner Expended	-19,715	±2,760	
Vehicle At Stage III Burnout	711,244		±5.5
Jettison Step III	-177,228	±3,625	
Vehicle At Stage 4 Start	534,016		±1.2
Step IV Main Propellant	-337,000	±1,719	
Step IV Injectant Available	-7,313	±37	
Step IV Liner Expended	-3,286	±1,127	
Step IV Vernier Propellant Available	-19,821	±99	
Vehicle At Stage 4 Burnout	166,596		±2.4
Jettison Step IV	-36,596	±1,430	
Payload	130,000		

Table 2.3-II. STL Design Point Solid NOVA Step Weight Statement

	Step I	Step II	Step III	Step IV
Propulsion - Main	1,599,560	686,883	132,953	22,348
Case	1,242,203	532,373	70,920	11,820
Liner (1/2 of Total)	57,173	24,500	19,715	3,286
Nozzle	300,184	130,010	42,318	7,242
Propulsion - Vernier				3,945
Secondary Injection	128,881	26,351	13,564	1,111
Structure (Inter and Intrastage)	319,371	110,952	30,711	6,192
Shroud	1,260			
Guidance Compt.				3,000
Step Jetison Weight	2,049,072	824,186	177,228	36,596
Main Propellant	17,325,000	7,425,000	2,022,000	337,000
Vernier Propellant				19,821
Secondary Injection Fluid	744,975	155,925	105,144	7,313
Liner (1/2 of Total)	57,173	24,500	19,715	3,286
Step Gross Weight	20,176,220	8,429,611	2,324,087	404,016
$\sigma = \frac{\text{Step Burnout Weight}}{\text{Step Gross Weight}}$	0.1016	0.0978	0.0763	0.0906

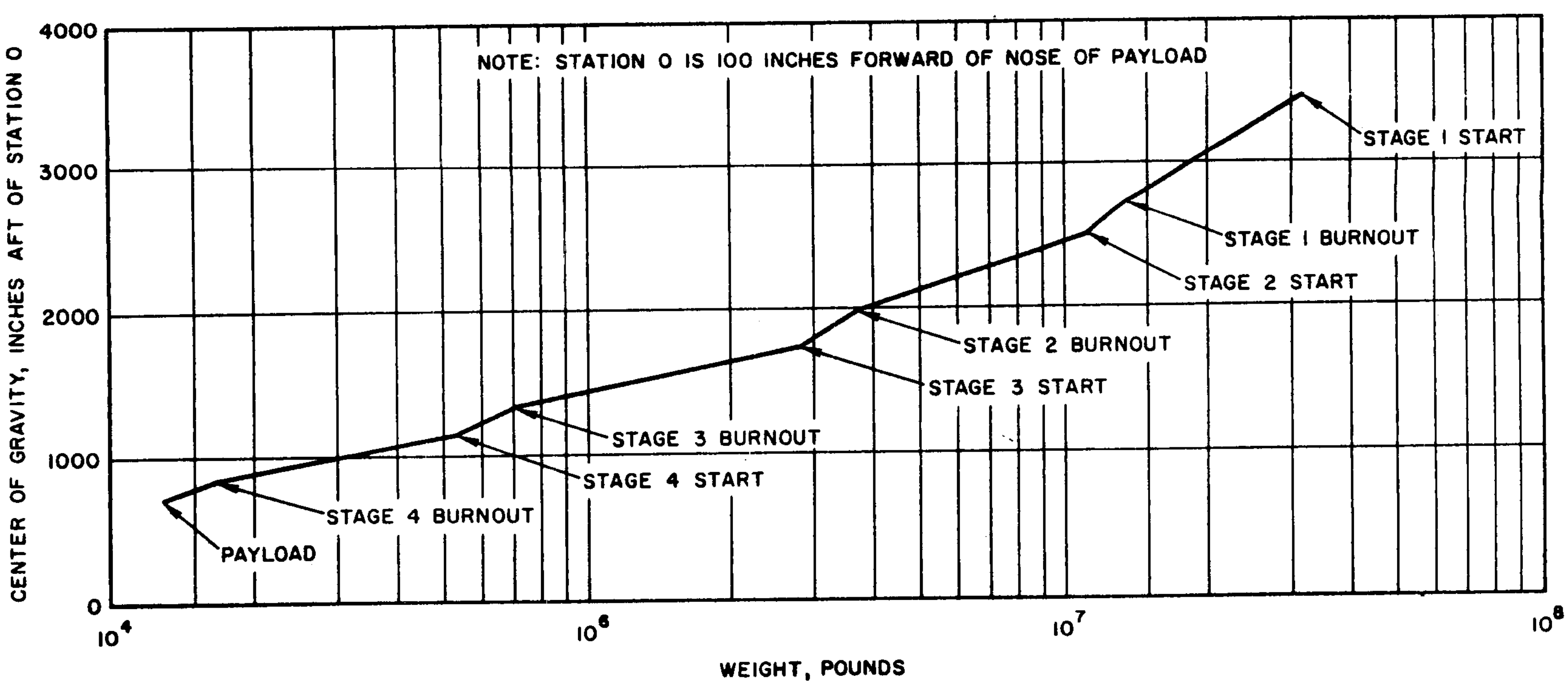

Figure 2.3-5. Weight and Center of Gravity, STL Solid Propellant NOVA.

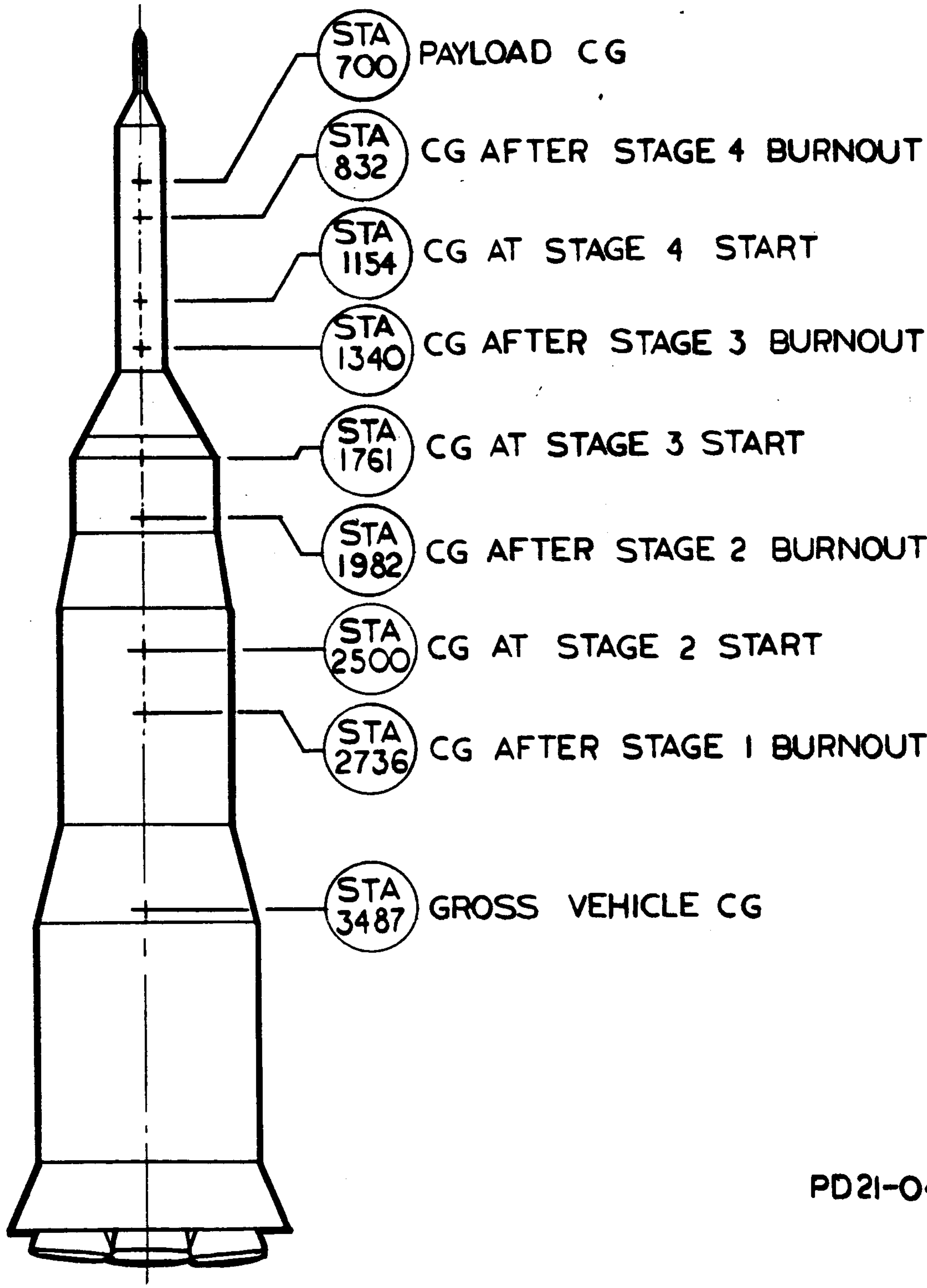

PD21-041

Figure 2.3-6. Center of Gravity Locations, STL Solid Propellant NOVA.

2.3.1.2 Engines

Type "A" engines were scaled from the JPL design as a function of contained propellant weight. Type "B" engines as shown by JPL were too far from optimum and were therefore redesigned to the following criteria:

a) P_c = 590 psi nominal

b) Step III, expansion ratio = 28:1

c) Step IV, expansion ratio = 33:1

d) Case diameter = 165 inches

e) Closure major to minor axis = 2

f) Volumetric loading = 88 percent

g) Material is steel with ultimate tensile strength = 225,000 psi

h) Factor of safety = 1.4 between nominal chamber pressure and ultimate strength.

Weight savings could also be realized on the "A" engines but were not large enough to affect the feasibility study. At the present design point, the inert weight saving would be of the order of:

Step I = -340,000 pounds

Step II = -145,000 pounds

2.3.1.3 Secondary Injection

Based on STL studies, the system weight of the Step I and II liquid injection systems appeared realistic. JPL maintained this ratio essentially constant for all stages. However, the step III and IV system weights should be a smaller fraction of the required fluid because of the lower engine chamber pressure. In the STL weight analysis, therefore, the ratios have been adjusted to account for an upper stage chamber pressure.

In the table below is presented a comparison of the weight factors used by STL in sizing the liquid injection system compared with those used by JPL. Also shown is the possible weight saving which would result from the use of a solid propellant gas generator, rather than the high pressure helium, for pressurizing the injectant.

Step	JPL		Used for STL Weight Calculations		Possible Gain Using Solid Propellant Gas Generator Pressurization	
	W_F/W_P	W_S/W_F	W_F/W_P	W_S/W_F	W_S/W_F	Weight Saving (pounds
I	0.043	0.173	0.043	0.173	0.140	-24,500
II	0.021	0.169	0.021	0.169	0.137	-5,000
III	0.052	0.161	0.052*	0.129	0.106	-2,400
IV	0.022	0.184	0.022	0.152	0.128	-200

Where W_F = Fluid Injectant Weight

W_P = Main Engine Propellant Weight

W_S = System Weight Less Fluid = Tanks, Helium, Plumbing, Supports

2.3.1.4 Vernier System

Storable propellants with a specific impulse of 300 seconds are assumed. A velocity requirement of 300 ft/sec prior to Stage 4 start and 200 ft/sec after Stage 4 burnout is used. System weight, less propellant was assumed to be 20 percent of propellant weight.

*Current STL estimates shown in Section 2.7 indicate a requirement for only about half the fluid weight ratio shown above for step IV. This means a weight saving of about 50,000 lb of fluid and 6000 lb of system weight in step III is possible. This has not been reflected in the weight statement.

2.3.2 Weight and Center of Gravity Tolerances

Weight tolerance performance was estimated for step jettison weights, expended propellants, inerts, and liquid injectant. In determining propellant, inert, and engine burnout weight tolerances, considerable use was made of Thiokol experience and data from the Minuteman first stage engine. (See Reference 4.) In general, it was assumed that a similar percentage weight accuracy could be expected in any single engine item (i.e., propellant loading). Where necessary, adjustments were made in the tolerances to account for the large difference in size of the engines being compared.

Table 2.3-III indicates the elements for which tolerance analyses was made and shows the derivation of the tolerance.

Table 2.3-III. Weight Tolerances

Item	Tolerance	Derivation
1. Engine Propellant	± 0.51 percent of Nominal	Thiokol Chemical Co.
2. Step Propellant Expended	-	RBS of Engine Tolerance
3. Engine Liner Expended	±34.3 percent of Nominal	Thiokol Chemical Co.
4. Step Liner Expended	-	RSS of Engine Tolerance
5. Liquid Injectant	±0.5 percent of Nominal	Assumed
6. Vernier Propellant	± 0.5 percent of Nominal	Assumed
7. Engine Burnout Weight	-	RSS of Case Tolerance and 3
8. All Inert Weights (Interstage, etc)	±3.26 percent of Nominal	Thiokol Chemical Co. Total Inert Tolerance
9. Step Jettison	-	RSS of 7 and 8 and TVC Resid. Tolerance

After calculating individual step center of gravity displacements, the steps were then combined into a vehicle using the concentricity and perpendicularity assembly tolerances presented in 2.3.2.1. The tolerances were applied in such a way that each step contributed to a maximum vehicle radial center of gravity displacement in the same direction. The vehicle center of gravity was then calculated at ignition and at burnout of each stage. In each case, the center of gravity was determined with reference to the roll axis of the step whose engines were firing (i.e., Stage 1 burnout center of gravity is referenced to the step I roll axis). The resulting center of gravity displacements are listed in Table 2.3-IV.

Table 2.3-IV. Vehicle Radial Center of Gravity Displacements

	Ignition		Burnout	
	Weight (pounds)	Center of Gravity (inch)	Weight (pounds)	Center of Gravity (inch)
Stage 1	31,463,934	±4.4	13,336,786	±6.9
Stage 2	11,287,714	±3.2	3,682,289	±5.4
Stage 3	2,858,103	±2.8	711,244	±5.5
Stage 4	534,016	±1.2	166,596	±2.4

2.3.2.1 Derivation of Radial Center of Gravity Tolerances

In the center of gravity tolerance analyses, the following reasonable assumptions were used:

a) Each engine can be aligned radially ±1.0 inch

b) All structure and sub-systems can be positioned radially within ±1.0 inch of their desired positions

c) Each stage can be aligned concentrically on a lower stage ±1.0 inch

d) The perpendicularity for each stage on assembly is ±0.4 foot (±1 inch in 72 feet)

e) The loaded center of gravity tolerance of each engine equals 0.46 percent of the engine's diameter (based on Thiokol Minuteman data)

f) Each engine burnout center of gravity tolerance was determined by removing the burnout weight tolerance from the maximum radius of the engine (A check against Thiokol burnout center of gravity data indicates good correlation.)

g) Weight tolerances were based on Table 2.3-III.

Using the above assumptions, maximum radial center of gravity displacements were calculated for each individual step at gross weight and at burnout. These displacements were determined by using one engine as the geometric reference point and then shifting the other engines and components in one direction. It was further conservatively assumed that the center of gravity of each component was shifted in the same direction and that light and heavy engines were located to maximize the magnitude of the shift.

2.4 PROPULSION SYSTEM

The rocket engine development required to implement the proposed all solid propellant NOVA vehicle has been examined and is believed to be feasible within the time scale described in the STL development plan. The engine performance requirements, as described by JPL, are considered by STL to be necessary if the vehicle weight is to be restricted to manageable proportions. These requirements can be met but they cannot at this time be considered to substantiate a conservative approach since they utilize to the fullest the capabilities which have been developed for Polaris and Minuteman. In certain areas, as for example, engine burning time and propellant burning rates, even greater capabilities are desired. These too are, however, believed to be achievable.

On an overall basis, the engine development feasibility is believed to be assurable. However, there are a few development areas where basic data are not really sufficient to permit a clear cut picture of the recommended mode of implementation. Intensive study will be required during the initial preliminary systems design phase to provide if possible, a basis for development choice so that parallel developments are eliminated or at least minimized. Thrust vector control by liquid injection or gimballed nozzles, nozzle throats made of graphite or ablative material and segmented or unitized rocket motors furnish three examples of potentially expensive parallel developments. In addition, viscoelastic data on contending propellants are too scanty to permit a definitive assurance that creep-collapse can be avoided without special development and design efforts which may in the end be attended by some performance penalty.

The development program must provide a highly reliable engine system. To this end, STL recommends emphasis on full scale flight weight rocket engine static testing. Subscale tests cannot be relied upon for data on survivability or reliability since these factors are strongly dependent on fabrication and quality control. For the present program, the lead time for the large A engine is sufficiently long to permit the B engine to be a fairly good subscale representation. Indeed, the B engine may provide a more stringent test of some portions of the design than is desired.

The required propulsion system development program must also include an adequate effort on production facilities and techniques. The very large size rocket cases will require an extension of current fabrication methods if economical production is to be obtained. The very large quantities of propellants that are required similarly demand development activity to provide the degree of quality control called for by both performance and reliability. The engines used in the STL vehicle are shown in Figures 2.4-1 to 2.4-5.

2.4.1 Rocket Engine Design

2.4.1.1 Unitized and Segmented Rocket Engine

One of the basic design choices to be made is between unitized and segmented rocket engines. In the STL study, this issue was glossed since it did not appear that a definitive consideration would be decisive to determining overall system feasibility, schedule and cost. As a result, the system study was essentially limited to consideration of unitized engines. A detailed investigation of the consequences of selecting one or the other of the two approaches should be carried out during the preliminary system design study.

2.4.1.2 Engine Cases

The method described by JPL for setting the relationship between engine operating and case burst pressure is considered optimistic. For example, on the "A" engine the nominal pressure is 800 psi. To this is added 11.2 percent to account for 3 sigma pressure and temperature variations. The case is then designed to this pressure. One hundred and sixty-five thousand (165, 000) psi yield strength material is used with wall thickness that result in a 9 percent factor of safety based on 180, 000 psi ultimate strength.

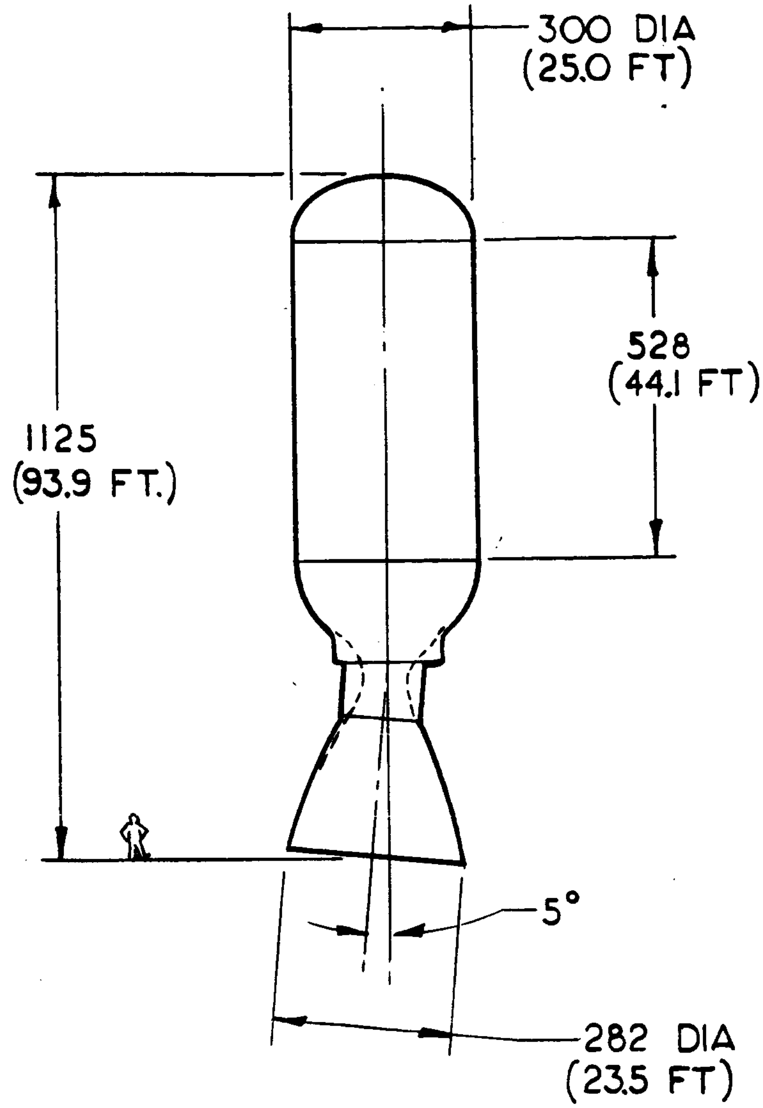

EXPANSION RATIO, ϵ = 10:1
CHAMBER PRESSURE, P_c = 800 PSI
THRUST, F = 8,800,000 LBS
WEIGHT = 2,711,647 LBS

PD21-05

Figure 2.4-1. Rocket Engine, Step I, Canted Nozzle.

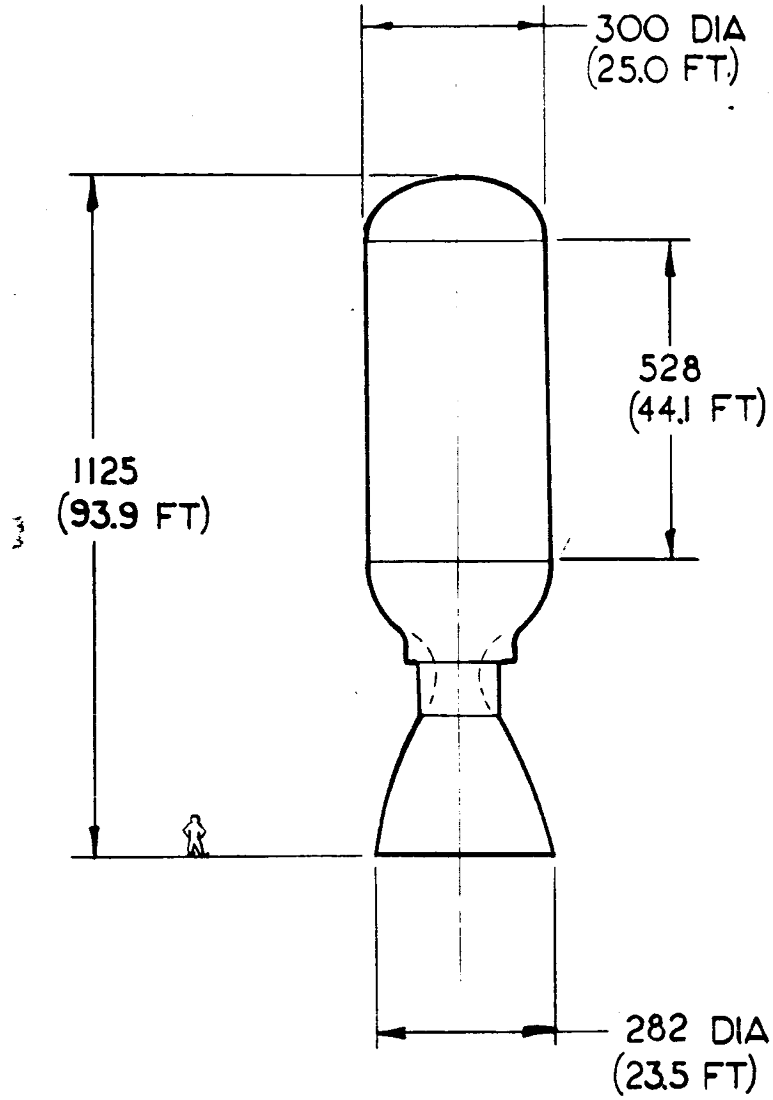

EXPANSION RATIO, ϵ = 10:1
CHAMBER PRESSURE, P_c = 800 PSI
THRUST, F = 8,800,000 LBS
WEIGHT = 2,711,647 LBS

PD21-050

Figure 2.4-2. Rocket Engine, Step 1, Straight Nozzle.

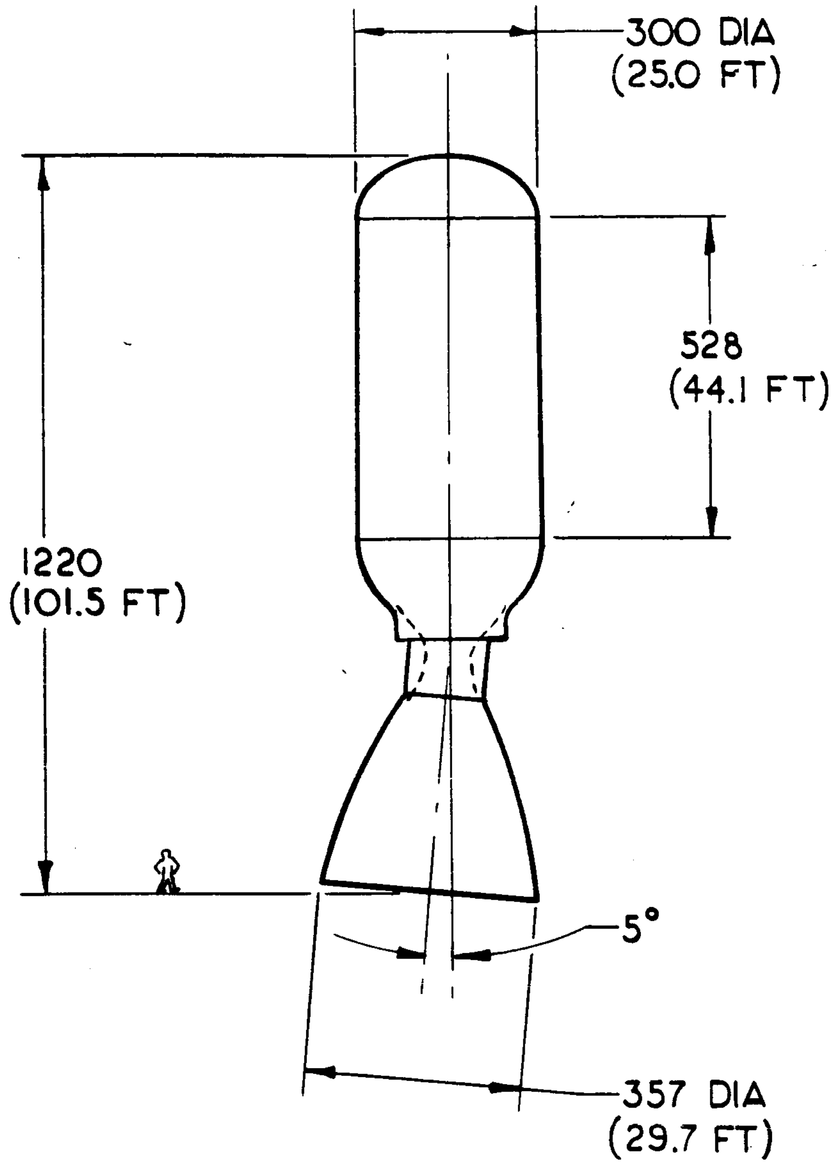

EXPANSION RATIO, ϵ = 16:1
CHAMBER PRESSURE, P_c = 800 PSI
THRUST, F = 8,800,000 LBS
WEIGHT = 2,711,647 LBS

PD21-052

Figure 2.4-3. Rocket Engine, Step II.

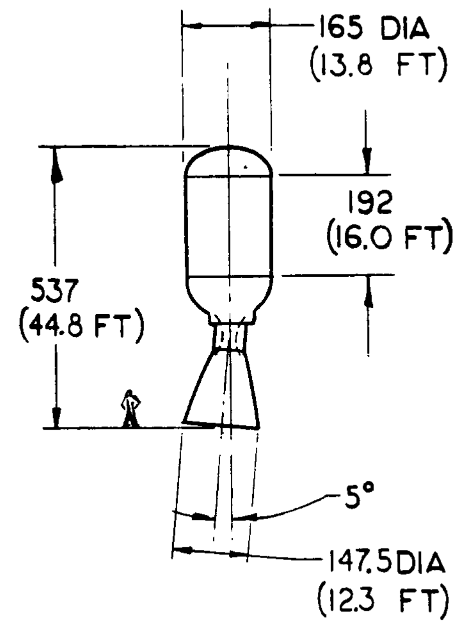

EXPANSION RATIO, ϵ = 28:1
CHAMBER PRESSURE, P_c = 590 PSI
THRUST, F = 760,000 LBS
WEIGHT = 362,445 LBS

PD21-053

Figure 2.4-4. Rocket Engine, Step III.

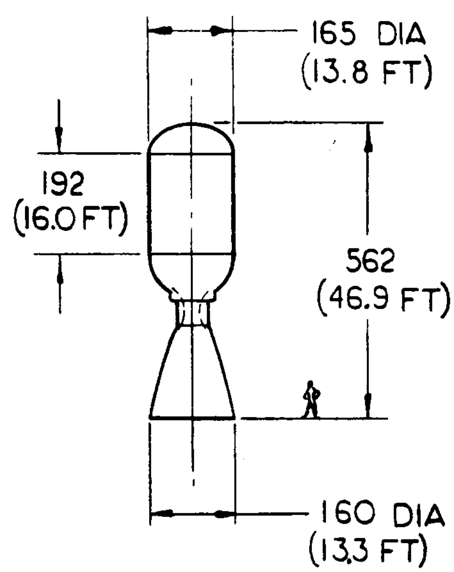

EXPANSION RATIO, ϵ = 33:1
CHAMBER PRESSURE, P_c = 590 PSI
THRUST, F = 760,000 LBS
WEIGHT = 362,634 LBS

PD21-054

Figure 2.4-5. Rocket Engine, Step IV.

In contrast to the above, it is recommended that the higher strength (225, 000 psi ultimate) steels employed on Minuteman be used. Minuteman Stage 1 experience, with a star grain configuration shows that a 15 percent pressure difference between peak and nominal pressure can be expected. To this must be added a 3 sigma allowance of 5 percent for pressure variation and 1 percent for temperature variation. These produce a design pressure 21 percent above the nominal. A conservative safety factor of 25 percent should then be applied. Calculated case weights for the "A" engine are comparable using either method because of the counterbalancing effects of the higher strength steel and more conservative safety factor.

The "B" case described in the JPL reports appears to have been designed as a blunt cylinder with 2/1 elliptical ends. A spherical case of the same diameter could have been employed at a significant saving in weight. However, a spherical shape leads to complications in clustering and interstage structure and does not appear desirable. For this reason, and in the interest of conservative star grain design, a smaller diameter and longer engine is more desirable. The weight allowance made by JPL is, however, considered to be reasonable for the elongated configuration.

The fabrication of cases in the sizes proposed appears to be feasible. Use of roll ring forgings, either hydro-spun or machined to final configuration, is considered mandatory to achieve the necessary uniformity of quality. Steels such as Ladish D-6 AC can be heat treated to 225, 000 psi ultimate in 3/4-inch sections without undue difficulty. Heat treating of welded assemblies is a common practice.

The concept proposed by JPL of introducing interstage structural loads as concentrated loads on pads on the engine domes is not consistent with good engine design. Such problems as case stress concentrations and failure of the propellant-to-case bond due to case flexing could be expected. Both intra and interstage loads should be applied as uniformly as possible into the ends of the cylindrical section through skirts on the engine.

2.4.1.3 Internal Insulation

The JPL allowances for internal liner and insulation weight appear reasonable for the A engine and conservative for the B engine. Design and manufacture of internal insulation does not appear to present any new problems because of the larger engine size. The materials to be employed were not identified by JPL. The internal insulation employed on Minuteman stages and recommended on this application is silica-filled Buna N rubber. The cylindrical section case liner should be of the same polymer employed for the propellant fuel-binder. It was not stated in References 1 and 2 how the consumption of insulating material during engine burning was treated in calculating performance. The methods employed by STL on Minuteman have proven remarkably accurate and are recommended.

2.4.1.4 Propellants

2.4.1.4.1 Performance. A propellant specific impulse of 245 seconds under standard conditions was assumed in the JPL study and related to highly aluminized propellants with either polyurethane or PBAA binders. This performance has been achieved in Minuteman size engines with the PBAA propellant, but only 242 seconds has been realized with polyurethanes having sufficient binder content to develop acceptable physical properties.

JPL extrapolates the specific impulse of the "A" engine operating at 800 psi with a 10/1 nozzle to 281 seconds (vacuum). Choosing a γ of 1.18 and using the 245 seconds standard, the STL method of extrapolation, based on Minuteman experience, predicts a value of 267.5 seconds. A similar calculation for the "B" engine with its higher (33:1) expansion ratio yields 288 seconds as opposed to 294 seconds obtained by JPL. These values do not include nozzle scale effect.

It is important to note that theoretical analysis of performance losses of solid propellants containing approximately 16 percent aluminum show that a large fraction of the loss in the Minuteman size engines may be attributed to velocity lag of the fluid particles. This loss will probably be significantly reduced in NOVA size engines because the longer dwell time of the particles in the longer nozzles will permit acceleration to near velocity equilibrium with the gas stream. Using a method developed at STL (Reference 5) it is estimated that the performance gain in an engine of "B" size will be about 4. 5 seconds and in "A" size about 5. 5 seconds.

2. 4. 1. 4. 2 Mechanical Properties. The stress in the propellant and the deformations (slump) of the propellant under acceleration both increase with engine diameter since the propellant is on the average farther from the engine wall and therefore not as well supported as in smaller engines.

The propellant in an engine case standing vertically produces a shear stress at the propellant-to-case bond of approximately 4 psi for the type "A" engine and 3 psi for the type "B" engine. These are average values over the entire case and may be exceeded in certain local areas. The estimated average stress encountered during the first stage acceleration is 15 psi. This compares with 5 psi for the Minuteman second stage in an 8. 5 g field. Although the 4. 8 psi stress in the Minuteman has proved to be tolerable, it is not known whether this can be safely exceeded by a factor of 3, since data on the tolerable stress levels are not presented available. It is, therefore, conceivable that the higher stress levels in NOVA could cause propellant failure, especially in areas of stress concentration such as at the base of the star perforation, unless the propellant were specially supported or reinforced.

The harmful effects of propellant slump are to alter the internal geometry of the rocket and possibly to induce cracking in the propellant or in the propellant-to-case bond. The amount of slump depends on the amount and duration of load, the propellant properties, and the degree of support given by the case to the propellant. It is estimated that immediately after erection of a Type A engine into the nozzle-down position, a vertical slump of approximately 1. 5 inches at the bottom inside of the grain will occur just due to its own weight. On this basis, the slump in the step II engines at step I burnout (3. 8 g) could be 5. 7 inches and possibly even more. By comparison it has been estimated that the maximum equivalent slump in

Minuteman second stage engine is less than 0.1 inch at Stage 1 burnout (8.5 g). It may also be anticipated that the amount of slump would be increased by long term creep effects during transportation and storage unless the propellant were properly supported. It is difficult to predict the creep behavior of the NOVA propellant charge since reliable creep data are not available. The stress levels in the type "A" engine would be roughly five times greater than those in the first stage Minuteman engine. Thus, even if slump due to creep in the Minuteman propellant should be tolerable, as indicated by preliminary results from tests now in progress, it could still turn out to be a disabling factor in NOVA.

The severity of the propellant stress and slump problems and their effect on mission feasibility cannot be determined on a short time scale. The stress which will cause grain failure under specified conditions is not known and cannot readily be determined. The amount of long-term slump can be evaluated only with data which is not presently available on the actual propellant and then only after a fairly long study.

The propellant mechanical properties required for a study of propellant stresses and deformation are the instantaneous shear and tensile modulus of the propellant and the shear and tensile compliances. Time to failure date under constant stress conditions for both shear and tensile stress states are also needed. Some of the data may be available now, the rest would have to be determined by experiment.

In determining long-term creep properties, there is no known method of scaling up test time. Thus, to determine the creep expected in six months of storage would require six months of test time. Some of the other required tests could be conducted in a time period much less than six months. Once the propellant properties are available, analysis can be performed to determine the potential seriousness of both short or long term grain slump. This analysis should result in approximate estimates of the changes in internal grain geometry resulting from radial slump and time to failure of the grain under static loading due to either flight or storage conditions.

LEFT BLANK INTENTIONALLY

If the results of the above studies indicate a critical problem due either to high in-flight stress levels or to long-term slump, several means could be employed to alleviate the problem:

1) It is envisioned that the engines would be shipped and stored in a vertical position, nozzle end upward; this would have the beneficial effect of minimizing slump. It may also be feasible to leave a propellant support mandrel in place until the nozzle must be attached.

2) Propellant mechanical properties can be enhanced at the expense of slightly lower performance by using an increased fuel binder content.

3) The use of a single nozzle allows support of the bottom of the grain on the aft closure. In this case slump would manifest itself as an inward movement tending to close up the grain port. The ballistic effects of this constriction could be minimized by tapering the port (use of tapered casting mandrel).

4) The concept of using mechanical supports in the propellant appears feasible but would require very extensive development and full scale testing and is certainly not state-of-the-art. It could be expected to severely influence the engine development cost and time required.

5) Segmented engine construction would tend to minimize stress and slump problems and at the same time permit easier mechanical support of the grain segments if required. This would be obtained, however, at the cost of reduced performance and reliability.

2.4.1.4.3 <u>Burning Rate.</u> Burning rates for conservative star grain designs in both engines are about double those obtained in Minuteman propellant formulations but are considered achievable using catalysts. This will require a significant propellant development program. Six pointed star perforations with web thicknesses of 1/2 engine radius have been assumed. The port to throat ratio should be made less than two so that erosive burning is avoided, since this phenomenon is not readily predicted. Extra conservatism in engine aft end insulation would therefore be required. Reproducibility of engine thrust and total impulse would probably also be adversely affected. Principally in the interest of conservative grain design and to allow development to proceed at an earlier date, it is desirable that the "B" engines be resized to about 14 foot diameter.

2.4.1.4.4 Combustion Instability. Ample evidence is available from Minuteman and other programs to support the conclusion that combustion instability will not occur in highly aluminized composite propellants.

2.4.1.4.5 Propellant Selection. JPL considers both polyurethane and PBAA formulations as candidates for both engines. At present, the principal advantage of polyurethane is its somewhat better mechanical properties. In comparison, PBAA propellant is most readily processed, and is simpler to control (it has only 1/3 as many ingredients), is relatively unaffected by moisture and high humidity, and can be cast under ambient pressure conditions, rather than requiring a vacuum. A promising development of a PBAA type polymer having chain-terminated carboxyl groups would improve the propellant properties to a level comparable with polyurethane. STL believes that selection of the propellant should strongly consider the potential processing problems since the propellants are otherwise generally equivalent.

2.4.1.5 Nozzles

The nozzle concepts described in References 1 and 2 represent an overly optimistic evaluation of nozzle design problems. Experience on high performance, long duration engines has shown that the primary structural problems result from the large thermal expansions that occur, and these cannot be completely resolved by subscale tests.

Throat design becomes very difficult in the extremely large sizes considered (approximately 6' for "A" engine, approximately 3' for "B" engine). Graphite as a throat material should be the primary effort as recommended by JPL. However, a steel backup structure is not adequate without an insulating layer interposed. Multiple piece graphite construction is proposed by JPL. Adequate cements capable of withstanding the temperature environment are not currently known. A single annular piece of graphite is preferable but for the "A" engine a piece of this size is not presently available. An immediate program to generate the high density graphite manufacturing capacity would be required and capacity for rings about 9 feet in diameter and about 12 feet long is necessary. Pieces about 4 feet in diameter will be necessary for the "B" engine. This latter size is not presently available in the desired grade but is available on special order in a lower grade. It is believed that acceptable graphite for both engines can be obtained on the required time scale and that multiple piece construction can be avoided. Two companies making graphite have indicated their capability to make pieces 80 - 100 inches diameter within one year.

There are two principal problems with graphite throat inserts, erosion and structural failure. Although some erosion can be tolerated, breakout cannot. Unfortunately, available analysis techniques are grossly inadequate to predict thermal stresses and an early program of tests of materials and nozzle configurations should be implemented to help establish a better method of predicting thermal stress in large nozzle inserts.

Erosion data on large graphite nozzles are lacking but will become available as firings on fairly large segmented engines take place. Data from these firings should be collected and analyzed as quickly as possible. Erosion estimates, for the present system, based on the limited data available for ATJ graphite are:

"A" Engine	3 percent area change
"B" Engine	6 percent area change

Lower quality (density) graphite would erode more, perhaps as much as 50 percent greater change. Nevertheless, such area increases are tolerable from a performance standpoint.

The high pressure-molded reinforced-phenolic-plastic ablative throats considered in the JPL study are attractive because throat structural problems are minimized. Erosion will, of course, be greater than with graphite; throat area changes are estimated to be:

"A" Engine	5 percent area change
"B" Engine	12 percent area change

These area increases are also tolerable if taken into account in the engine design. A subscale program using single nozzle Minuteman Stage 1 size engines is recommended to verify that predicted rates are not significantly exceeded.

Nozzle exit cones should, ideally, be of one-piece high pressure-molded phenolic-plastic construction. However, equipment limitations early in the program may necessitate fabricating the cone in ring sections. If the nozzles are of ring construction a fiberglas overwrap will be required for structural support. A metal support structure will probably be required with either one piece or built up construction to carry the side thrust loads (control forces) from the secondary injection system.

Nozzle weights given in the JPL study are believed to be in error. STL estimates for the JPL nozzles are compared below with those given in the study.

	JPL Value	STL Estimate
"A" Engine (10:1 nozzle)	34, 000	29, 000
"A" Engine (16:1 nozzle)	----	49, 000
"B" Engine (33:1 nozzle)	3, 500	15, 000

The very large weight penalty incurred with the "B" engine nozzle results from its very large surface area. An increase in engine chamber pressure from 350 psi (JPL) to 590 psi reduces the size and weight of the nozzle without exceeding the basic JPL engine weight allowance.

Nozzle cant is suggested by JPL and STL for the peripheral engines of steps I and II. In addition, STL suggests canting the nozzles of the step III engines. An analysis of vehicle dynamics at staging indicates that it is not necessary to align the thrust axis through the vehicle center of gravity just prior to staging but that a small amount of cant eases the control problem. The cant angles to align the thrust through the center of gravity would amount to 9 degrees for the engines of step I, 10 degrees for the engines of step II, 13 degrees for the three corner engines of step III and 7 degrees for the three interior engines of step III. The guidance and control system and staging analysis which have been performed in the present study (2.7) indicate that 5 degrees of cant is adequate. This greatly minimizes the performance loss that would be incurred if the full nozzle cant were required.

Of perhaps more importance than the performance penalty is the considerable increase in engine design difficulty because of asymmetrical flow problems introduced by large nozzle cant, which would result in a need for more full-scale development firings to achieve a satisfactory design. Design difficulties are expected to increase in proportion to the magnitude of cant angle. Below 5 degrees, design complications are minimized and performance loss is very small. At angles above 8-10 degrees, however, additional full scale tests and development time would probably be required to solve the problems encountered. It is also quite possible that the lack of symmetry in the aft closure and nozzle, aggravated by erosion as burning progresses, would result in thrust misalignments that would not occur in a straight nozzle design, and that the theoretical control advantages of cant would not be fully realized. Since both canted and uncanted nozzles appear to be required, full-scale firings are required to demonstrate adequacy of each nozzle. Consequently, the trade-off between producing the necessary control force capability with the thrust vector control system rather than relying on nozzle cant to minimize the required control forces should be studied in detail.

2.4.1.6 Igniter

JPL considered two types of ignition systems and selected a pellet basket pyrotechnic igniter over a rocket (Pyrogen) type. Experience with both types in the Minuteman program would lead STL to the opposite choice. The rocket type igniter has been employed on Stage 1 with a minimum of development problems. Average ignition time for the engine is 0.135 second with a reproducibility of 0.025 second (3σ). The pellet-basket type has been found more difficult to design for reproducible ignition transients. Functioning characteristics are greatly influenced by manufacturing variations, particularly in the pellets. It was found that the specific surface of the flake aluminum powder in Alclo pellets closely influenced functioning. The specific surface of commercial flake aluminum powder varies from lot-to-lot and ignition transients have shown close correlation with aluminum flake lot. Another design factor influencing functioning is basket confinement. Variations arising from inherent variability of the design are amplified by the high pressure exponent of the pellet material. It is anticipated that variability problems of the pyrotechnic igniter will be greater in the larger sizes.

Ignition times of Minuteman size engines are comparable with either type igniter. Methods have been developed in the Minuteman program for rocket igniters to control the ignition time by variations in the igniter propellant materials. For example, ignition times can be decreased by increasing igniter propellant aluminum content. Mass flow and direction also influence ignition characteristics. The rocket type igniter can be designed and adjusted using well-established principles and can be sealed more readily than the pyrotechnic type with no special problems due to increased size. It is therefore recommended for primary development.

The use of some form of auxiliary ignition safety device to increase handling safety of solid propellant engines is mandatory for military systems and is becoming rapidly more widespread in space applications. An electromechanical device (S and A) is employed on Minuteman to short out the squibs and impose a physical barrier between them and the ignition charge when in the safe position. Another scheme not yet state-of-the-art but perhaps worthy of further development is to use a squib which requires a very high initiation energy (exploding bridge wire). Present practice is to arm all such devices on the launch pad and monitor their armed condition. The requirements of a manned vehicle may modify this philosophy to require in-flight arming of upper stages as is done on warhead fuzes. Realiability and other system implications of such a move should be carefully investigated, however. The use of redundant squibs and circuitry is recommended. Completely redundant igniters should be avoided, if possible, since this introduces the probability of excessive variability in ignition and engine peak pressure.

2.4.1.7 Engine Uniformity

Clustering introduces some problems due to small differences in performance between individual engines of a cluster. Variations in ignition delay, thrust, and burning time affect the control forces required to trim the vehicle, particularly at staging. This affects the design of the control system and in the present application has led to a requirement for nozzle cant (section 2.7). Anticipated variations in operating characteristics (based on extrapolation of Minuteman data) are compared below with the assumptions of the JPL study:

	Standard Deviation	
	JPL Value	STL Estimate
Average thrust	1.23%	1.23%
Instantaneous thrust	--	2.46%
Total impulse	0.16%	0.25%
Ignition delay	0.01 sec (pellet igniter)	0.020 sec (pellet igniter) 0.010 sec (rocket igniter)

Variations in the tailoff portion of engine thrust (from final peak to 10 percent average thrust level) are generally greater than in the main portion of the engine operation and are due to thermal gradients in the propellant grain, manufacturing dimensional variations, and flaws. JPL assumed a (nominal) linear tailoff lasting 10 percent of the burning time. This appears reasonable. The tailoff interval may, however, vary by as much as 25 percent (3σ). The control system analysis described in section 2.7 revealed the desirability of staging steps I and II during the thrust tailoff phases. Staging at a thrust level of about 10 percent of the thrust prior to start of tailoff was found to be satisfactory and produces essentially no degradation in vehicle performance since the impulse lost is less than the standard deviation of total impulse.

2.4.2 Thrust Vector Control

STL has conducted fairly detailed studies of thrust vector control of large solid propellant engines and has concluded that only two of the many possible schemes proposed or used in previous missile applications have real merit for a NOVA class vehicle. These are gimballed nozzles and secondary fluid injection. Jet vane systems have been rejected for very large, long duration engines because of forbidding problems in vane design for survival. A study of vane materials and fabrication techniques has led to the conclusion that only a refractory metal leading edge (tungsten alloy) could survive. Further, techniques are not available or in sight for making these parts either in one piece or by reliable built-up construction.

2.4.2.1 Gimballed Nozzles

The extensive experience gained in the successful development of hinged nozzles for the three stages of Minuteman makes the concept of the basically similar gimballed nozzle attractive. Indeed, such a system is under development for Skybolt. The problems with hinged nozzles are well-known and have been solved, though in the case of Minuteman with considerable difficulty and development effort. A trend toward increased difficulty with engine size and burning duration has been established. Use of a single center-mounted nozzle for each engine, in the present NOVA concept, rather than the 4-nozzle configuration of Minuteman, should tend to minimize some of the problems which have been encountered and which were connected with asymmetrical flow into the nozzle. Nevertheless, the seal, thermal growth, torque, stiffness, and other problems with gimballed nozzles introduce potential failures in initial tests despite the most careful design, and an extensive development program would be required to achieve a successful design. A gimballed nozzle design is, however, believed feasible for this application.

Control aspects of gimballed nozzles are reasonably well understood from Minuteman experience and can be scaled to larger vehicles.

2.4.2.2 Secondary Fluid Injection

This system involves injection of a fluid (liquid or gas) through orifices in the nozzle expansion cone wall to create an oblique shock wave and thus divert the exhaust stream. By spacing around the wall orifices controlled by separate valves, it is possible to control in both pitch and yaw planes. Separate roll control is necessary in single engine stages with single nozzles of either the secondary injection or the gimballed type. A schematic diagram of a secondary injection system is shown in Figure 2.4-6.

Secondary injection is a relatively new control scheme and has not yet been tested in flight, although several organizations have conducted static firings. It is planned for use on Polaris A-3 Stage 2 and is being actively investigated for possible application to improved versions of Minuteman, Stages 2 and 3. Several tests are planned in the near future on large engines in connection with feasibility firings of the large segmented solid propellant engine program.

Since movement of the engine nozzle is not required with the secondary injection scheme, its development is relatively straightforward compared to that of a gimballed nozzle. Thus careful attention to implementation of the detailed design should assure a relatively high probability of survival.

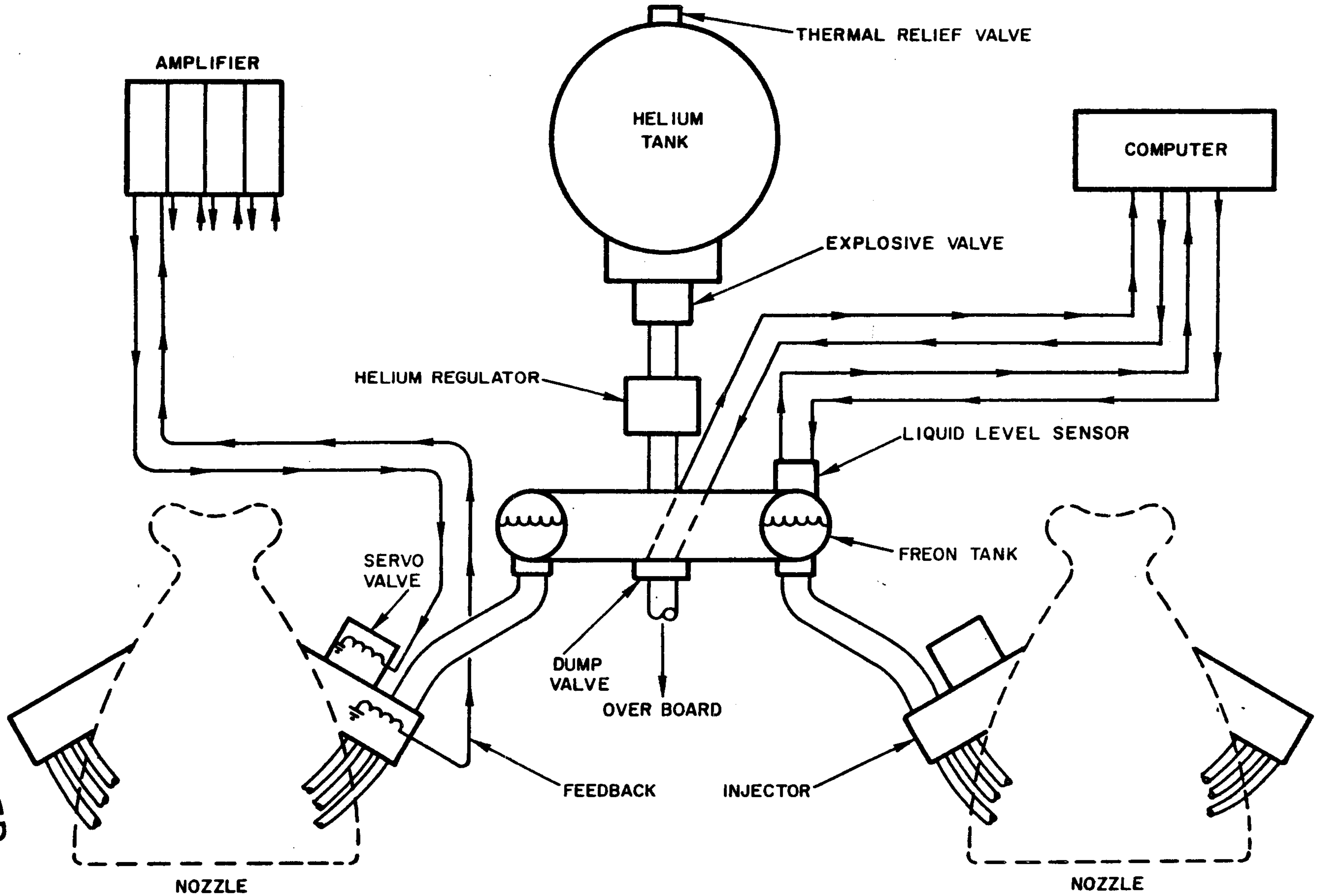

Figure 2.4-6. Schematic Diagram, Secondary Injection T.V.C. Systems.

Further, design and testing of injectors, valves and port locations can proceed using smaller size engines to provide a reasonable basis for design of the full-scale engine. However, the following unknowns for this system still exist: dynamic response characteristics, the degree of non-linearity in thrust deflection versus flow rate, effects of the flow field on heat transfer rates (erosion), effects of flow separation in the nozzle, and contour and scaling effects on performance. Many of these unknown areas are now under investigation and it is felt that no insurmountable problems exist. The difficulty of control feedback is probably the most serious potential problem and deserves special attention in the detailed preliminary design study. Such a study should also very accurately determine the requirements for maximum side force and total side impulse, as these have a significant effect on the design. The estimates for these quantities used in the JPL study are, however, consistent with those made by STL for the present vehicle system. Recent studies by STL have indicated that the dry weights of gimballed nozzle and secondary liquid injection systems are comparable. Jet vanes compared unfavorably in weight with either system and the drag losses due to the vanes, estimated at 3 percent or more, further degrade performance. Secondary injection imposes a small performance penalty due to the weight of the injectant fluid carried. This can be minimized by programming the dumping of excess fluid if it is not consumed in steering the vehicle as anticipated, and the overall effect on vehicle size is almost negligible.

STL concurs with the selection of a pressurized rather than a pump fed system and tentatively recommends FREON 114B-2 as the injectant. Assumptions used in sizing system capacity appear reasonable. Dumping of excess injectant is also considered feasible and the possibility of dumping through the nozzle to enhance performance appears worthy of further detailed study. The use of a solid propellant gas generator for tank pressurization is within state-of-the-art and is preferred over a high pressure helium supply on the basis of lower overall weight. An auxiliary benefit of such a scheme for step IV propulsion is that the gas generator may be oversized and the excess gas used for roll control by bleeding it into suitable nozzles.

JPL weight estimates for secondary injection tankage, plumbing, valves, etc., appear somewhat high. These weights are nevertheless a relatively insignificant fraction of the inert weight and do not affect vehicle feasibility.

It is not presently possible to define much of the secondary injection hardware in detail. The preliminary design study should include a survey of existing designs and investigate such appealing schemes as use of the injectant for nozzle cooling, use of the nozzle as part of the injectant tank and stiffening of the nozzle by integrating it with the tank, use of engine gas for pressurization, etc.

2.4.3 Growth Potential

Growth potential, within the concept of an all solid vehicle, may be anticipated in two areas. One of these is the reduction in the number of individual engines in the vehicle by the development of larger engines as this becomes feasible. This can be expected to enhance reliability considerably and performance to some extent.

Incremental increases in propellant performance of perhaps 2 seconds specific impulse per year for the next 4 years are probable through increases in propellant solids content. Eventually a further improvement might be obtained from increasing fuel-binder energy level by nitrating provided that propellant mechanical properties are not degraded thereby to an unacceptable level. The increased solids content also results in a small density increase. Significant performance increases (14-20 seconds specific impulse), can be realized through the introduction of beryllium-loaded propellants in the upper two stages. These propellants are basically similar to those studied except for the substitution of beryllium for aluminum. The performance increase arises from the lower molecular weight of the exhaust products rather than from an increase in flame temperature. Therefore, engine hardware problems are not adversely affected. At present these propellants are in the early development stage and testing has been confirmed to very small engines since the exhaust products are extremely toxic and test facilities are limited. Beryllium is also very expensive ($100/lb) at present but might drop an order of magnitude in price if large quantities were used. The availability of the large quantities that would be required has not been considered and should be studied further. The toxicity would not be a problem on upper stages except in the event of a vehicle failure in which the upper stage burned so that significant quantities of its gases could be inhaled, or an area contaminated by particle fallout. Over-water launching is believed to solve this problem adequately. It is estimated that use of the beryllium propellant will be state-of-the-art for large engines in about 4 years. It should, therefore, be considered for follow-on development only.

2.5 VEHICLE AERODYNAMICS

2.5.1 Scale Effects

It can be shown that the influence of aerodynamics on the performance and controllability of a vehicle diminishes in importance as the vehicle grows in size. The equations of motion for steady flight in the atmosphere are given below, with the notation as defined in Figure 2.5-1.

$$\frac{\ddot{x}}{g} = \frac{F}{W} - \frac{A}{W} - \cos\theta$$

$$\frac{\ddot{y}}{g} = \frac{F\sigma}{W} + \frac{N}{W} - \sin\theta$$

$$\ddot{\theta} = \frac{Nl_1}{I_{CG}} - \frac{F\sigma l_2}{I_{CG}}$$

The axial and normal aerodynamic forces, A and N, are proportional to a reference area, typically a cross-sectional area of the body, and hence to a linear dimension squared. The vehicle weight, W, on the other hand is proportional to a linear dimension cubed. Thus, the axial and normal "g's" due to aerodynamic forces, A/W and N/W, diminish inversely as the size of the vehicle. Similarly, the aerodynamic moment, Nl_1, is proportional to a length cubed whereas the moment of inertia of the body, I_{CG}, is proportional to the fifth power of a length. Thus, the contribution of the aerodynamic moment to the angular acceleration, Nl_1/I_{CG}, falls off as the square of the vehicle size. In other words, very large booster vehicles are too massive and have too much inertia to be significantly influenced by aerodynamic lift and drag.

The above conclusion has been verified in the performance and control studies performed for the solid propellant NOVA configuration presented in Reference 2. Axial and normal force and center of pressure

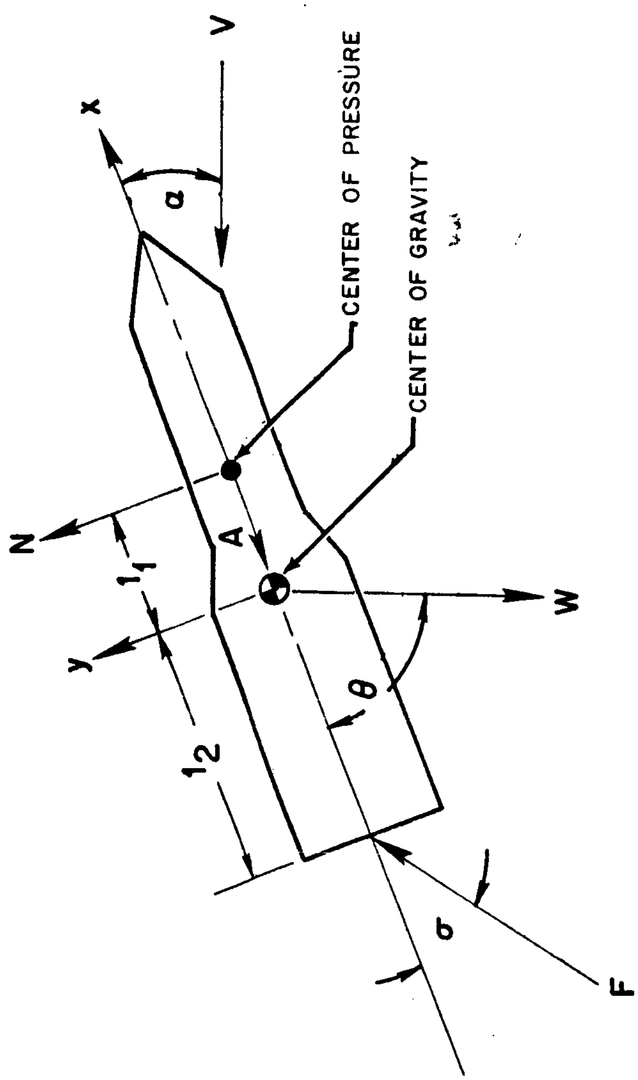

Figure 2.5-1. Vehicle Notations.

estimates for this configuration are presented in Figures 2.5-2 through 2.5-4. Drag curves are shown for a completely unfaired vehicle and for two partially faired vehicles. The reduction in drag attainable by use of the fairings is seen to be significant. Nevertheless, trajectory calculations using both extremes of drag give practically identical results. Similarly, control system studies reveal that regardless of the degree of aerodynamic instability of the vehicle, a very minor amount of thrust vector offset (less than 1/2 degree) is required at any point in the trajectory to control the vehicle. It thus appears that from the standpoint of vehicle performance only, it is not necessary to use shrouds or fairings or to take other steps to minimize air drag.

Although the aerodynamic influence on the performance and stability and control of a vehicle diminishes as the size increases, this does not imply that the effect of the airload on the structure also tends to become less important. It was shown that the aerodynamic moment was proportional to a length cubed. The resisting structural moment can be considered as a stress times an area times a distance, and hence is also proportional to a length cubed. Thus, structural requirements due to aerodynamic loading are independent of vehicle scale factor.

2.5.2 Unsteady Aerodynamic Effects

Unsteady flow effects may be significant for an unfaired vehicle, particularly at transonic and low supersonic speeds. Flow separation, local shock-boundary layer interaction, and vortex shedding phenomena are expected to occur with clustered rocket cases which are exposed directly to the airstream. The resulting fluctuating pressure fields would give rise to buffeting and acoustic problems which must be examined with respect to their influence on gross bending moments of the vehicle, local structural stresses, vibration, and noise. The magnitude of these problems cannot be assessed without extensive and careful wind tunnel testing. Even with such tests, reliable design data cannot be guaranteed because the

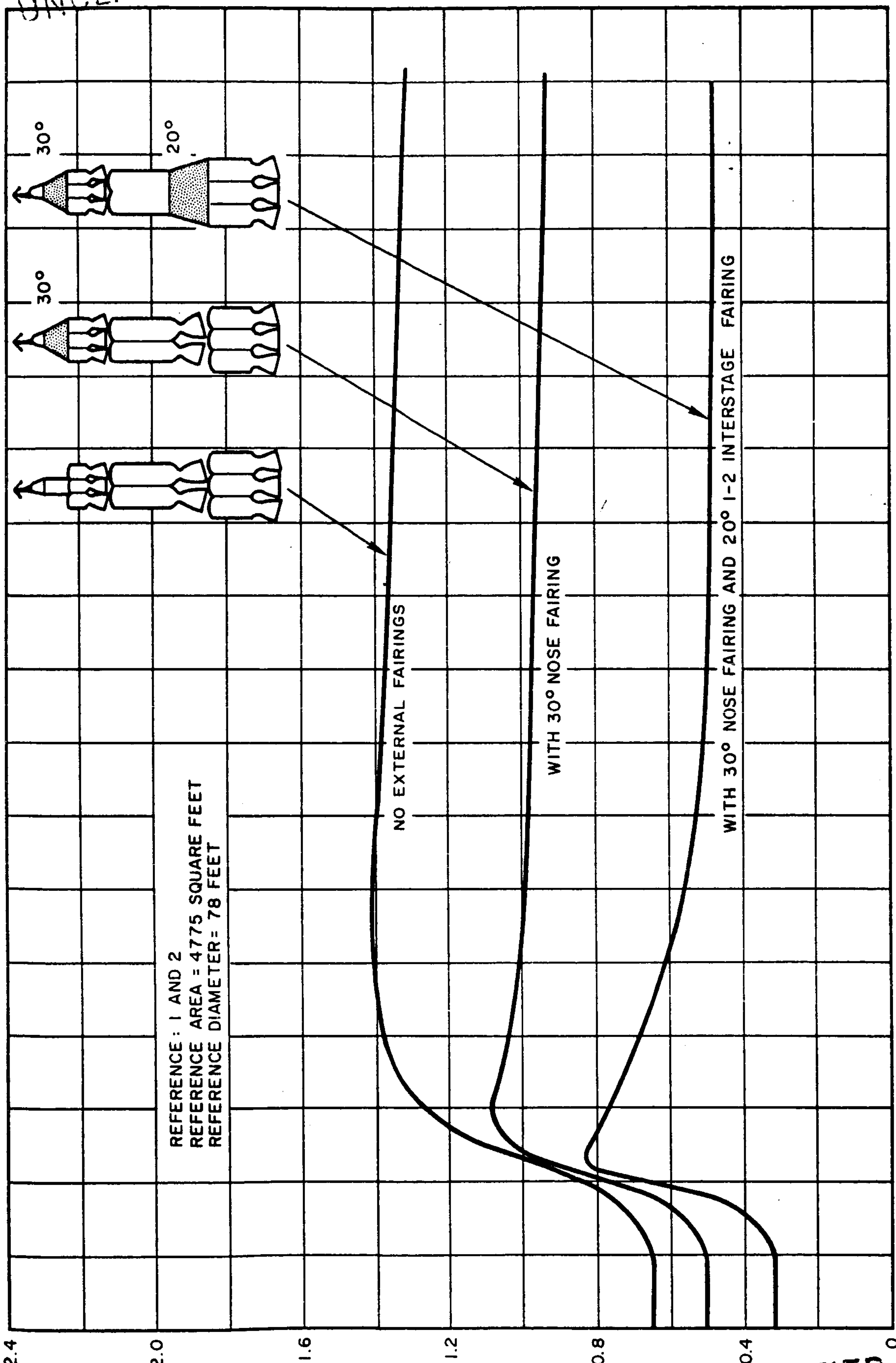

Figure 2.5-2. Estimated Normal Force Coefficient, JPL Solid Propellant NOVA.

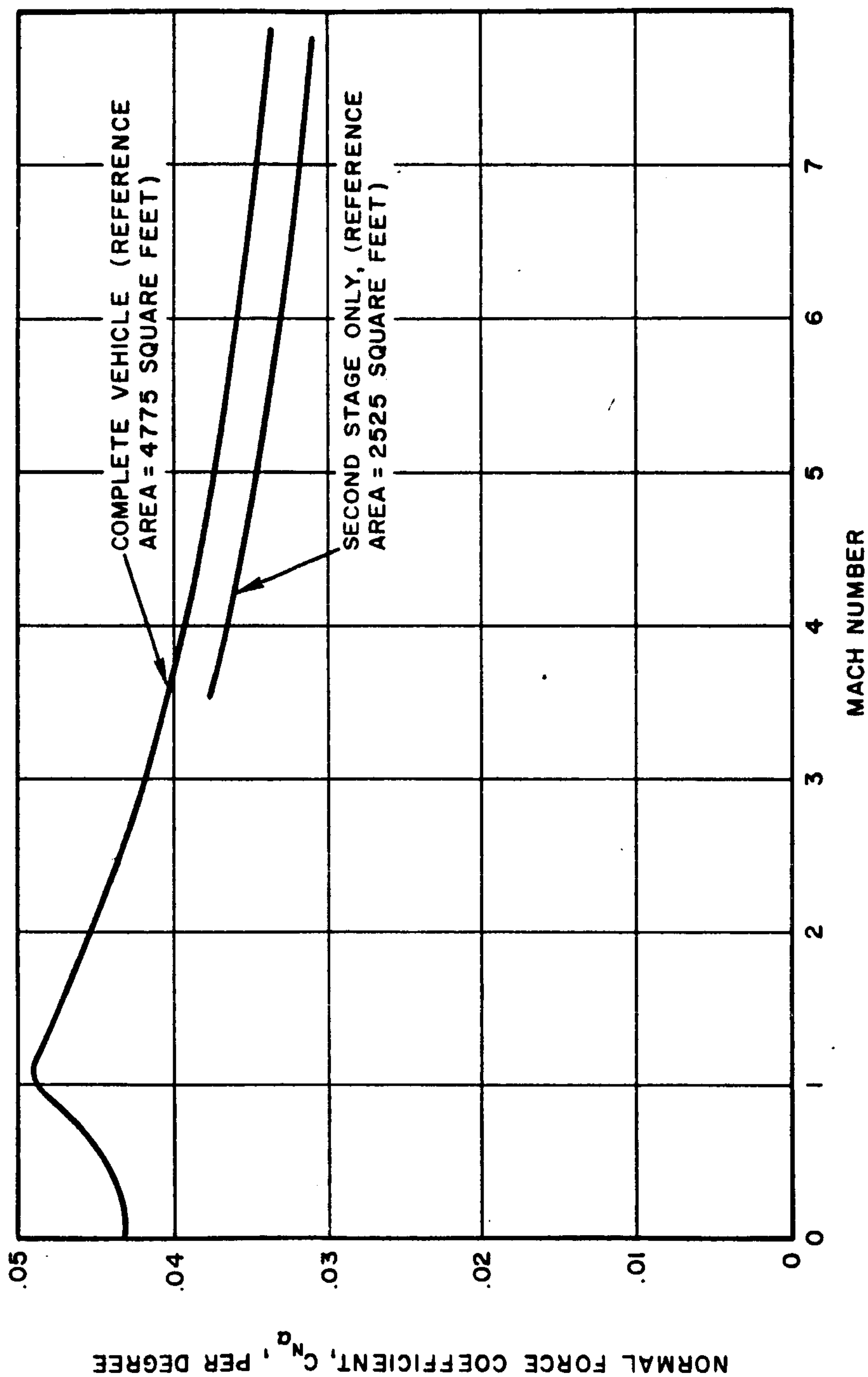

Figure 2.5-3. Estimated Normal Force Coefficient, JPL Solid Propellant NOVA.

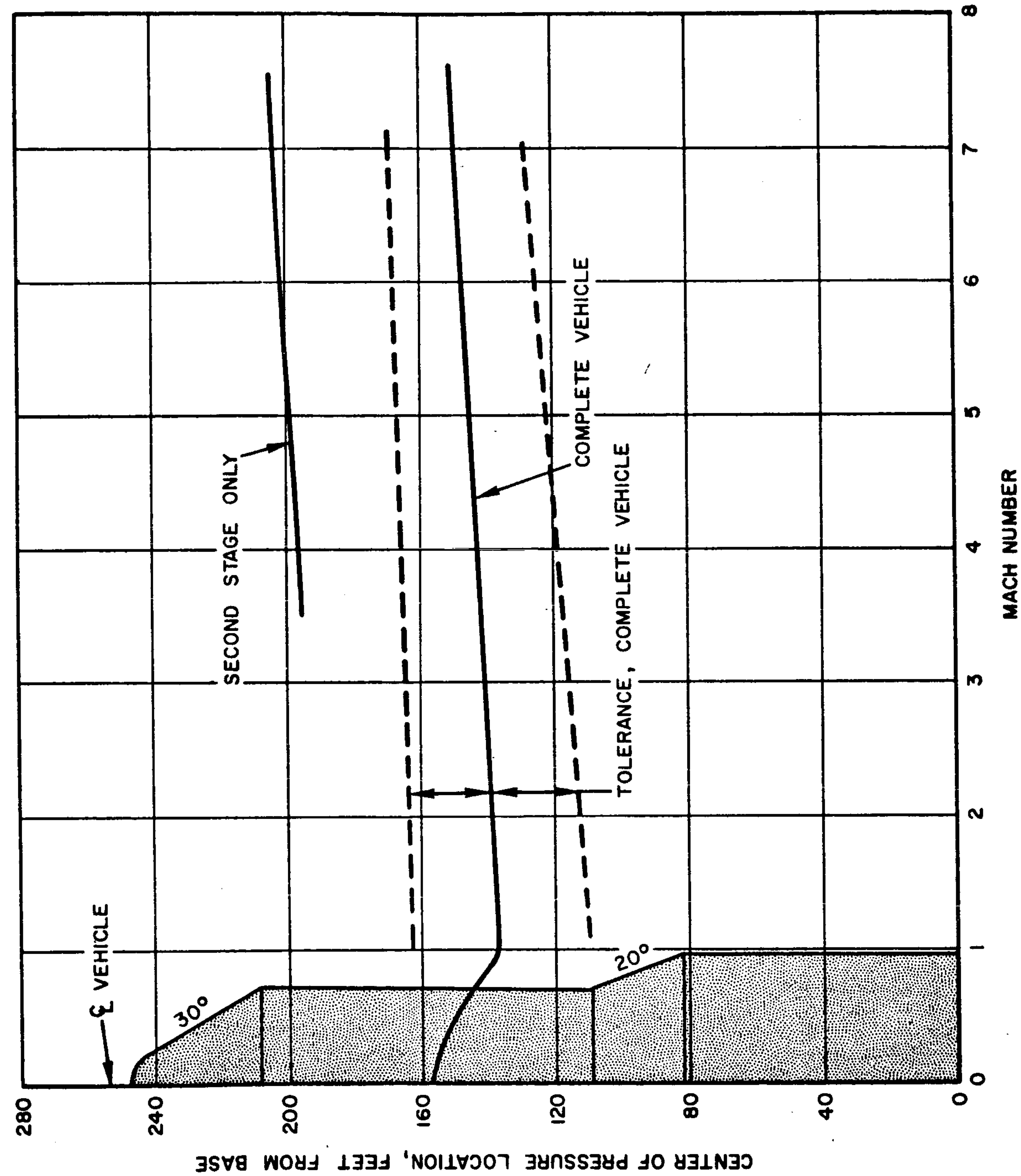

Figure 2.5-4. Estimated Center of Pressure, JPL Solid Propellant NOVA.

scaling laws for transient flow phenomena involving separated, viscous flows are not known. However, based on past experience with Mercury-Atlas, Mercury-Redstone, Atlas-Able, Thor-Able Star, and Titan flights, in all of which buffeting and associated phenomena were encountered, one can confidently predict that an unfaired solid-propellant NOVA will likewise experience such difficulties. Their correction is expected to be a major design and development problem.

It appears sensible, therefore, to attempt to minimize the buffeting and acoustic phenomena by shielding the head ends of the rocket clusters in each step behind aerodynamic fairings. The capability of judiciously designed fairings to reduce buffeting effects was clearly illustrated in the recent Mercury-Redstone flights that carried the U.S. Astronauts. In the first flight, vibration due to transonic buffeting was severe enough to impair the vision and coordination of the Astronaut. On the second flight the buffeting response was significantly reduced by adding an aerodynamic fairing on the Marman ring clamp that attached the Mercury capsule to the adapter. The solid-propellant NOVA considered by STL in the present study, is therefore predicated on the use of fairings to completely enclose each interstage and the junction of the payload with the fourth step. (See Figure 2.1-2.) Estimated aerodynamic coefficients for this configuration are presented in Figures 2.5-5 through 2.5-7.

Even with fairings covering the interstages, there still may be concern for unsteady flow phenomena around the clusters of rocket cases in the first and second steps. Scaled wind tunnel models instrumented with high frequency response pressure transducers will be needed to expose regions of intense buffeting, and to evaluate local fairings designed to alleviate such activity.

Wind-induced oscillations of the vehicle on the launch pad is another problem area in which unsteady aerodynamic effects may be significant. In addition to the steady drag force, ground winds give rise to unsteady

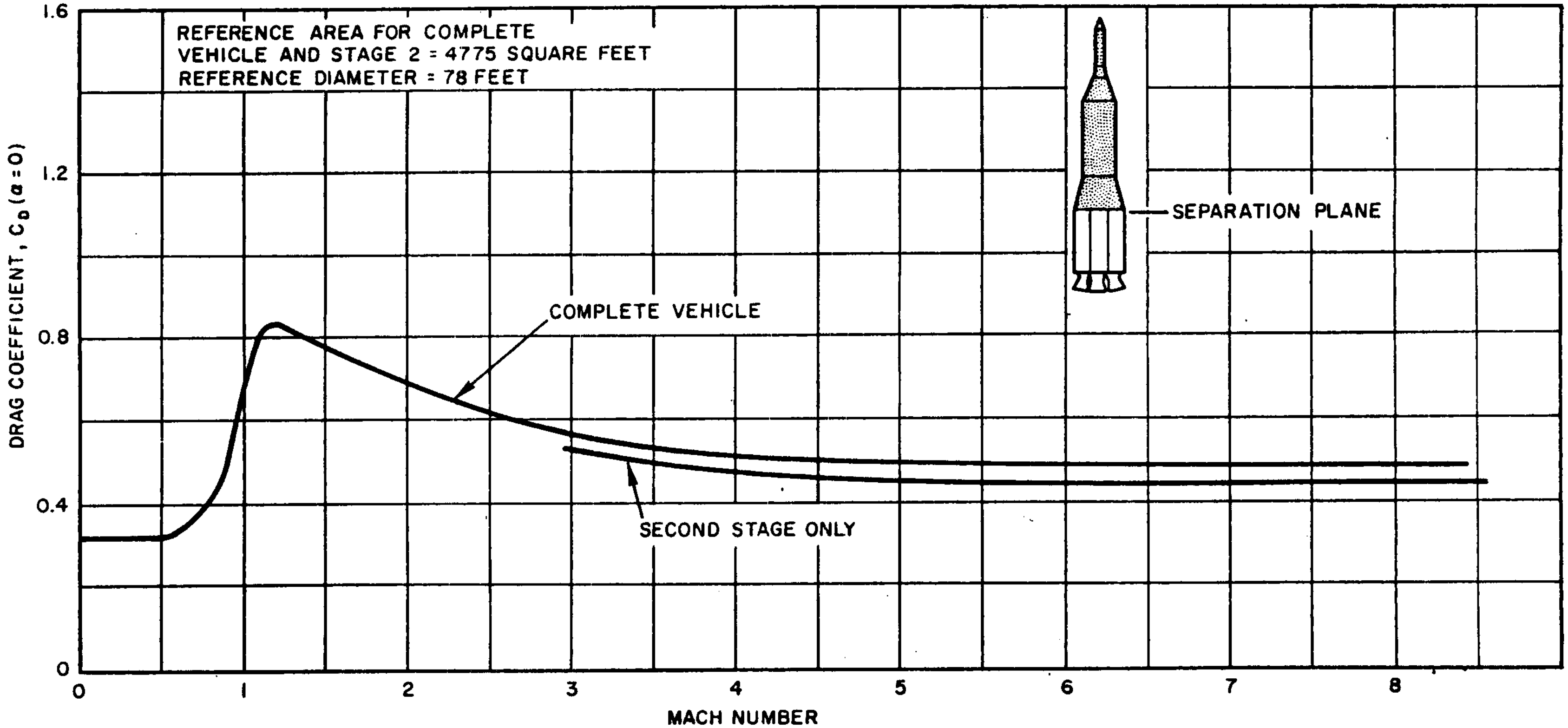

Figure 2.5-5. Estimated Drag, STL Solid Propellant NOVA.

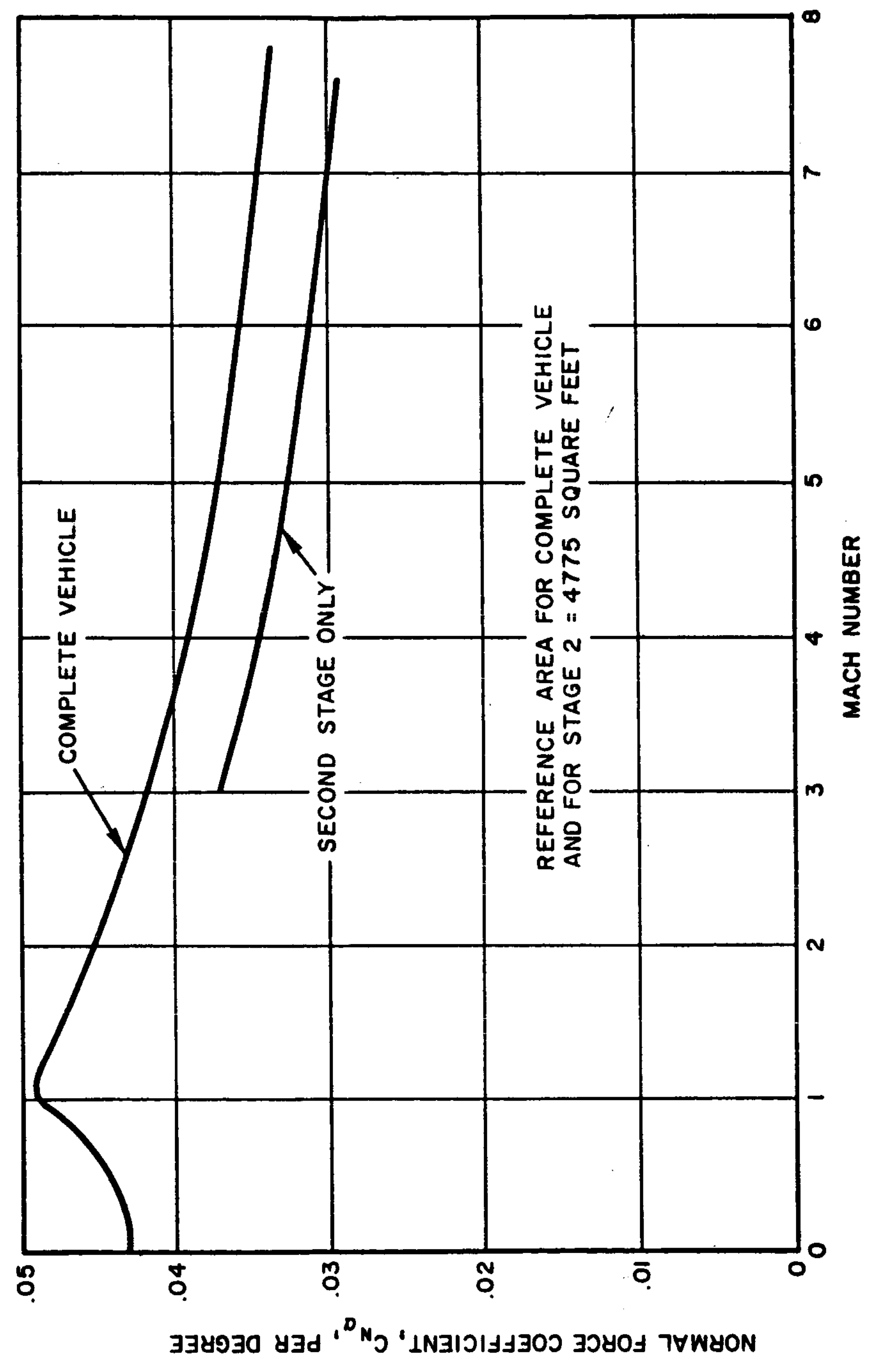

Figure 2.5-6. Estimated Normal Force Coefficient, STL Solid Propellant NOVA.

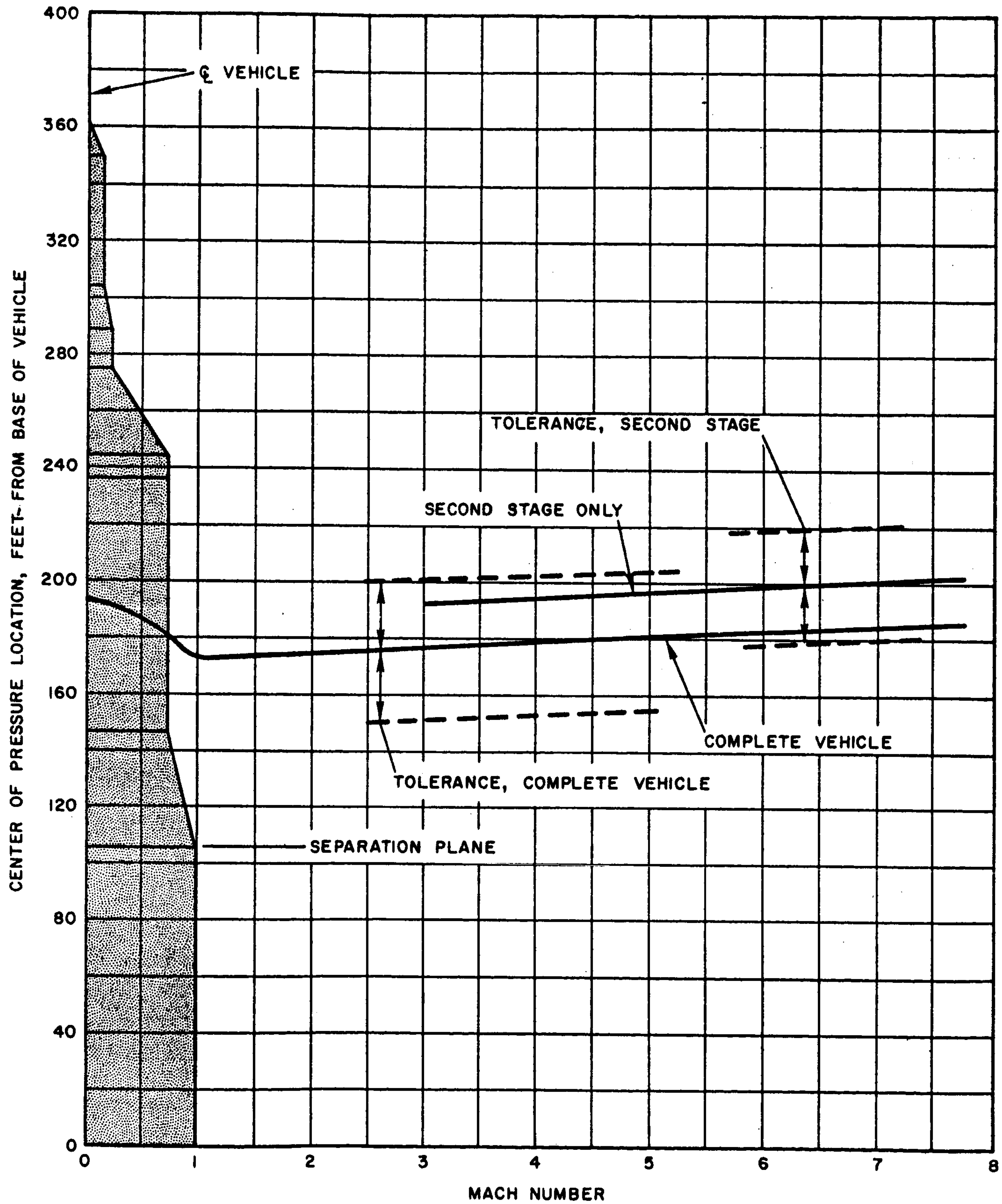

2.5-7. Estimated Center of Pressure, STL Solid Propellant NOVA.

drag and crosswind forces due to the random shedding of vortex sheets along the length of the vehicle. Such forces excite the combined vehicle-launch stand structural modes of vibration. In the case of the Titan missile, the unsteady lateral forces produced the critical ground wind loading. Multi-body (clustered) configurations may present different characteristics, however. Recent data from a dynamically similar 1/13-scale model of the Saturn (Reference 6) showed that the steady drag load, rather than the unsteady lateral loads, was critical. A similar situation may be true for the solid-propellant NOVA; however, a wind tunnel test should be performed to obtain the necessary design information.

The effects of unsteady aerodynamic forces on the stability of the control system of a large elastic vehicle have always been considered unimportant in the ballistic missile and space vehicle programs under STL cognizance. The unsteady forces referred to here are those associated with the beam bending vibration modes of the complete vehicle. Some approximate calculations of the magnitude of these forces were made using unsteady slender body theory. The calculations were based on numerical data for the Titan A missile, under the assumption that it was oscillating harmonically in its first bending mode at the maximum dynamic pressure conditions in flight. The in-phase and out-of-phase generalized aerodynamic forces were compared with the corresponding generalized mechanical terms, with the following results:

$$\frac{\text{Aerodynamic stiffness}}{\text{Mechanical stiffness}} \sim \frac{1}{2000}$$

$$\frac{\text{Aerodynamic inertia (vertual mass)}}{\text{Generalized mass}} \sim \frac{1}{1000}$$

$$\frac{\text{Aerodynamic damping}}{\text{Structural damping}} \sim \frac{1}{5}$$

Of the three aerodynamic terms, only the damping seems of any significance. Recently, some NASA Ames Laboratory tests (Reference 6) on a flexible model of a so-called "hammerhead" missile configuration* disclosed the existance of negative aerodynamic damping at transonic speeds when the model was excited in its fundamental bending mode. The unsteady slender body theory mentioned above will always predict positive aerodynamic damping. The negative damping found experimentally is probably due to unsteady shock-boundary layer inter-action and flow separation.

While it cannot be stated, a priori, that a solid propellant NOVA vehicle may encounter a similar phenomenon, it is considered important, in view of the vehicle's relative flexibility and general lack of a clean aerodynamic configuration, to perform aeroelastic model wind tunnel tests in conjunction with rigid model buffeting test.

2.5.3 Aerodynamic Heating

Aerodynamic heating has been examined for the solid-propellant NOVA, and is not considered to be a problem area. The trajectory used in the analysis is shown in Figure 2.5-8. Four locations on the airframe were examined and the results are tabulated in Table 2.5-I. The locations on the interstage skin or shroud were assumed to be reasonably remote from heat sinks such as ribs. On the Step III tank, the inside surface of the case was assumed to be insulated. The aerodynamic heating rates were calculated using incompressible flat plate skin friction coefficients, the reference enthalpy method for compressibility corrections, and the modified Reynolds analogy relating skin friction to heat transfer. The local edge-of-the-boundary layer flow conditions at each location were based on the arbitrary assumption of conical flow corresponding to the

---

*A "hammerhead" configuration is one in which the nose of the vehicle is larger in diameter than the stage immediately below it; the term is generally applied to configurations which are susceptible to severe transonic and supersonic buffeting.

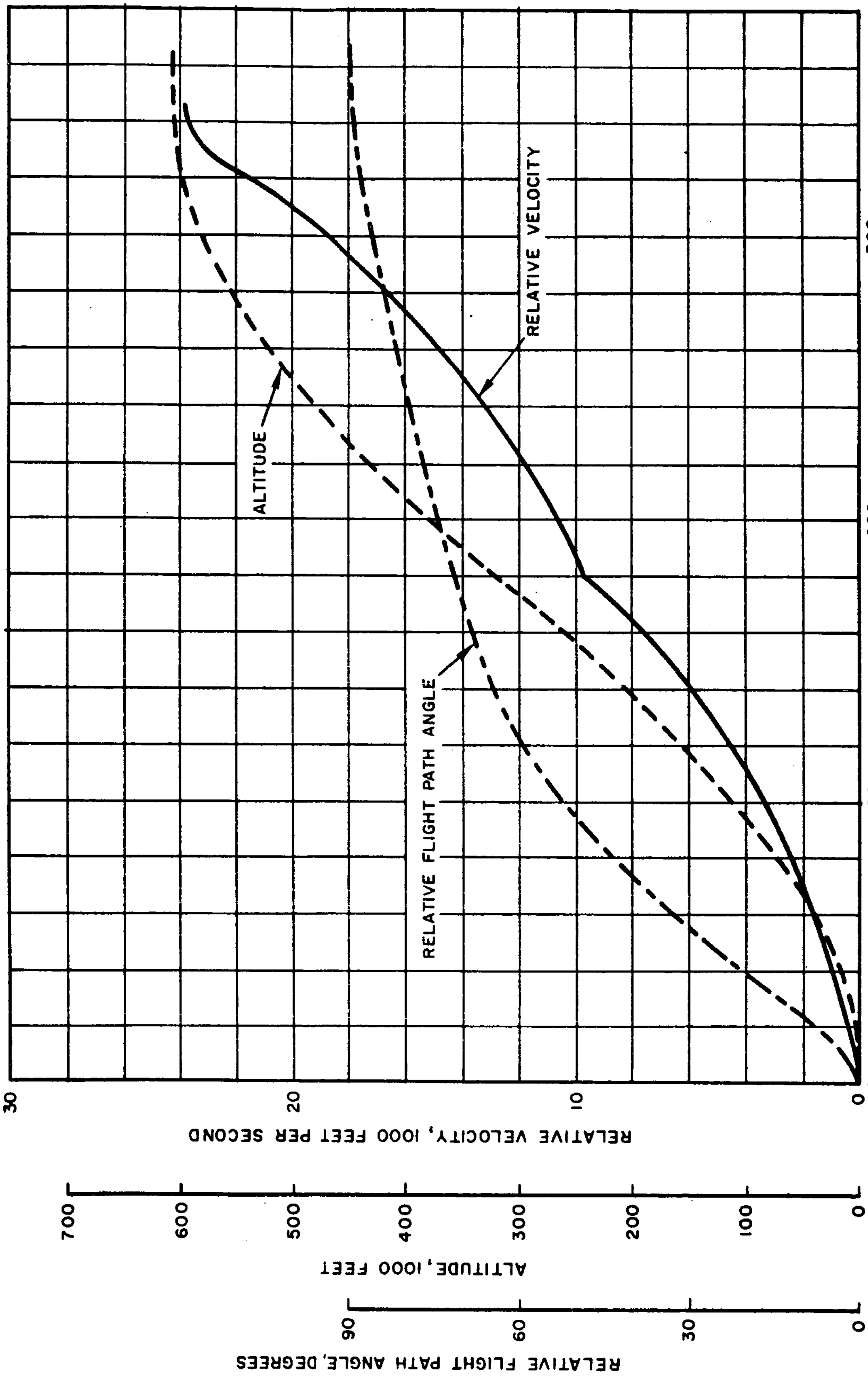

Figure 2.5-8. Aerodynamic Heating Trajectory Parameters.

Table 2-5-I. Aerodynamic Heating for Solid Propellant Nova

Location	Material	Thickness, inches	Maximum Temperature, ^{o}F	Allowable Temperature, ^{o}F
1-2 Interstage Skin	Aluminum	0.25	140	300
3-4 Interstage Skin	Aluminum	0.10	290	300
Step 3 tankage	Steel	0.25	101	300
Step 3 shroud	Aluminum	0.10	150	300

angle each surface makes with the axis of the vehicle. Where this angle is zero, as on the step III tankage or shroud, the local flow was assumed identical to free stream flow. Temperature gradients normal to the surface were ignored. An initial temperature of 80°F was assumed.

The only location which approaches the limit temperature (these are very rough estimates only) is the step III-IV interstage skin. A more realistic aerodynamic heating analysis, using a better estimate for the local flow, would probably give a lower temperature. In any event, the aerodynamic heating near the forward end of the vehicle can be considered as a detail design problem. The fact is that this NOVA trajectory is extremely mild from an aerodynamic heating standpoint; the heating parameter, $\int qvdt$ where q is dynamic pressure and v is velocity, is lower than the values encountered in typical Atlas and Titan trajectories (Figure 2.5-9.)

2.5.4 Base Heating

Base heating due to recirculation of exhaust gasses must be considered as an important problem area, and definite measure must be taken to protect critical areas and components in the base of each of the first three steps. Laboratory and flight experience from Polaris and MINUTEMAN have demonstrated that clustered solid propellant rockets

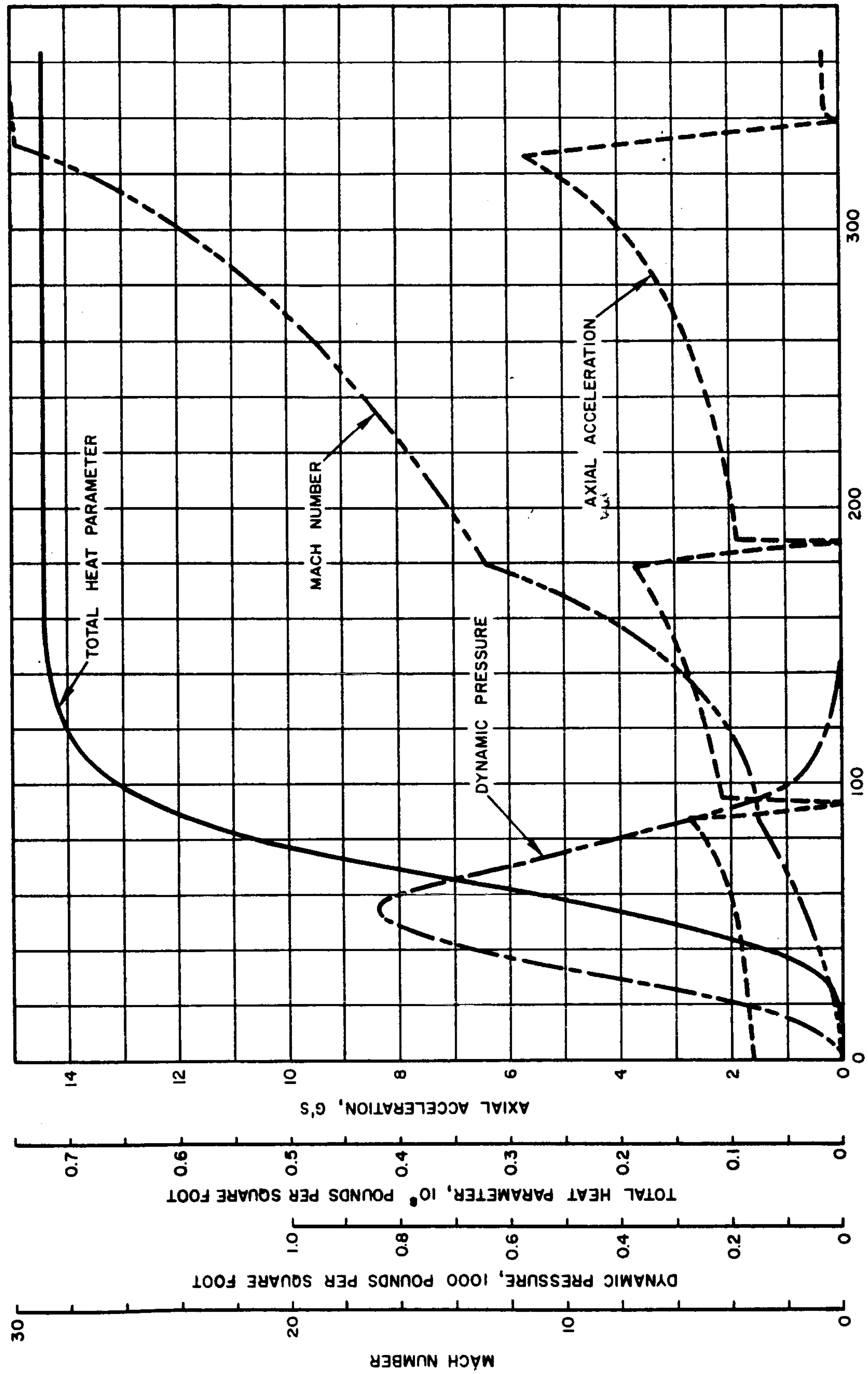

Figure 2.5-9. Estimated Aerodynamic Load and Heating Parameters.

give rise to severe recirculation and intense radiative and convective heating. It is not at all certain that the model test results from Saturn are applicable to a solid propellant NOVA, and it is believed essential to perform scaled hot rocket model tests in an altitude facility in order to establish the thermal environment and determine optimum protective measures. The Minuteman currently uses a heat deflector located between the nozzles and flush with the exit plane. Similar devices seem to be indicated for the all-solid NOVA. On Step I, the individual jets will begin to coalesce at about 80,000 feet, and the base heating rates will rise steeply to some high level as the vehicle rises above this altitude. Below this altitude, the base heat rates will be relatively low. Steps II and III, on the other hand, will experience a nearly uniform, high level of heating.

The importance of the radiant component of base heating must be emphasized. As the reversed exhaust flow encounters the heat deflector, it is forced to escape laterally between the individual nozzles. This gas-particle mixture is at nearly the stagnation temperature; hence any component of the thrust vector control system or any portion of the nozzle exterior or aft closure seeing this lateral stream will receive intense radiant heating. Also, if fairings are used on the interstages and if the stage separation plane is near the nozzle exit plane, the lateral jets of recirculated gases will burn through the skin. This actually occurred during altitude chamber tests of the Minuteman third stage. Either the separation plane must be moved forward or some portion of the interstage fairing must be jettisoned after staging.

The third step of the JPL NOVA configuration (Figure 2.1-1) would present a very critical problem in protection against base recirculation. If a heat shield were used, it would be of the order of 18 feet in diameter and must be designed for a steady-state pressure loading between 0.2 and 0.5 psia resulting from impingement of the recirculated gases. It must also be designed to withstand whatever pressure pulse loading accompanies the staging process; this has not been estimated, but the order of magnitude is believed to be about 10 psia. The alternative to, a heat deflector across the opening between the step III nozzles would be to insulate all surfaces of step III and step IV rockets which will be exposed to the radiant and connective heating.

This particular problem is minimized in the cluster of step III rockets used in the STL version of the solid-propellant NOVA (see Figure 2. 1-2). A series of small deflectors can be used with this configuration in a manner similar to steps I and II.

The fourth step, consisting of a single rocket, will not experience any significant radiant or convective heating from the exhaust plume.

2.5.5 Staging

Staging of multistage ballistic vehicles presents a number of problems in structural, propulsion, performance, and hardware areas. All these, however, can be solved by careful design, analysis, and subscale testing. The following are among the items which must be considered: nozzle-to-dome clearance, requirement for blast ports, location of the separation plane, environment inside the interstage compartment and associated design criteria, staging sequence including thrust level of tailing-off step at initiation of staging, thrust build-up characteristics of ignited step, etc. Gas dynamic analyses of the build-up in pressure in the interstage compartment, together with a dynamic analysis of the motions of the separating bodies, generally yield fairly reliable results for preliminary design. Also, some rules of thumb are available, based on past experience with staging problems to aid the designer. As an example, a nozzle-to-dome distance of one throat diameter is an approximate rule for avoiding severely fluctuating asymetrical flow separation in the nozzle being ignited. On the other hand, with heavy fixed nozzles, the side forces due to flow separation may not be a design condition. It is believed that subscale hot rocket tests should be performed in an altitude facility to provide design data needed to assure an optimum and reliable staging operation. Such tests, performed statically with a mock-up of the retreating stage fixed at successively greater distances from the firing stage, have been successfully carried out for Titan II. They were not only a useful but also an essential part of the Titan II development program.

2.6 VEHICLE STRUCTURE AND DYNAMICS

2.6.1 Structure

The structural feasibility of the JPL proposed solid propellant NOVA injection vehicle concept presented in the referenced reports has been studied. Important aspects considered include design concepts, design criteria, loads, weights, fabrication and assembly techniques, development requirements, production facilities, schedules, and costs for the primary structure. Time prevented any serious consideration of secondary structures. No attempt was made to establish optimum design approaches through detailed studies, but estimates of the effects of a 40 percent increase in gross weight were considered. The main results of and conclusions drawn from the investigation of structural feasibility of the concept are briefly summarized below. Additional details are discussed later.

Some of the specific detail design concepts and fabrication practices recommended in the report are believed to be undesirable; for example, the concept of applying large concentrated loads to the engine case membranes through welded structural attachments. However, it is believed that technically acceptable alternatives for all such features exist which are consistent with the basic conservative philosophy desired for design and development. Therefore it has been concluded that the design, fabrication, and assembly of the structural hardware for the design concept is technically feasible using conservative practices based on current technology. The development schedule for the structure indicated in the report does not appear to be unreasonable. Some extensions of the present state-of-the-art in large engine case and nozzle design fabrication will be required, but it appears that the validity of the vehicle concept does not depend on achieving optimum or unusually efficient structures. Thus, a vehicle structure sized conservatively may also in the end possess an inherent growth potential of great value.

In general, the loads criteria employed in the study are believed to be conservative, and the resulting interstage structural weights are not unreasonable even for considerable variations in structural philosophy, including integration of interstage structures and aerodynamic fairings. Such fairings are believed to be required during first stage operation; the feasibility of jettisoning forward interstage fairings after first stage separation (as indicated in the report) has not been established, and it is recommended that the vehicle concept and sizing not be made dependent on this feature if possible. It may be noted that the reported weight estimate neglected step I launch support structure, a possible design for which has been estimated to weight about 95,000 pounds for the 25 million pound vehicle and about 130,000 pounds for the 35 million pound vehicle.

The cost of the structural hardware required for this program as shown in the JPL report is believed to be underestimated for the 25 million pound vehicle, and it is recommended that commulative average costs of at least 10 dollars per pound should be used, for estimating all the primary structure metal parts (including rocket cases). (Even this figure should be optimistic unless unusually competent and integrated engineering, production, and management capabilities are brought to bear.) The major hardware cost underestimation in the report appears to be for the engine cases, which are also the major structural cost item.

Facility requirements for engine case manufacture do not appear unreasonable, but contrary to what is stated in the report, additional roll-ring forging facilities might be required for this program, not only to support the sustained volume output required, but also to circumvent the possibility of delayed transportation from the north during severe winter months. This is particularly important if Ladish, in the Great Lakes area (Cudahy, Wisconsin) is envisioned as a major supplier of roll-ring forgings. However, if a new facility for roll forming (either supplementary or as principal supplier) were built nearer the assembly plant, this would be felt not only as an additional facilities cost but also probably as higher cost per pound for case hardware, due to higher intangible costs.

Schedules for facility development indicated in the report do not appear to be unreasonable. However, considerable ingenuity will be required in extending existing state-of-the-art in developing large machine tools for shear spinning. It should be noted that achieving low hardware cost is critically dependent on successfully shear spinning the large roll-ring forgings into longer "sleeves," resulting both in maximizing the yield of finished weight per pound of raw material, and in minimizing the number of welds required in assembly.

2.6.1.1 Design Loads and Criteria

2.6.1.1.1 Flight Loads. Load estimates based on JPL assumed design conditions have been made and it appears that the interstage loads so derived are quite conservative, except possibly in the III-IV interstage region. However, these latter loads will not materially affect the structural weights used in the analysis. The loads near the forward end of the vehicle are quite dependent on the aerodynamic properties of step IV; hence it is virtually impossible at this time to estimate these loads accurately.

The JPL weight estimates were based on loads data derived from the following condition (Reference 2, Page 18).

Axial load	6.0 g
Transverse load (bottom)	0.2 g
Transverse load (top)	1.0 g

The axial load factor exceeds present estimates of the burnout accelerations and is conservative. The transverse load factors are estimates that include aerodynamic loading and are assumed to vary linearly along the vehicle. It was conservatively assumed that the maximum axial and transverse loads occur simultaneously. For interest, the JPL loads at the interstages are compared with STL estimates in Figure 2.6-1.

The maximum dynamic pressure loads are based on $n_{axial} = 2.5$ g's, STL drag estimates, and the JPL normal aerodynamic force data presented in Reference 2, Page 118. The first stage burnout loads are based on $n_{axial} = 6.0$ g's and an assumed lateral acceleration of 0.3 g's.

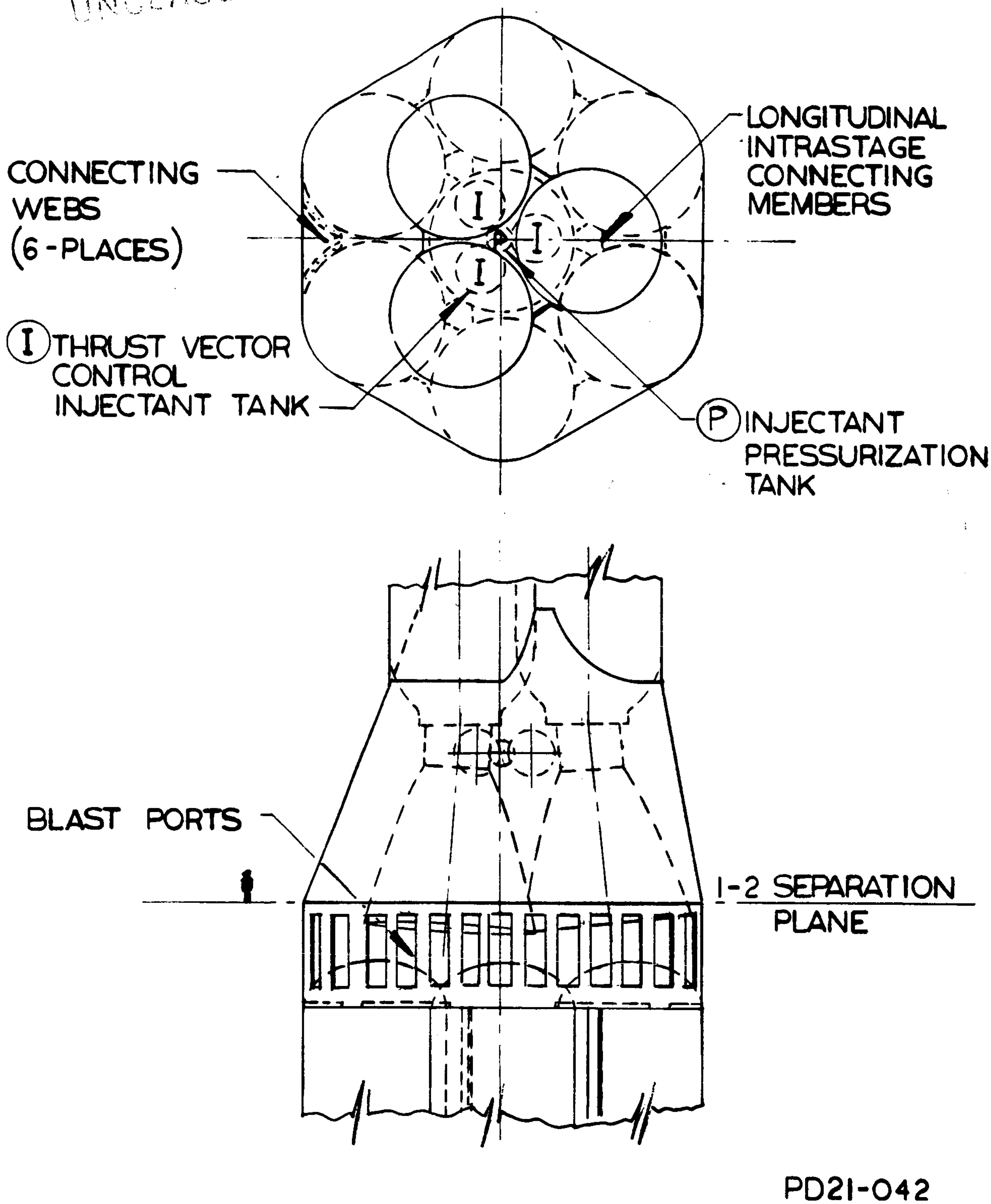

Figure 2.6-1. Interstage Structure, Step I-II, Design 1.

Table 2.6-I also shows the STL load estimates for large version of the NOVA (35,000,000 pounds liftoff weight).

It is apparent from the P_{EQ} column in Table 2.6-I that the axial load provides the major contribution to the total load at the interstages. This would tend to minimize the influence of variations in normal force, center of pressure, and control force on the design loads for the interstages.

2.6.1.1.2 Ground Handling. The points presented by JPL with respect to ground handling loads are extremely important. Because of the size of the vehicle and structural components, it may not be economical to design all ground support, transportation, handling and assembly equipment so that the handling or transportation loads are below the flight loads. In general, it is very desirable to avoid penalizing the vehicle structure for ground conditions. However, there may be instances (which should be minimized as much as possible) where it may be necessary to design to ground conditions even though this philosophy is contrary to most missile or space booster design experience.

If the vehicle performance margin is large enough, it could be economical—in the long run—to allow ground conditions to design some structural components.

2.6.1.1.3 Safety Factor. The ultimate factor of safety used by JPL for design of the interstage is 1.25. STL concurs with the use of this factor for major structural components. It must be recognized that if arbitrarily larger safety factors are imposed on man-rated vehicles, structural weights will increase accordingly.

2.6.1.1.4 Aerodynamic Heating. Aerodynamic heating of the interstage structures and engine cases has been estimated (see Section 2.5) and should not be a problem. This results primarily from the fact that the vehicle is relatively slowly accelerated and because of the great heat sink provided by these structures.

2.6.1.1.5 Conclusions and Recommendations. In general, it can be stated that load computation for a vehicle of the NOVA size is within the state-of-the-art. The major inputs that must be defined early in the design phase

Table 2.6-I. Solid NOVA Loads Summary (Limit Loads)

Vehicle	25,000,000 Pounds			25,000,000 Pounds			25,000,000 Pounds		
Condition	JPL Design Condition			STL Max q			STL I BECO		
Location of Structure	P (kips)	M (in-kips)	P_{EQ} (kips)	P (kips)	M (in-kips)	P_{EQ} (kips)	P (kips)	M (in-kips)	P_{EQ} (kips)
Aft III-IV Fairing R = 348 inches	4,600	384,000	6,800	5,860	428,000	8,320	2,304	50,000	2,591
Aft II-III Interstage R = 348 inches	19,200	1,640,000	28,620	11,630	744,000	15,906	16,151	280,000	17,761
Aft I-II Interstage R = 462 inches	63,000	5,350,000	86,200	31,697	504,000	33,877	56,151	2,100,000	65,251

Vehicle	35,000,000 Pounds			35,000,000 Pounds		
Condition	STL Max q			STL I BECO		
Location of Structure	P (kips)	M (in-kips)	P_{EQ} (kips)	P (kips)	M (in-kips)	P_{EQ} (kips)
Aft III-IV Fairing R = 348 inches	7,821	470,000	10,521	2,304	50,000	2,591
Aft II-III Interstage R = 348 inches	13,591	735,000	17,811	16,150	250,000	17,590
Aft I-II Interstage R = 462 inches	41,741	795,000	45,181	56,150	2,900,000	68,650

include aerodynamic properties, thrust-time histories, and ground handling and assembly criteria. It is believed that a fairly conservative design approach can be employed to arrive at design loads. It is expected that only a moderate portion of the vehicle structure will be designed by external flight loads; hence, a very conservative design approach should not significantly affect the vehicle performance (payload) capability.

2.6.1.2 Interstage and Intrastage Structures

2.6.1.2.1 Designs Studied. Two alternative designs to those shown in the JPL report were studied for the step I-II interstage structure, two designs for the step II-III interstage structure, and one design for the step III-IV interstage structure.

The first step I-II interstage design (Figure 2.6-1) has a cylindrical structure extending forward from the step I rocket engine cases to the separation plane. This structure has open blast ports located around the cylinder to relieve nozzle back pressures at step II motor ignition. A conical stiffened sheet metal structure extends forward from the separation plane to the aft skirts of the step II rocket cases. The outside motors of step I are tied together by six shear plates located around the skirts of the rocket motors, and the center motor is connected to the outer motors in the cluster by longitudinal shear ties at the skirts. In this design, the structure also serves as an aerodynamic fairing between the two steps.

The second step I-II interstage design (Figure 2.6-2) has a sheet metal structure, containing blast ports, which wrap around three of the outside step I rocket motor upper skirts, and extends forward to the separation plane. In view from above, this structure forms a triangular shape which closely matches the shape of the step II rocket motor cluster, and a conical stiffened sheet metal structure extends forward from the separation plane to pickup the aft skirts of the step II rocket cases. The remaining three outer step I rocket cases are supported by intrastage shear ties, and the axial load is distributed through the conical structures which attack to to the main interstage structure. The center step I rocket motor is attached

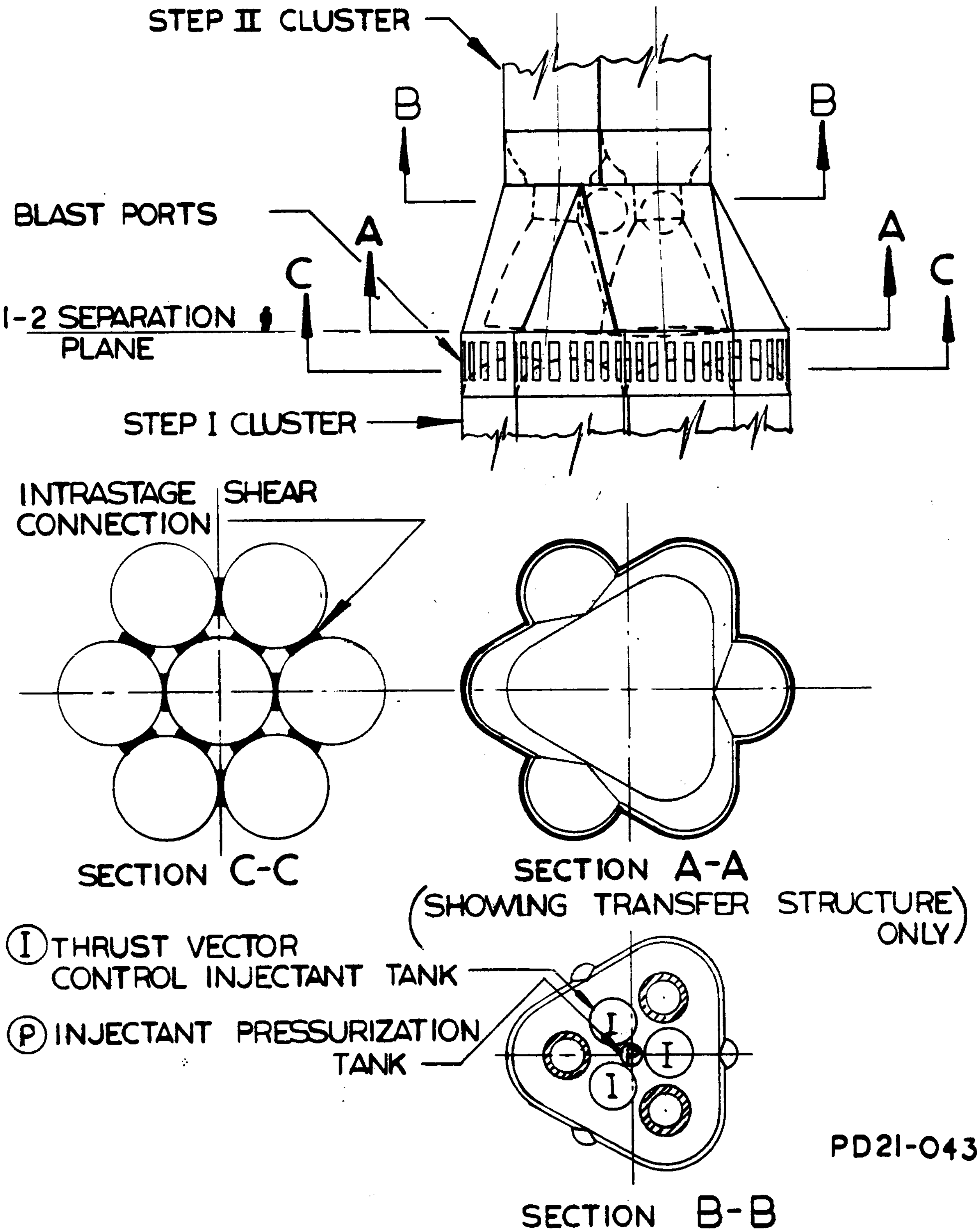

Figure 2.6-2. Interstage Structure, Step I-II, Design 2.

to the outer rocket motors by shear connections at the fore and aft skirts. This interstage structure provides a better load path than the first design and distributes the loads around a larger portion of the step I rocket motors.

One type of step II-III interstage structure studied is shown in Figure 2.6-3. With this method, a structural skirt from the cases of the three step II motors continues up to the separation plane. This section contains open blast ports to relieve the pressures at step III motor ignition. Three shear attachments join the step II motors together at the upper end. An interstage structure blends the envelope shape of the three step II motor cases at the separation plane into the shape of the six clustered step III motors at the aft end of their cylindrical section.

The other type of step II-III interstage studied is shown in Figure 2.6-4. The method used here is similar to the one described above, the only difference being the clustering of the six step III motors in a circular pattern instead of the triangular pattern used previously.

The step III-IV interstage is shown in Figure 2.6-5. The six step III motors are joined together with shear ties located on short skirt extensions of the cylindrical motor cases. The lower portion of the conical interstage structure also attaches to these skirts. The interstage structure blends the shape of the six clustered step III motors into the circular shape of the single step IV motor at its aft skirt. Blast ports are not provided in this interstage section, since separation of the two steps is achieved by using the step IV vernier system. A separation plane located further forward would be desirable, but the position shown is necessary so that the vernier thrust chambers can be located far enough aft to prevent impingement of their exhaust gases on the step IV nozzle. Further study of this area is necessary to optimize the design.

2.6.1.2.2 Materials. The interstage structure and most of the intrastage structure will be designed on the basis of buckling considerations. Both aluminum and steel were studied and it is believed that while steel could be used, a heat treated aluminum alloy, such as 2014-T6, will provide a more

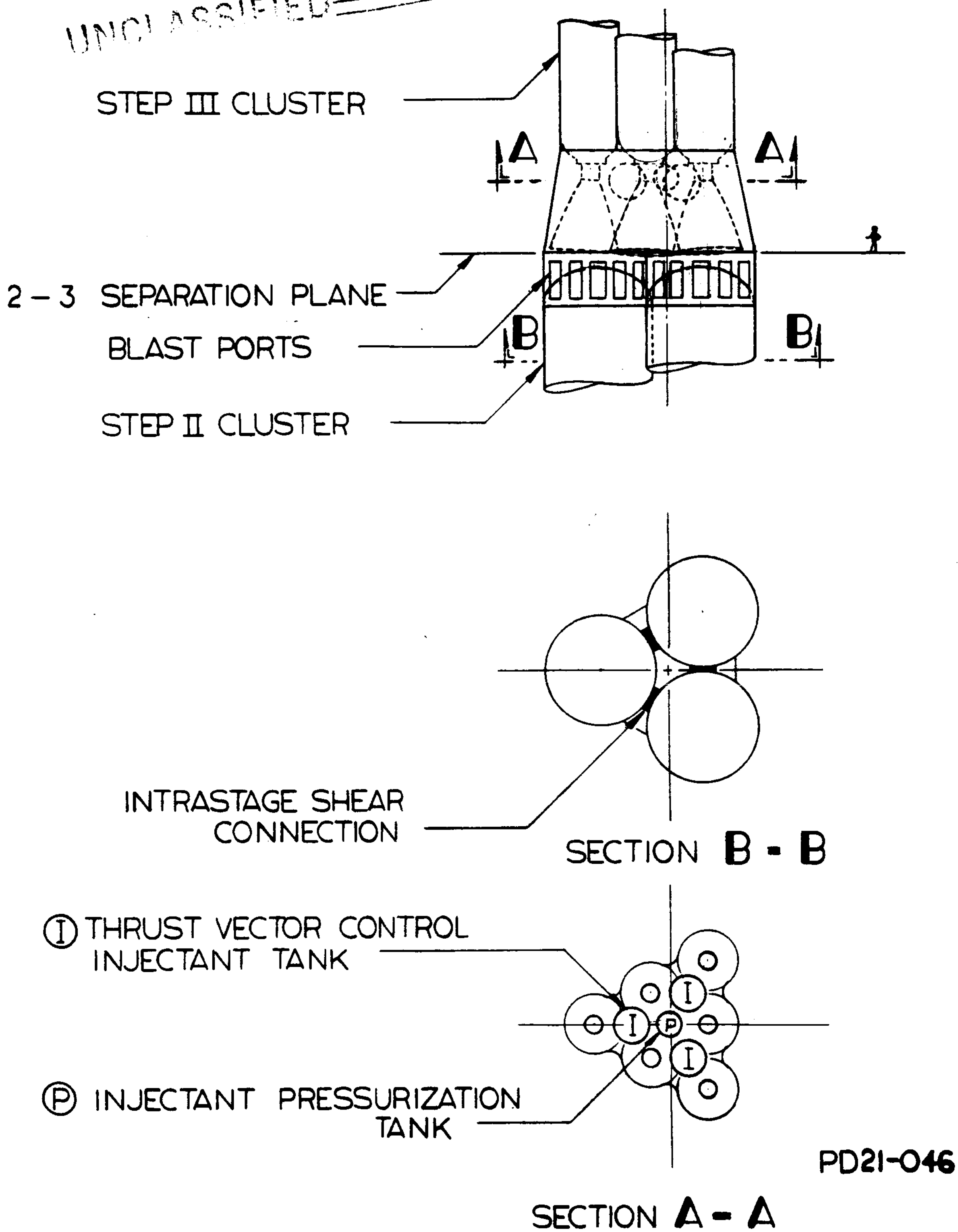

Figure 2.6-3. Interstage Structure, Step II-III, Design 1

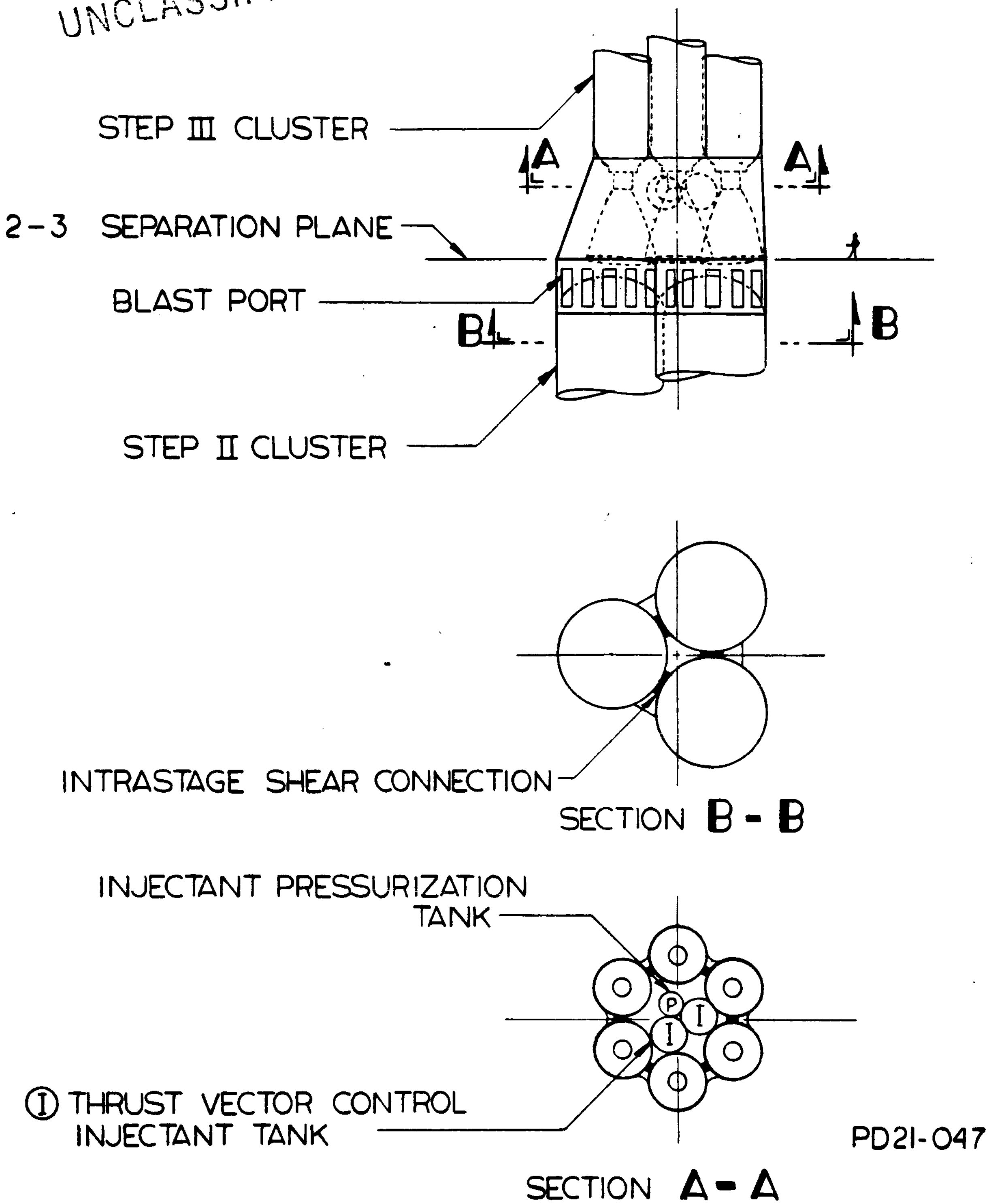

Figure 2.6-4. Interstage Structure, Step II-III, Design 2.

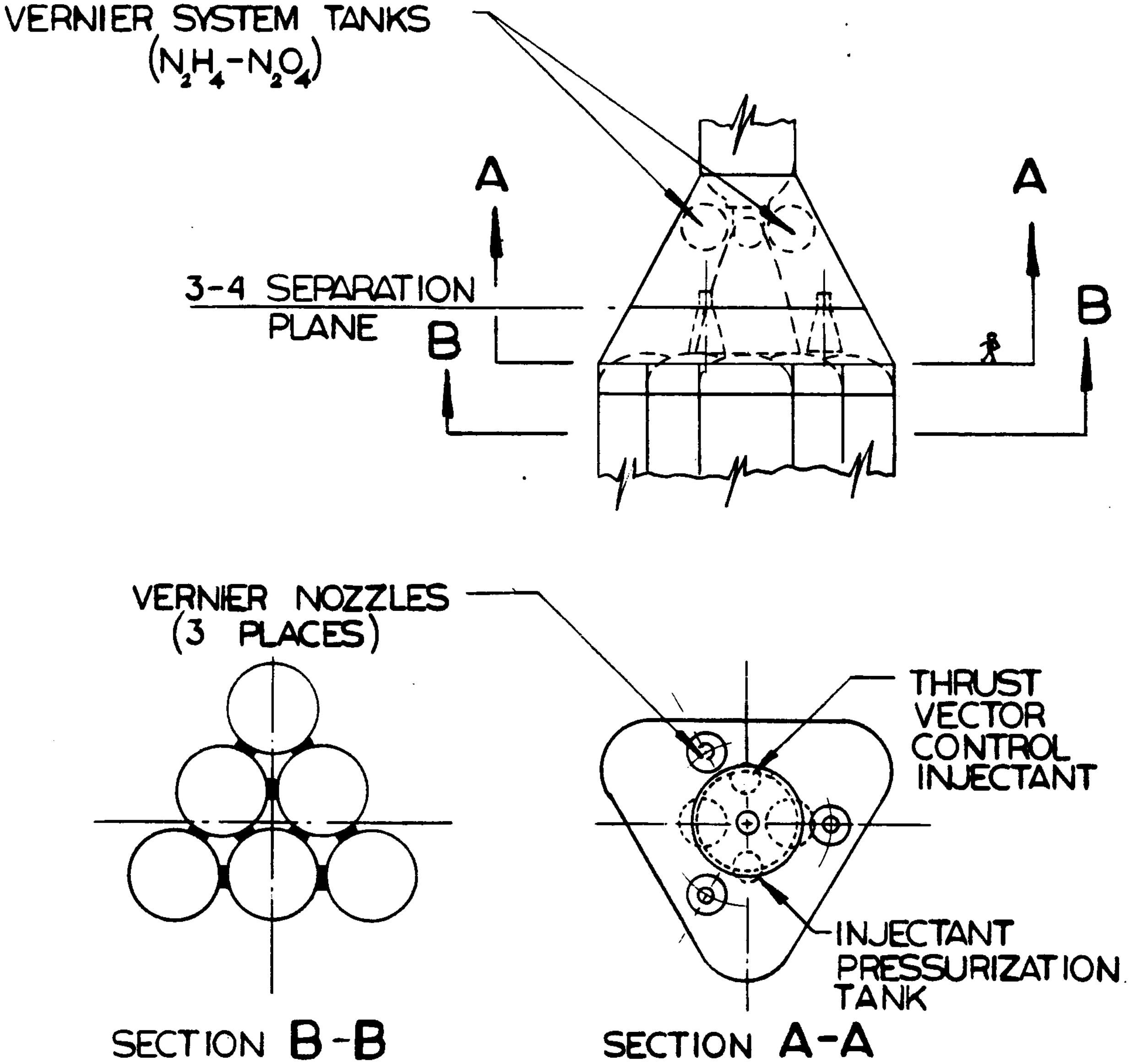

PD21-048

Figure 2.6-5. Interstage Structure, Step III-IV.

efficient structure with more reasonably configured structural members. If aluminum is considered rather than steel, the stringers are less susceptible to local crippling or column buckling and the thicker skin panels are less susceptible to panel flutter.

Preliminary cost estimates indicate that an aluminum interstage structure would be less expensive to produce and assemble than one of steel. Aluminum can be easily machined in a heat treated condition. Critical dimensions should be easier to control in a riveted aluminum structure than in a welded steel structure.

2.6.1.2.3 Load Paths. JPL suggested two methods for transmission of loads between step I and step II. The method presented in Figure 7 of Reference 2 appears to be undesirable on the basis that it results in large radial kick loads in addition to large concentrated axial loads which would be detrimental to the step I engine cases weight.

The method presented in Figure 8 of Reference 2 is somewhat better but it still transmits highly concentrated loads. In addition, an aerodynamic fairing is believed to be necessary and would require considerable additional weight. Thus, a concentrated load transmission system was found to be undesirable when compared with a structural fairing.

Lugs, clips, or stringers should not be welded to the motor cases to transmit primary loads because of stress concentrations, material degradation, and cost. A far better solution lies in the utilization of skirts at the ends of the cases to which shear webs, stringers, brackets, etc., can be riveted in a conventional manner (i.e., Minuteman practice). This would also permit prefabrication of the intrastage and interstage structures and should significantly reduce the assembly time. The load transfer into the cases would be more uniform and reinforcements should not be necessary to provide for point loads as would be the case for the configurations shown in the JPL study. This concept permits the interconnection of the cases during assembly and would reduce the amount of temporary bracing required.

It was found that a structural fairing between step I and II could be used to transfer loads more uniformly into the step I and II cases. Peak compression stresses are approximately 40,000 psi. A cursory check of step II case buckling was made for the assumed 6 g axial load factor. Average compressive stresses would be quite low, but the effects of the expected nonuniform loading are at this time not amenable to analysis. This particular question would have to be studied in greater detail to establish whether or not it could be a critical condition.

2.6.1.2.4 <u>Stiffnesses.</u> Estimates of step and interstage stiffness were obtained from JPL for the 25 million pound vehicle. These data re compared below in Table 2.6-II with independent calculations.

Table 2.6-II. Comparison of Step and Interstage Stiffness

	JPL Data		STL Calculation	
Interstage	A in^2	I in^4	A in^2	I in^4
I - II	500	10×10^6	500	8 to 27×10^6
II - III	200	0.5×10^6	200	0.5 to 1.0×10^6
III - IV	—	—	—	— 0.2×10^6
	JPL Data		STL Calculation	
Step (Engine Cases)	A in^2	I in^4	A in^2	I in^4
I	6300	63×10^6	4950	55×10^6 min
II	2700	27×10^6	2120	24×10^6 min
III	—	—	—	—

The STL estimates for the interstage moments of inertia are presented as a range, thus indicating the effect of going from a truss type interstage to a structural fairing with a greater effective radius. (The dynamic studies were performed using the STL data.) It can be seen that the use of a structural fairing rather markedly improves the bending stiffness in the interstages.

The JPL estimates of the moments of inertia for the engine cases are about 10 percent greater than that which is obtained if it is assumed that each engine case bends independently with no shear transfer to the adjacent case. The JPL data were used as a reasonable lower bound for the dynamic studies.

Shear stiffnesses were permitted to range from ∞ down to KAG with K = 0.5. It could be argued that K will be lower for the engine cases if they are attached to one another only at the ends, but a much more detailed analysis would be necessary to properly establish a lower value. For the range studied, shear stiffness was unimportant and it is believed that this will remain true because of the relatively short engine cases.

2.6.1.2.5 Recommended Design for Intrastage and Interstage. The use of a structural fairing was found to be quite feasible if a conventional ring-stringer, buckling skin configuration is used. This type of structure has been used in numerous programs with considerable success. A stiffened cylindrical aluminum skirt would be riveted to a short steel cylindrical skirt on each engine case. The length of the steel skirt must be sufficient to permit a transfer of shear from one case to another and to properly distribute the loads from the concentrated stringers into the engine case.

An analysis was performed to estimate the size of a stringer in the step I-II interstage. It was found that the configuration shown in Figure 2.6-6 would be structurally adequate and that the weight would fall within the JPL estimate. Three or four rings (including the separation frame) would be required to limit the lengths of the columns. It can be seen that the members are of a size which is well within present technology. No significant problems are anticipated in the design of this structure.

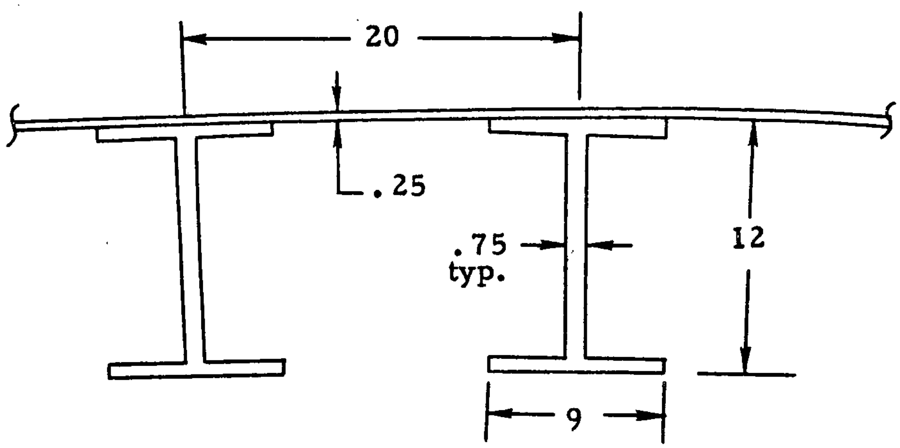

Figure 2.6-6. Typical Skin-Stringer Panel Step I-II Interstage, 35×10^6 Pound Vehicle

2.6.1.3 Vehicle Support Structure

The JPL report omits any mention of vehicle support structure. Some vehicle assembly and launch requirements clearly dictate that some structure be provided, the effect of such a structure on the vehicle must be examined. With closely clustered tanks and large nozzles of the step I motors a clearance problem may exist if the vehicle were to fly out of a fixed support structure permanently attached to the launch pad instead of the vehicle. Realizing then, that a major portion of the vehicle support structure would have to be permanently mounted to the vehicle, two designs were considered.

The first design considered as a support structure with uniform load distribution at the structure-pad interface (Figure 2.6-7). This structure

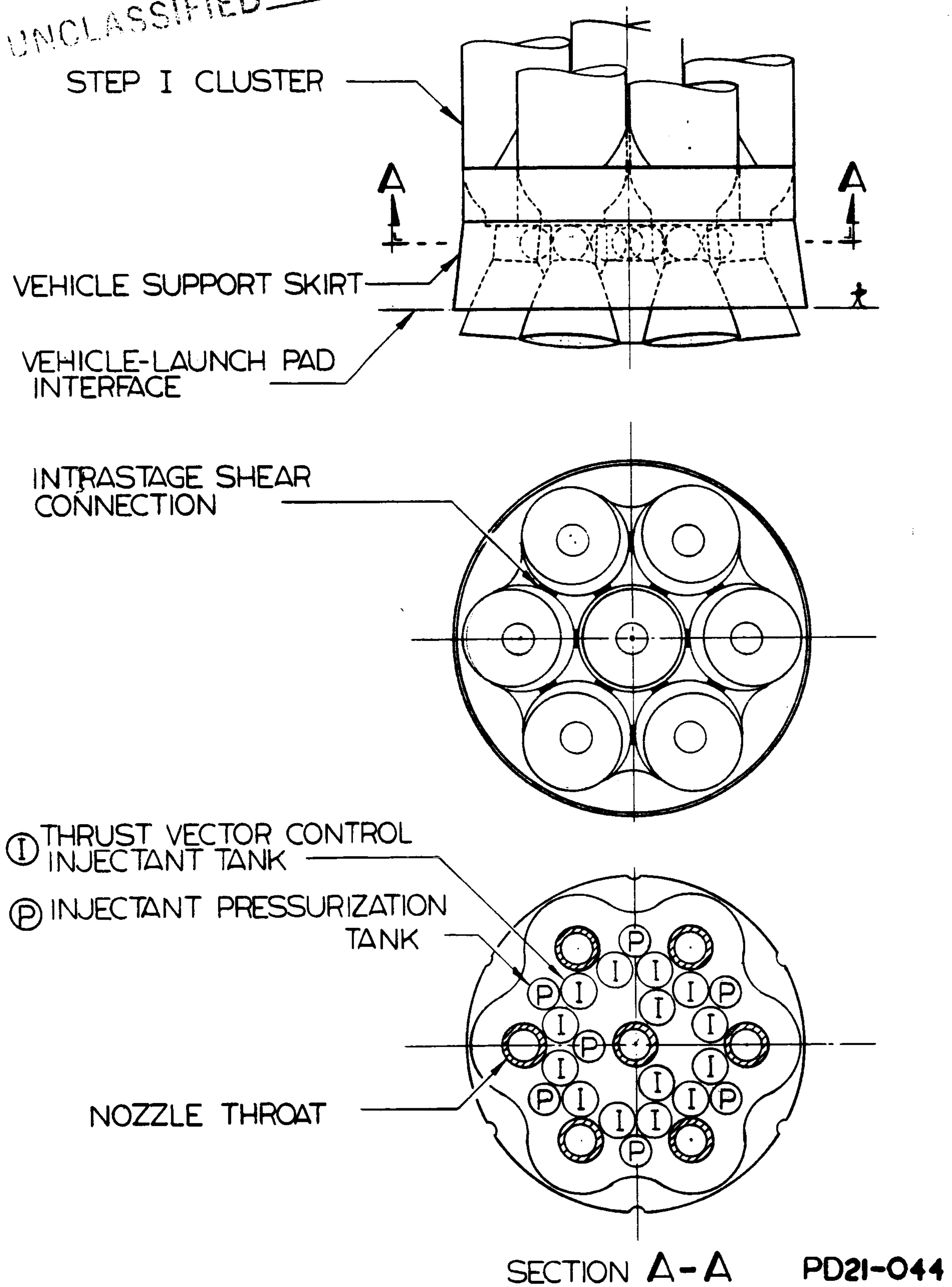

Figure 2.6-7. Vehicle Support Structure, Distributed Load Type.

distributes the vehicle dead load uniformly from the structure-pad interface to a portion of the aft skirts of the six outer rocket cases. The skin of this support structure is formed so as to fair from a circular section at the launch pad interface to a scalloped section at the aft skirts of the rocket motors. The center rocket is attached to the outer rockets by the intrastage shear connections. The skin of this structure is made of a low density material such as aluminum alloy or magnesium alloy to increase buckling efficiency. Valves, plumbing, etc., for the liquid injection system are partially supported by the structure.

The second design considered is a support structure with concentrated load points at the structure-pad interface (Figure 2.6-8). This structure is basically the same as that discussed above except that the loads from the skirts of the rocket cases are redistributed to six concentrated load points at the structure-pad interface. With six concentrated load points to carry the vehicle dead weight, some means to assure equal loads at each point must be provided so that a weight penalty will not be imposed on the structure if a structural failure and possible severe damage to the missile is to be avoided.

Both of these structures are feasible and can be built by present fabrication techniques. Further design study would be necessary to produce an optimum support structure.

An estimate of the strength requirements and weight was made for the six point support design. Heat treated aluminum stringers, skin, and frames of conventional design would be employed, in design quite similar to the step I-II interstage structure. Approximate weight estimates, based on conservative working stresses, indicate approximately 100,000 pounds is required for the 25 million pound vehicle and approximately 130,000 pounds for the 35 million pound vehicle.

2.6.1.4 Engine Cases

2.6.1.4.1 Basic Philosophy. The weight of the engine cases for one vehicle is nearly 1.5 million pounds, in about 60 percent of the entire inert weight of

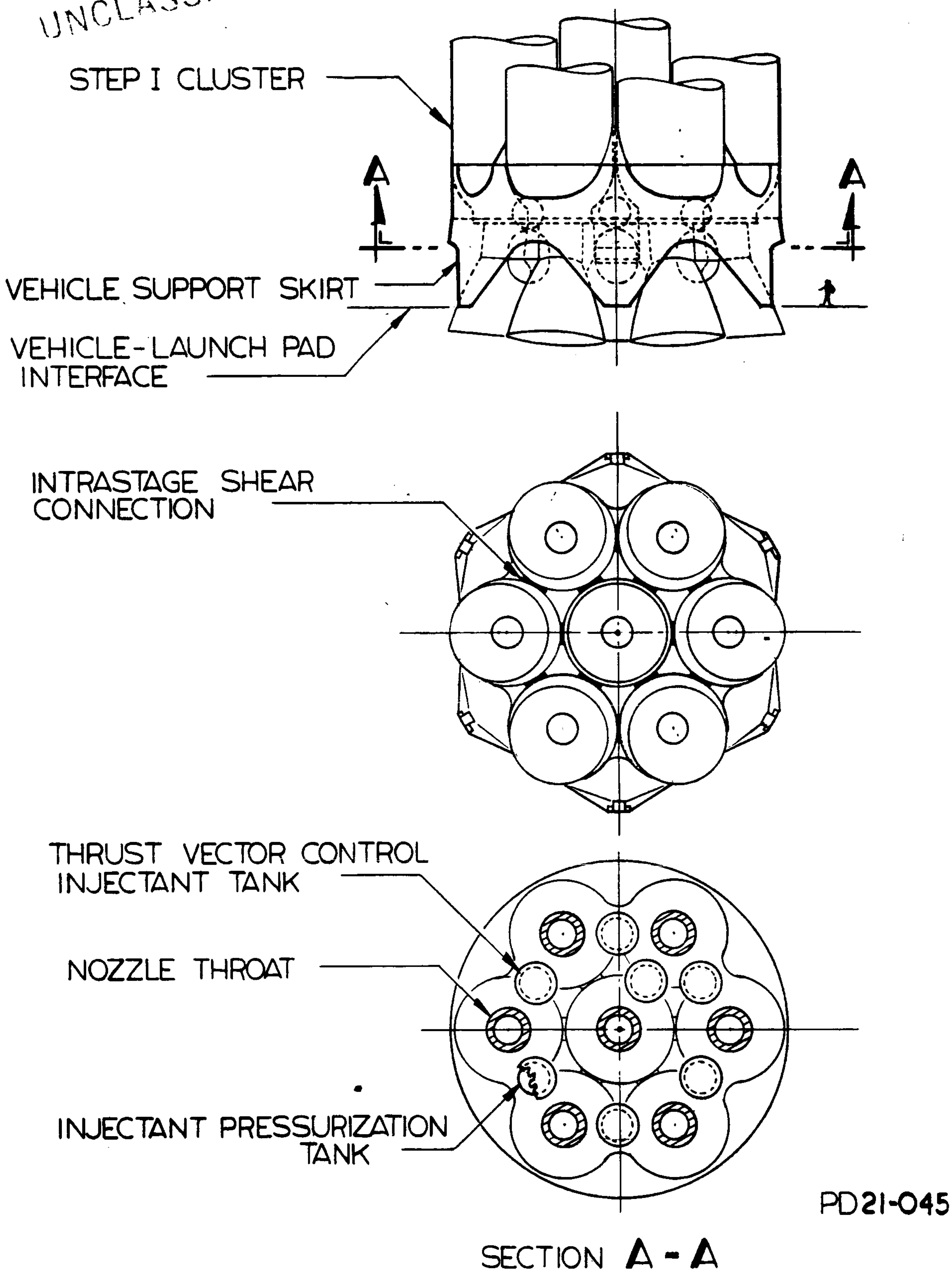

Figure 2.6-8. Vehicle Support Structure, Multiple Point Support.

the 25 million pound vehicle. Each Type A engine case weighs about 140,000 pounds (roughly seventy times the weight of the Minuteman first stage case) and nearly 200,000 pounds each for the 35 million pound vehicle. Costs of the initial Type A motor cases would run several million dollars each, and any hardware of this price demands special consideration. The cost of excessive development effort and of rejects in production could become a major program cost, proportionally larger than in any other program, past or present, and enormous in an absolute sense. The cost of unreliable case performance in flight is simply untenable.

It is important to appreciate at the outset that despite their large size, these cases are highly efficient pressure vessels designed to a small factor of safety in order to achieve the desired mass fractions, and that there is no justification for assuming that because they are large they may be accorded any less serious attention to important design detail than their smaller counterparts in current programs. If any difference exists between these and smaller cases of comparable design, it might easily be that the large cases are more sensitive to defects and stress concentrations, and therefore must be treated with additional respect.

All the foregoing considerations confirm the necessity for employing JPL's indicated fundamental design philosophy of basic design simplicity and conservatism to avoid excessively time consuming and costly development programs, as well as avoiding any practices which would result in doubtful reliability. Despite the stated philosophy, it is believed that some of the detailed design and fabrication practices described in the reference are unconservative, specifically the recommended practices of applying large concentrated loads to the case membranes, and of welding structures directly to the case membranes to effect such load transmission. Experience in several programs has produced convincing evidence that these practices must be avoided if any measure of success and reliability is to be achieved. Super-imposing extremely large and complex stress concentrations with metallurgical discontinuities by using a welded attachment method which is basically quite variable and incapable of adequate inspection, and for which there can be no adequate proof test, is an untenable combination in a program of this importance, urgency, and cost.

Fortunately, the intrastage and interstage transmission of loads need not depend on this approach. As described earlier, more conventional attachments to integral case skirt extensions are feasible, and this is the recommended solution to the problem. Welding of the cases should be limited to circumferential welds for the joining of segments, knuckle joints, domes, etc.

2.6.1.4.2 Materials and Allowables. The selection of a moderately high strength steel for the cases is appropriate, but only steels of high cleanliness and homogeneity should be used. Such a steel is Ladish D6AC, as used in Minuteman cases. The technology for this steel at moderate strength levels is well developed, and the superiority of a vacuum melted steel such as this over high quality aircraft grades of air melted steels of similar strength capabilities lies principally in the greater uniformity and superiority of properties, particularly in biaxial stress fields, and will be reflected in greater reliability. It is recommended that vacuum melted steel be used here even if it were not priced as low per pound as high quality air melt aircraft grade steels; however, at this time there is no significant difference in price, and this should continue to be so. The present industrial capacity for vacuum melted steel should be adequate for the development part of the program, but would undoubtedly have to be expanded to meet the production rate. This would be relatively inexpensive, and could probably be expected to be financed by industry rather than by government facilities money.

Present Minuteman working stresses in D6AC are 10 percent greater than the 165 ksi value recommended in the report. Although there is no evidence to show that the present Minuteman strength level (225 ksi burst), factor of safety (1.25), and working stress (180 ksi) would be unsafe to use in cases of significantly greater wall thickness than Minuteman (6 times as great), any size effects would be determined in the subscale (development) test program in time to influence the final design. To be conservative, 165 ksi working stress seems reasonable now for initial sizing and weight estimates, keeping in mind that even a few percent increase in working stress produces a significant performance gain.

The possibility of employing significantly larger allowable stresses than those used on Minuteman could not seriously be contemplated without considerable development testing and experience with presently unknown factors associated with very large cases. Significant changes in fabrication techniques would undoubtedly be required, and it is doubtful if any welding at all should be used with significantly higher allowables.

2.6.1.4.3 Detail Design and Fabrication. Fabrication of the cylindrical sections should be done from roll ring forgings, as suggested in the report, in order to eliminate longitudinal welds which have always constituted a major development problem and source of trouble. Cylindrical segments can be machined to final size from the forgings, or hydrospun to net wall thickness thereby elongating each segment and reducing the number of circumferential joints. Hydrospinning would probably effect significant savings in raw material and machining costs as well, and it is believed the net cost per pound of finished hardware would be reduced by this approach.

Circumferential joints could be welded or bolted, and certain advantages and disadvantages are apparent for each method. It is not possible to state firmly at this time which approach should be employed, and considerable additional study of the overall requirements and consequences should be made. If other considerations should finally require that the motors be segmented, then obviously bolted joints would be employed. Bolted joints would naturally provide for attaching interconnecting and secondary structures, as well as temporary work platforms (which in no event should be welded to the case membrane), and local reduction of allowables due to welding after heat treatment would be avoided. Furthermore, the use of nonwelded assemblies would make the use of significantly higher allowable and working stresses more feasible.

Present Minuteman case practice includes heat treatment of the entire case after welding. Serious consideration of this philosophy should also be made for these cases. The alternative approach with welding after heat treatment of detail parts is to accept the local reduction of allowable in the weld zone and to use appropriate local reinforcement thickening as determined from development tests. If welding is performed after heat treatment, additional local post weld treatment of the weld zone will undoubtedly be required to develop a soft and ductile weld. Development testing to determine the requirements and techniques would be mandatory.

One piece heads appear to be feasible, and should be employed to avoid welding. Blanks from which heads would be spun could be obtained from opened and flattened tubes 10 feet in diameter and 30 feet long. These tubes would be formed by hydrospinning roll ring forgings. Some machining prior to spinning might be done to tailor the thickness and to provide for the igniter boss and edge reinforcement as required. The amount of material for each head is roughly the same as for each of the segments going into the cylinder assembly.

The method of assembling domes to cylindrical sections requires additional study, but in any event a short, integral cylindrical skirt should be provided to accept loads, as discussed previously. One approach is to use a separate Y joint made from a roll ring forging, another would be to form a similar joint integrally with either the cylinder or the dome.

2.6.1.4.4 Facilities. The facilities cost estimates in the report appear to be reasonable, but it is believed that the rate of production may require additional equipment or tooling. It appears that the shear forming equipment for cylindrical segments would require significant advances in current state-of-the-art, and the development of this tooling would demand ingenious solutions to many problems. However, it is believed entirely feasible, even if costly.

Additional roll-ring forging capacity would be required, contrary to what is stated in the JPL report, to sustain the desired volume and to provide a hedge against possible delays in transportation from the north in winter, when, for example, navigation on the Great Lakes may be weather limited. This is appropriate to consider if the Ladish Co., at Cudahy, Wisconsin, is a potential supplier of roll ring forgings. They are one of only a very few concerns capable at this time of supplying these large forgings. If additional facilities are developed in the south, nearer the engine case fabrication facility, costs for the hardware could be expected to rise due to overhead and shakedown of a new facility. This matter should receive further consideration.

As mentioned before, additional vacuum melt capacity is required for the production runs, but would probably not represent a tangible program cost.

The heat treatment facility costs indicated in the JPL report would be low by about a factor of two if entire engine cases were heat treated.

2.6.1.5 Liquid Injection System

Although the structural problems involved in this system were not studied in detail, a few observations are pertinent.

The spherical, cylindrical, and/or toroidal pressure vessels for containing the liquids and gases are of major concern, and their development problems should not be glossed over nor permitted to become obscured simply by the magnitude of the development problems for the large engine cases. The tank weights for step I alone are between 5 and 10 times the weight (depending on allowables and safety factors) of all the pressurized structure in the largest current ballistic missile. The weights indicated in the report appear to be based on the same material and allowables used in the engine cases. There appear to be no new facility requirements for their fabrication, and several materials are feasible. Development costs and cost per pound estimates shown in the JPL report appear reasonable.

A problem of some importance is the manner in which these tanks are supported in the vehicle. Considerable study would be required to select the proper manner in detail in order to permit a logical assembly sequence and rational load paths. It appears feasible to consider supporting the tanks off the intrastage structures and engine case skirts.

2.6.2 Structural Dynamics

In present boosters, critical dynamic load conditions are due to winds, thrust rise transients, transonic buffeting, and other phenomena associated with the overall dynamic response of the vehicle. In the large solid propellant NOVA class booster, because of the scaling effects pointed out in the JPL study (Reference 2) and the moderate axial accelerations, the elastic response problem associated with the overall vehicle are less important and do not affect system feasibility. The more critical problems are associated with various local loading conditions. Specifically, the conditions which have been considered are:

a) Local acoustic effects on propellant and components.

b) Solid propellant dynamic response.

c) Unsteady aerodynamic loads.

2.6.2.1 Acoustic Environment

Independent calculations of the sound pressure levels (SPL) to be anticipated near large rocket engines were based on Reference 7. The SPL at 200 feet thus computed is 169 db, which is in good agreement with the calculation of Reference 2 where no ground reflection is assumed (3 db difference). The SPL between the nozzles will be somewhat higher, but should not exceed 194 db which is one atmosphere fluctuation. It should be noted that these values are somewhat conservative because total ground reflection has been assumed, far field theory was used for prediction at near field (short distances) and for high levels of SPL (where nonlinear effects tend to limit response), and because the effect of water on the jet was not considered (this tends to decrease levels).

When the acoustic environment is severe, structural failure or equipment malfunction can result. In the case of the NOVA booster, however, structural failure of the engines should not occur because of the relatively thick structure involved. Thus, for example, the first stage engine case thickness is approximately 0.750 inch, compared to 0.144 inch for the Minuteman. The maximum external SPL for the NOVA and Minuteman are approximately 181 db and 168 db, respectively. The mass-law attenuations through the wall thicknesses at 100 cps, for example, are 41 db and 27 db for the NOVA and Minuteman, respectively. Thus, the noise levels within the first stage of the NOVA and the Minuteman would be approximately the same, 140 db and 141 db respectively. It would appear, therefore, that the internal acoustic environment of the NOVA first stage engines is no greater than that of the Minuteman, which suffered no malfunctions from this cause.

The equipment in the vicinity of the first stage nozzles would be subjected to extremely high levels (180 plus db). Such equipment, however, would be subjected to these high levels during engine development phases and would be sufficiently ruggedized for this purpose.

From the foregoing, it appears that no insurmountable acoustic problems should be expected with the NOVA booster. A certain amount of component proof testing can and should be performed in the laboratories, but no large scale development programs are envisioned as necessary. A few acoustic tests on the structure of the upper part of the missile should be made in order to establish the structural integrity. These can be relatively simple tests on appropriate portions of the structure and performed with existing acoustical facilities. This conclusion is based partly on the fact that the NOVA wall thicknesses appear to be sufficiently heavy for adequate attenuation and partly on the assumption that adequate component shielding can be accomplished when necessary by adding sufficient mass without extreme weight penalties, as were sometimes encountered in the current missile programs. It will also be necessary to establish the vibration fragility of the various items of equipment. These fragilities must then be compared with the actual environment and appropriate protection or equipment ruggedization supplied.

2.6.2.2 Solid Propellant Dynamic Response

The dynamic stresses induced in the propellant do not appear to be serious. This is partly attributable to the damping inherent in the propellant, and partly due to the fact that the frequencies of the propellant modes relative to a rigid case appear to be significantly higher than the fundamental bending mode frequency and other elastic frequencies of the complete system. Extension of these qualitative conclusions to prediction of stress levels is too extensive a task for the present study.

It is also suggested, as a result of vibration measurements on Atlas, Titan and Minuteman missile flight tests, that the solid propellant acts to damp out structurally transmitted vibrations, so that engine induced vibrations tend to remain within reasonable limits.

2.6.2.3 Unsteady Aerodynamic Loads

It has been pointed out in Section 2.5 that fairings should cover the interstages to minimize the local buffeting effects due to unsteady flow. However, there still may be concern for unsteady flow phenomena around the clusters of engine cases in the first and second steps. Scaled wind tunnel models instrumented with high frequency response pressure transducers will be needed to discover regions of intense buffeting, and to evaluate local fairings designed to alleviate such conditions. Model tests should also be performed to evaluate the effects of horizontal winds blowing across the vehicle while on the launch pad.

2.6.2.4 Bending Frequencies and Mode Shapes for Liftoff Condition

To provide data for a control system stability investigation, approximate bending mode shapes and frequencies have been computed for the solid NOVA just after liftoff. Several cases were computed, with resulting frequencies as indicated below. Interstage stiffness was varied as a parameter. The effect of shear stiffness was investigated by computing each case with infinite shear stiffness, as well as with a resonable estimate of the stiffness. The idealized two-dimensional model used for calculating the bending motion of the multimotor stages probably makes the present frequency estimates somewhat higher than the actual values.

The total weight of the JPL configuration for which the computation was made was approximately 25 million pounds. The heavier configuration discussed in the present report would have somewhat lower frequencies.

The computed frequencies are summarized in the Table below.

Table 2.6-III. Computed Bending Frequencies

Interstage Flexural Rigidity ($lb\text{-}in^2$)		Natural Frequencies (cps)		
Step I-II	Step II-III	First Mode	Second Mode	Third Mode
2.4×10^{14}	*15×10^{12}	1.04	2.80	5.57
2.4×10^{14}	30×10^{12}	1.29	3.01	5.90
8.1×10^{14}	15×10^{12}	1.06	3.12	7.23
8.1×10^{14}	30×10^{12}	1.33	3.47	7.64

*JPL configuration

Results of this study indicate the following:

a) The most realistic estimate of the bending frequencies at liftoff is:

First mode:	1.0 cps
Second mode:	2.8 cps
Third mode:	5.6 cps

b) The bending frequencies are quite sensitive to the II/III interstage stiffness. The lower of the two stiffnesses investigated, 15×10^{12} lb/in^2, is considered the most reasonable value. The frequencies could be raised about twelve percent by doubling this stiffness, with a significant weight penalty.

c) Fairly sizeable variations in the I/II interstage stiffness and overall shear stiffness do not appreciably affect the frequencies.

Representative mode shapes are shown in Figure 2.6-9. Because the assumed weight and bending stiffness distributions are necessarily somewhat arbitrary, they are reproduced for reference in Figures 2.6-10 and 2.6-11.

2.6.2.5 Conclusions

2.6.2.5.1 No insurmountable technical problems appear to exist in the structural dynamic area.

2.6.2.5.2 Two potential problems exist which may require considerable development time for solution. These are:

a) Vulnerability of components at high-level acoustic excitation. The severe acoustic environment which propulsion, guidance, and other components must withstand may well increase the development time required for these components. The fact that weight limitations are not critical offsets to a degree the severe environment by making it easier to design protective equipment.

b) Intrastage and interstage loads due to unsteady airflow between the motors forming an individual step may be minimized initially by using a complete fairing over the interstages. A series of model tests should be conducted to estimate the severity of the problem.

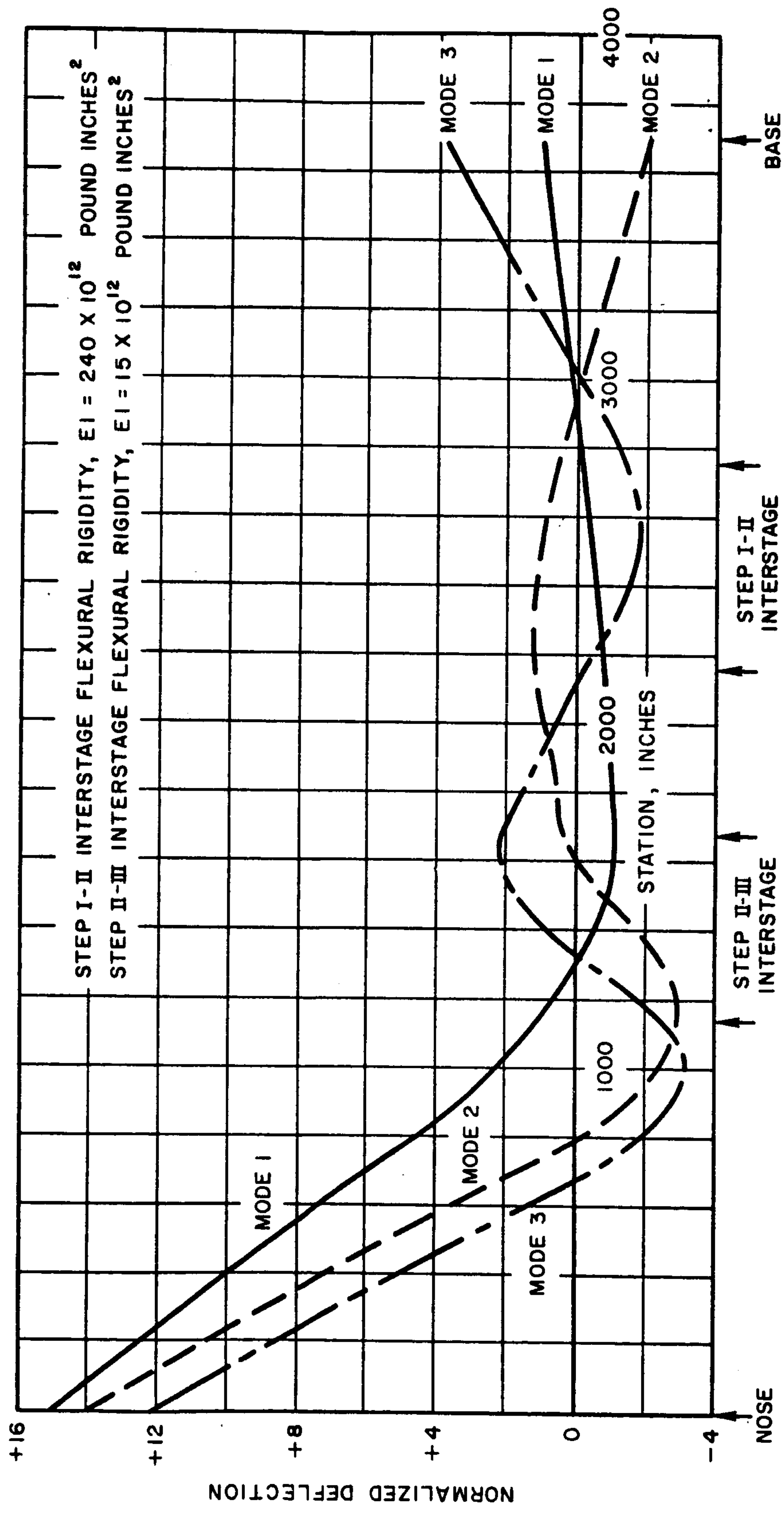

Figure 2.6-9. Estimated Bending Modes at Liftoff, Solid Propellant NOVA.

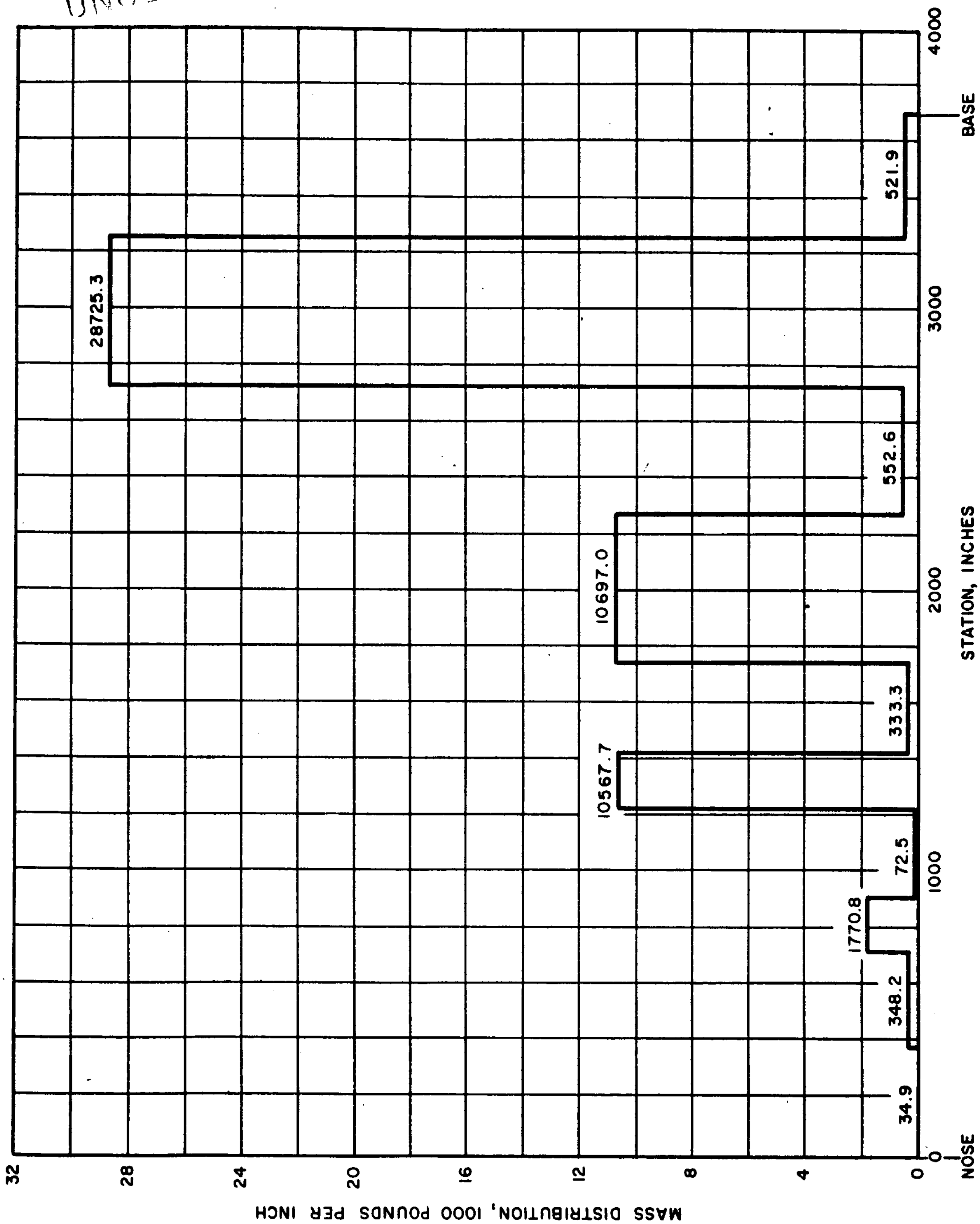

Figure 2.6-10. Mass Distribution at Liftoff, Solid Propellant NOVA.

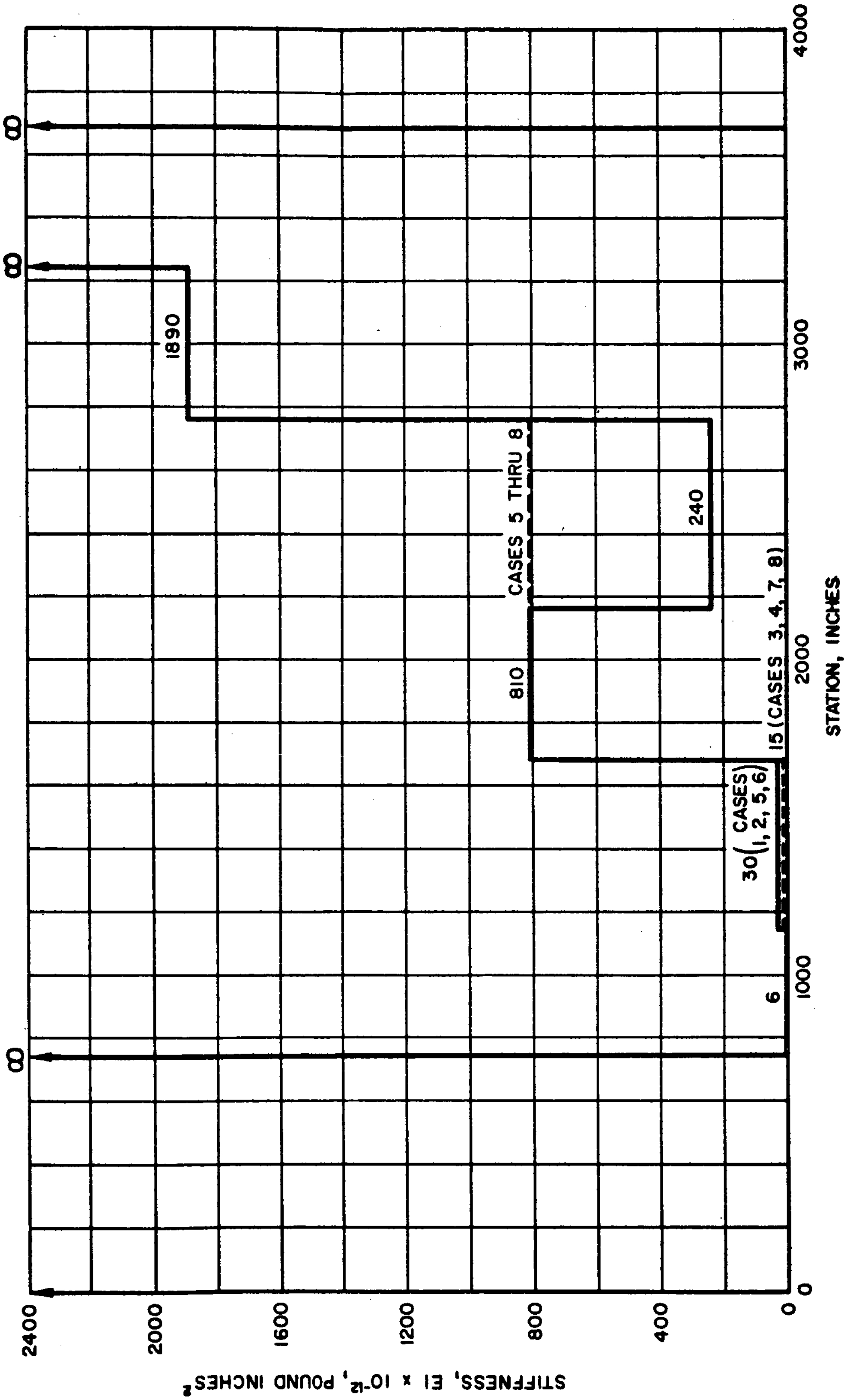

Figure 2.6-11. Estimated Stiffness Distribution at Liftoff, Solid Propellant NOVA.

2.7 GUIDANCE AND CONTROL SYSTEM

The major problem areas associated with attitude control for the all-solid NOVA vehicle have been identified, and can be separated into the following general categories:

a) Stability and accuracy considerations
b) Thrust vector control authority requirements
c) Total control impulse requirements
d) Control force generation system
e) Coast phase attitude control

An analysis of these areas has been performed to determine the salient features of the attitude control system. The results are described below.

2.7.1 Stability and Accuracy Considerations

An investigation was made to determine the control system gain requirements imposed by aerodynamic stability considerations. Although the vehicle is aerodynamically unstable during a major portion of its flight in the sensible atmosphere, it was found that this was not a limiting factor. That is, the minimum permissible attitude gain to provide closed loop aerodynamic stability was found to be considerably below the lower gain limit imposed by other considerations. The principal factor which determined the lower gain limit was the attitude accuracy in the presence of thrust unbalance during the thrust decay period just prior to burnout of each stage.

A secondary factor which contributed to the determination of the minimum allowable bandwidth was the guidance-control subsystem interaction. For this portion of the study, it was assumed that an inertial guidance system would be employed for all stages. It was further assumed that attitude commands would be generated to null the cross-trajectory velocity component. Maximum steering loop time constants of 10 seconds for first-stage, and 5 seconds for second- and third-stage operation were considered adequate. With these guidance constraints, control system stability analyses were performed, considering only rigid-body dynamics. Low frequency stability margins were thereby determined as a function of autopilot rate and position gains.

Having established the rigid body control system stabilization requirements, with particular emphasis on minimum allowable bandwidth, the effects of structural dynamics were next considered. Approximate bending mode calculations for first-stage at liftoff showed the natural frequencies to be 6.5, 17.6, and 35 rad/sec for the first, second, and third modes respectively. At first stage burnout these natural frequencies increase to approximately 7.1, 19.1 and 43.1 radians per second. The control system bandwidth varies from approximately 0.8 to 1.7 radians per second during first stage operation. In view of the fact that the first bending mode frequency is higher than the required control system bandwidth by at least a factor of 4 at all times during first stage flight, severe bending stabilization problems are not expected. A number of different approaches are possible for provision of bending stabilization, among which is the use of multiple rate transducer arrays as suggested by JPL. However, a relatively simple adaptive technique exists which appears attractive for this application, and this method is proposed in the interest of eliminating system complexity. A detailed description of this scheme is contained in Reference 8. Briefly, the system uses a pair of rate gyros located on opposite sides of the first mode antinode. The signals from these sensors are blended so that the output at the first mode frequency is small, and has a phase corresponding to that of the forward gyro. If the position gyro is also located forward of the first mode anti-node, phase stabilization of that mode can be accomplished by introducing an appropriate amount of lag by means of a shaping network. This theory can be extended to apply to higher modes as well, but for purposes of this study, it is estimated that modes higher than the first mode can be attenuated sufficiently to provide gain stabilization without introducing excessive phase shift at rigid body frequencies.

System stability, including the effects of body flexibility, was considered only for the first stage. However, this represents the worst case, and it can be safely assumed that comparable stability margins could be provided for the upper stages using similar techniques.

It is concluded from the above described studies that there is reasonable assurance that adequate stability of NOVA is achievable without undue difficulty.

It is not anticipated that aerodynamic load relief will be necessary in view of the relatively minor aerodynamic normal force effects. If, however, significant changes in the aerodynamic parameters occur during the evolution of the vehicle system and cause an aerodynamic load problem, load relief can be provided by a number of workable schemes. One type is currently being investigated by STL under a study contract with the Marshall Space Flight Center.

The attitude gain for the NOVA control system is expected to be in the vicinity of 0.5 degree thrust vector deflection per degree attitude error. During the thrust decay region near burnout of each stage, it will be possible to attain attitude errors as large as 6 to 10 degrees. To allow errors of this magnitude may imply some risk of losing attitude reference. Therefore, unless the attitude gain can be increased during this flight regime, (this is a strong function of bending stability) it may be necessary to resort to such techniques as the use of integral plus proportional control in the autopilot. An accurate determination of this necessity, and the establishment of autopilot design criteria is more properly the subject of a detailed design study. Although this factor may influence the control system configuration, it will certainly not impose problems of an insurmountable nature.

2.7.2 Thrust Vector Control Authority Requirements

In the establishment of maximum thrust vector deflection requirements, such factors as winds, misalignments, and staging transients normally require extensive investigation. In the system under consideration, however, the predominant factor in establishing the required control authority stems from the unbalanced thrust condition encountered when each step approaches burnout. Because of loss of propulsive efficiency, it is undesirable to cant the nozzles such that the thrust of each engine in the cluster passes through the stage center of mass at burnout. On the other hand, it is not practical to attempt to provide sufficient control authority to trim out all of the thrust unbalance effects. A study was therefore performed to arrive at a reasonable compromise between nozzle cant angle and thrust vector deflection capability. For the purpose of this study, it was assumed that all engines in a step had equal total impulse, the thrust decayed linearly during the last 9 percent of the total stage burning time for the nominal case, the impulse consumed during thrust decay was equal for all engines in the cluster, the 3σ variation in burning rate was 3.7 percent of nominal, and that burning rate was the only source of variation. On the basis of these assumptions, the study led to the decision to cant all nozzles 5 degrees (except for the center step I engine and the single engine of step IV). In addition, the three peripheral engines of the Stage III cluster, will burn nominally 10 percent faster than the three interior engines of that step. This configuration will require a thrust vector deflection capability of 5 degrees in pitch and yaw on each engine. The curves of Figures 2.7-1 and 2.7-2 represent the estimated 3σ values of thrust vector deflection as a function of time measured from the nominal start of thrust vector decay. Stage III calculations have also verified that a thrust vector deflection capability of 5 degrees is adequate, provided that the 5 degree cant angle is used and the three center engines burn 10 percent longer nominally than the outer three engines.

Thrust vector response to winds was calculated for the first stage utilizing a time-varying rigid body model, a simple autopilot, and wind profiles whose shear and velocity maxima were selected to occur at the most adverse time of flight. A typical thrust vector response to such a wind condition is depicted in Figure 2.7-3. The corresponding wind

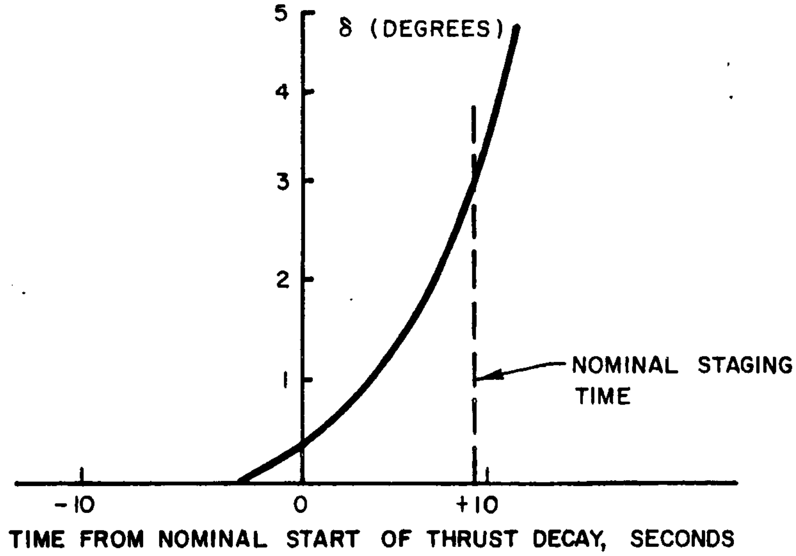

Figure 2.7-1. Stage I Estimated 3 Sigma Thrust Vector Deflection During Thrust Decay.

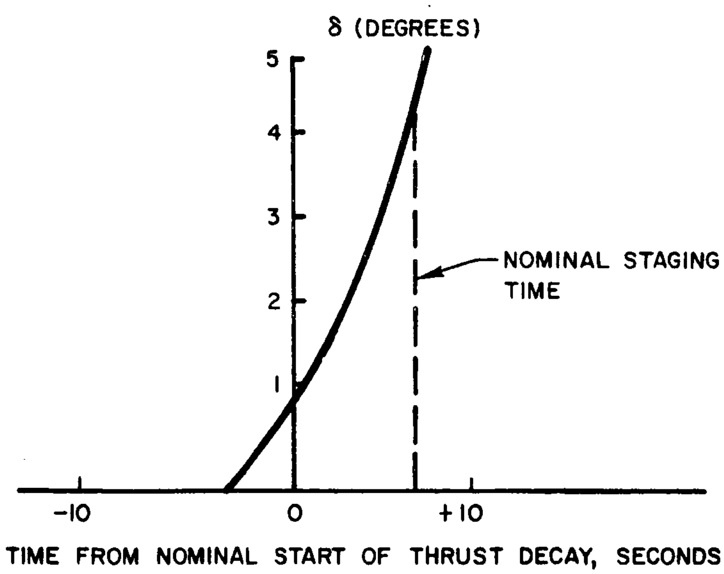

Figure 2.7-2. Stage II Estimated 3 Sigma Thrust Vector Deflection During Thrust Decay.

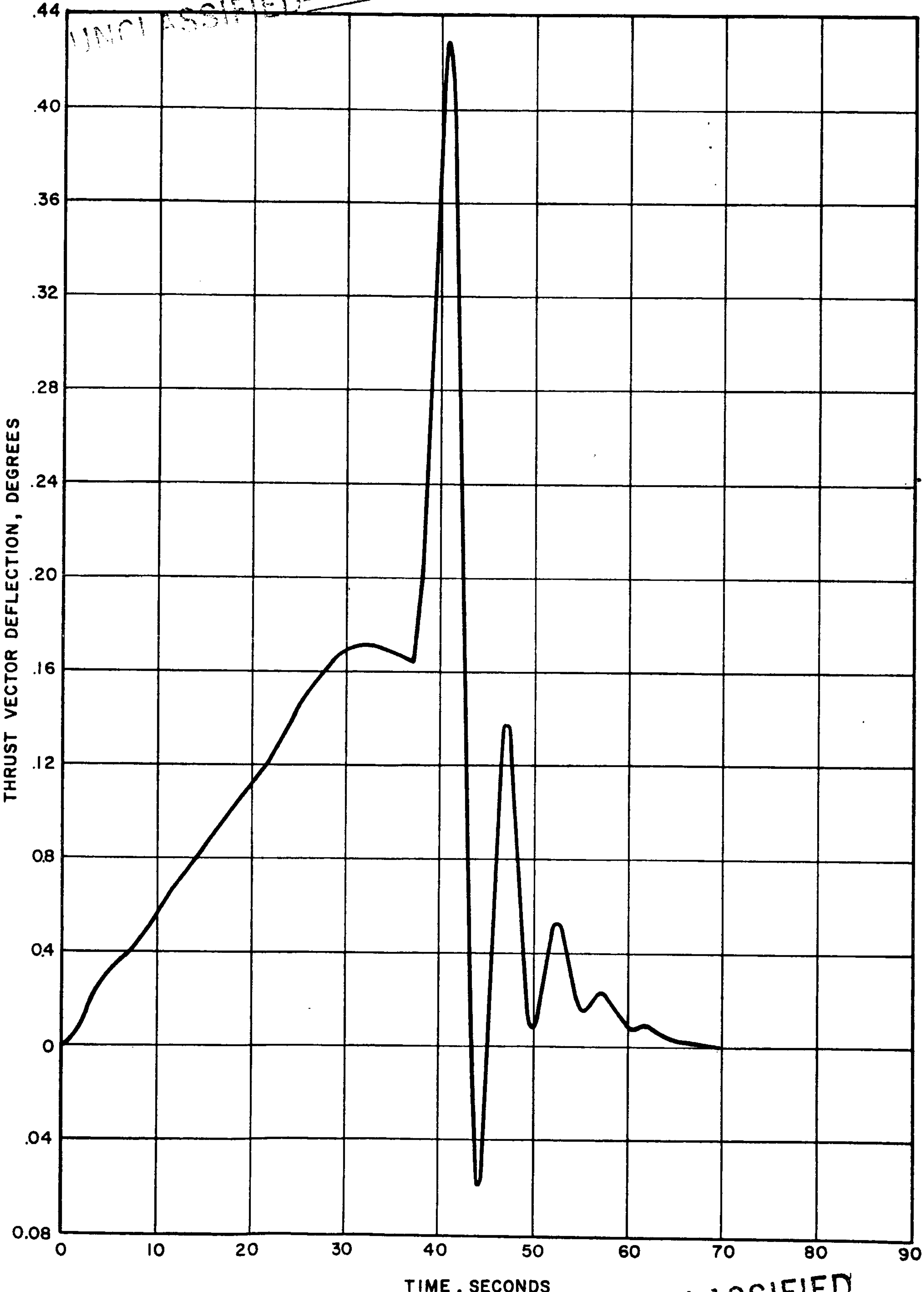

Figure 2.7-3. Stage I Wind Response.

profile is shown in Figure 2.7-4. Other factors which were considered, but estimated to have a negligible influence upon the maximum thrust vector deflection requirement, were thrust and center of gravity misalignments, and engine ignition transients. An estimate was also made of the maximum tolerable angle of attack at initiation of second stage operation. The tolerable angle was found to be much in excess of the value expected as a result of attitude reference constraints.

Because of the large thrust vector deflection capability in pitch and yaw, it seems apparent that adequate roll capability is assured. A conservative estimate would place the roll requirement on thrust vector deflection below 1 degree, which is easily attainable in all stages.

2.7.3 Total Control Impulse

Since secondary injection is assumed (for vehicle sizing purposes) as the method of control force generation, a determination of the total control impulse requirements is necessary to size the injectant storage system. This determination has been made in a conservative manner by summing the effects of winds, misalignments, thrust unbalance, steering and control. Table 2.7-I below summarizes these results.

Table 2.7-I. Control Impulse
(Expressed in Percent of Total Stage Axial Impulse)

Stage	I	II	III	IV
Wind	0.1	-	-	-
Misalign	0.5	0.50	0.75	0.7
Thrust Tailoff	0.2	0.25	0.20	-
Control and Guidance	0.3	0.30	0.30	0.3
Total	1.1	1.05	1.25	1.0

Note: A control impulse equal to 1.5 percent of each stage impulse would be a conservative estimate.

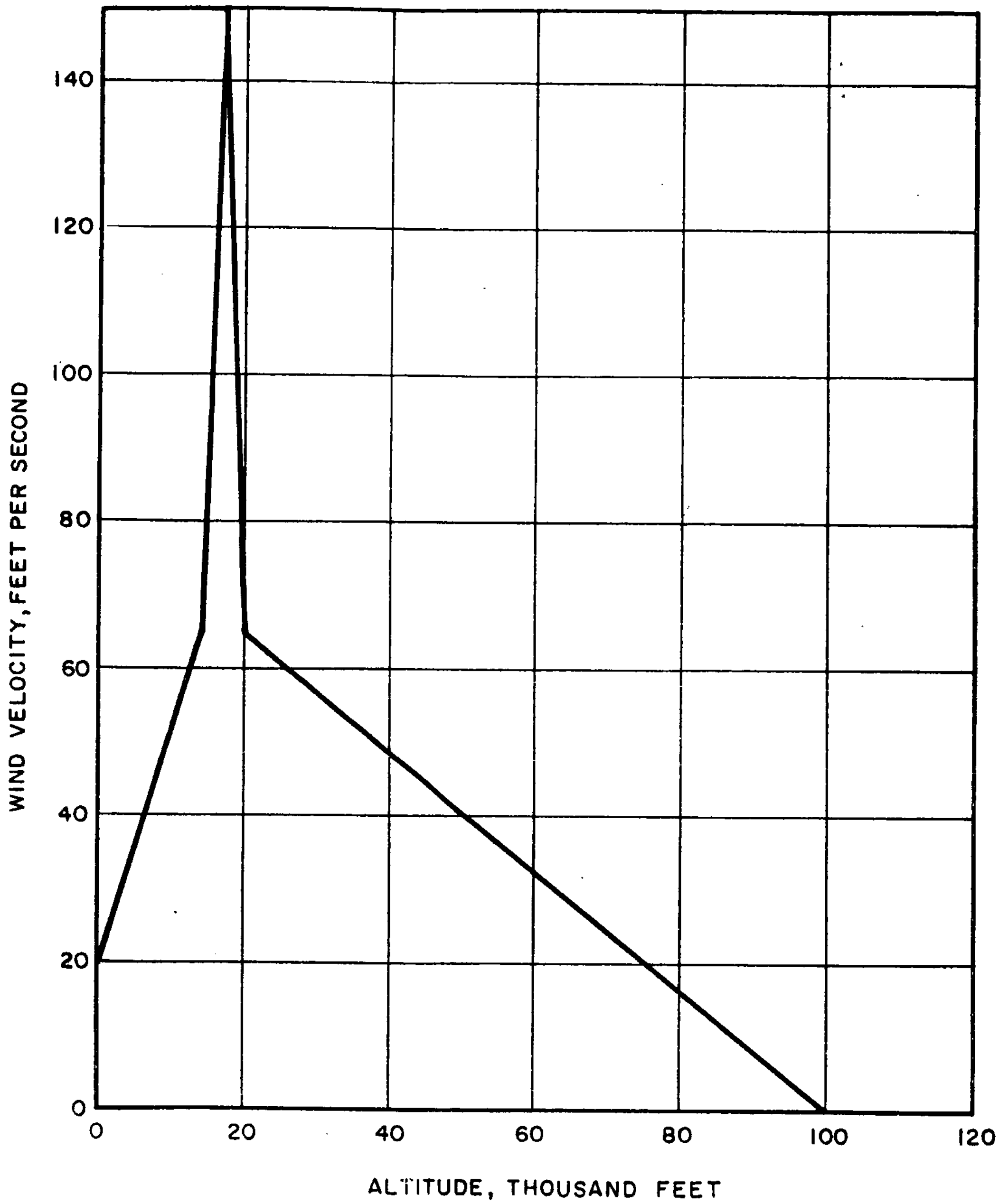

Figure 2.7-4. Wind Velocity Profile.

2.7.4 Control Force Generation System

Recent STL studies similar in nature to the one under consideration here have led to the conclusion that the secondary injection principle of thrust vector control appears to be the most promising approach. It should be recognized however, that from a control system viewpoint, this phenomenon is not yet fully understood. Theoretical and experimental data defining the dynamics of the injectant mass rate-to-side force transfer characteristic are extremely meager. Similarly, the nature and severity of nonlinearities in this characteristic are not well known. The best available engineering estimates indicate that no serious problem exists in this area, but experimental verification is necessary. Because of the randomly distributed injectant utilization requirements, it will be desirable to provide a means of dumping the unused injectant on those flights where less than maximum control requirements exist. This can be accomplished with the use of relatively simple circuitry which compares the amount of injectant remaining aboard with a predetermined curve, and dumps the excess at a constant rate. A small weight penalty will be incurred because of the need to provide sufficient injectant for large control deflections during the thrust decay region of each stage. This is not expected to be severe, however, because the time duration of the thrust decay period is a relatively small percent of the total flight time.

2.7.5 Coast Control System

During the coast phase of the NOVA mission, attitude control can be provided by means of mass-explusion jets, operating from a hot or a cold gas source, depending upon the detailed requirements. Since the design of such a system is well understood, no emphasis has been placed upon it in this study. It is considered to be a problem which is more appropriately associated with a preliminary design, rather than a feasibility study.

2.8 RELIABILITY

Launch vehicle reliability will determine the number of flights required to support the lunar operation. Two phases must be considered. The first phase, includes the initial flights of the complete vehicle and is intended to establish and correct design and development deficiencies. The second phase includes the lunar operations and utilizes vehicle systems which have demonstrated an acceptable level of both performance and reliability.

Examination of reliability records of existing missile and space vehicle systems shows a steady rise in reliability reflecting the elimination of design deficiencies. Eventually, a level is reached which reflects random failure. This level is determined both by the thoroughness and degree of proficiency exhibited in the assembly and checkout procedures and by the inherent reliability that has been developed into the components and subsystems which make up the vehicle.

2.8.1 Estimation of Reliability

As indicated in Reference 1 it is difficult, if not impossible, to make a priori estimations of vehicle reliability. Further, the number of flights will not be sufficiently large to establish a statistically sound reliability record.

Reference 9 further indicates that even if all component reliabilities were firmly established, it would still be improper to arrive at the overall vehicle reliability by combining the component reliabilities in such a way that each component has been decoupled from the vehicle. A more realistic means for deriving reliability estimates stems from empirical analysis of actual flight data. The following accumulative average reliability values have been extracted from Reference 9 and are listed as Table 2.8-I.

Table 2. 8-I. Reliability Records of Various Vehicle Systems

Vehicle	Flights	Reliability
Atlas	72	0.61
Titan	28	0.54
Polaris	79	0.67
Thor	65	0.79
Aerobee	40	0.98
V-2 (US Firings)	71	0.68
Discoverer	23	0.70
Vanguard	11	0.27

This table indicates that the more complicated vehicle systems have the lower cumulative reliabilities, a result which is hardly surprising. However, it is also seen that the reliability of 0.95 used by Reference 1 in costing the proposal is not easily obtainable in the limited number of flights scheduled. It is true that all of the vehicle systems listed in Table 2. 8-I were weight conscious and "pushed the state-of-the-art" to a varying degree. The question remains what vehicle reliability can be obtained if weight is not a consideration but time and money are considerations. It is contended that the relaxation of a constraint such as weight is certainly beneficial, but, nevertheless, the solid NOVA remains a very complicated vehicle, and its reliability record will possibly be rather similar to those listed in Table 2. 8-I.

Additional empirical reliability data is depicted in Figure 2. 8-1.

a) The overall flight system reliabilities for a 2 stage and 3 stage liquid propellant missile versus the number of flights. This curve has been obtained from Reference 9 and averaged from the liquid propellant Titan I, Atlas, Thor, and Jupiter.

b) The Blue Scout (Air Force) and NASA Scout reliability. The NASA Scout is a 4 stage solid propellant conservative design and should indicate the possible reliabilities of a new solid propellant vehicle during the early 10 flights.

~~CONFIDENTIAL~~ UNCLASSIFIED

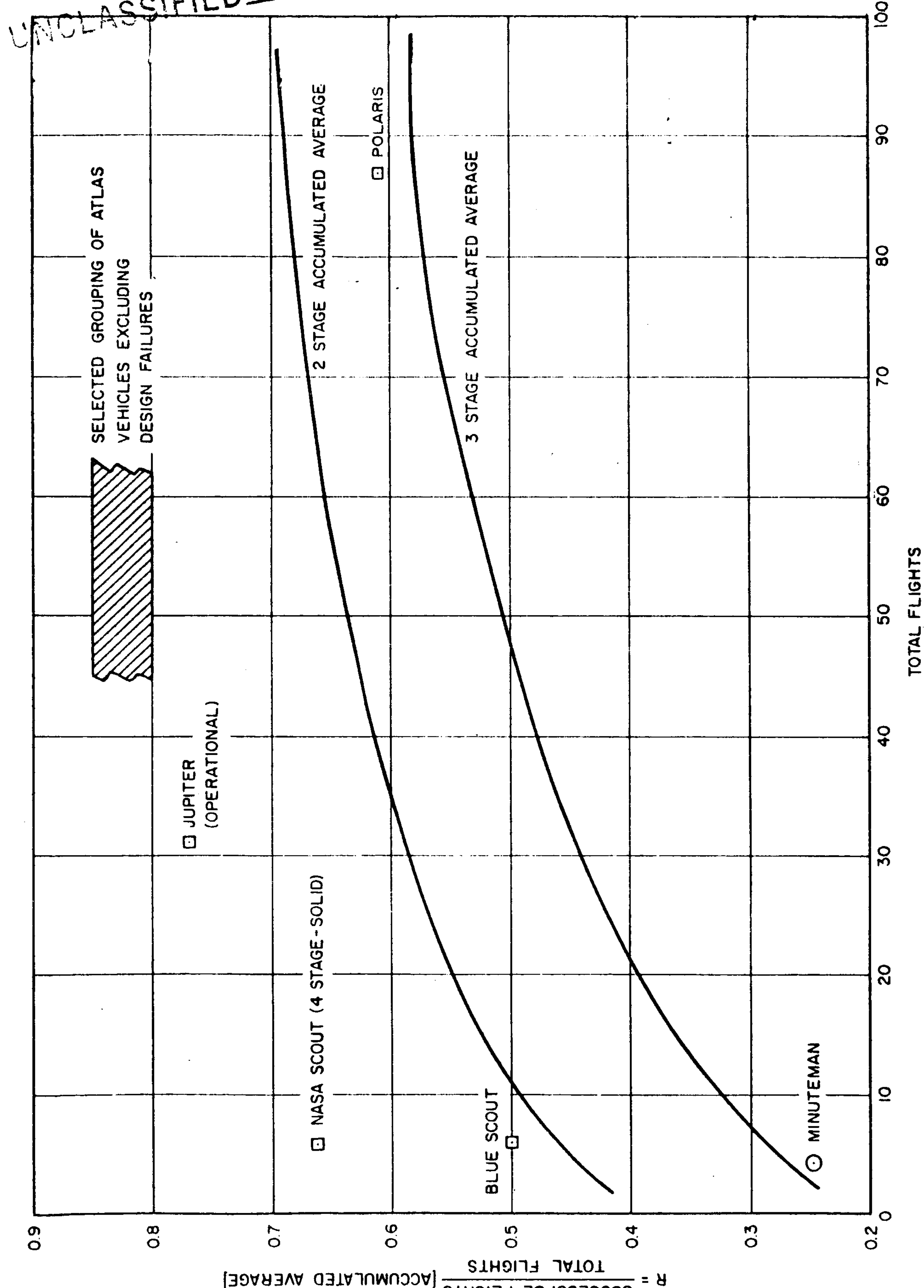

Figure 2.8-1. Missile Flight Test Reliability History.

~~CONFIDENTIAL~~ UNCLASSIFIED

c) Polaris, Minuteman and the operational Jupiter reliability.

d) A selected grouping of Atlas flights, in which failures due to design error were not included, only to quality control, random failures, etc.

This grouping gives an optimistic view of a liquid propellant reliability and is analogous to a conservative design. A supplement to this report will treat the relative reliabilities of liquid and solid propellant rockets.

2.8.2 Design and Testing Philosophy

The basic premise to design within the state-of-the-art without overemphasis on weight considerations, enabling safety margins and redundancy techniques to be utilized, is the most important concept in this program. Whenever there exists an established and proven reliable design, this should be used rather than a more advanced but unproven design with potential problem areas. Conservatism must be the theme of the program. In turn, this will demand strict management of the program. There should be no testing to improve performance at the expense of reliability. Attempts to improve performance frequently result not only in a reduction of the reliability of a component itself but also produce undesirable interactions with other components.

The development test philosophy suggested by JPL is not as convincing as the design philosophy. The test philosophy hinges on the premise that information from small scale engines can be scaled-up to the size considered. This is true to a certain extent but the validity of the statement is questioned with respect to reliability information. The total reliability of the system includes both design and manufacturing factors. The latter, especially, will require much time and experience in solving problems peculiar to the large size of the system. More emphasis should be placed on full-scale engine tests. Design manufacturing and quality control inadequacies will then be given greater opportunity for exhibition earlier than is contemplated in the stated development test program.

2.8.2.1 Full-Scale Testing

In order to obtain an estimate of the number of tests of full-scale engines that might be indicated, the first stage Minuteman engine development program was reviewed. It was thought appropriate to consider the Minuteman program beginning with the first full-scale engine test and concluding with the end of testing of the first established configuration, i.e., the PFRT engine. It is realized that the philosophies of the Minuteman engine program and the NOVA program differ in that there was to be no "dead end" testing in the Minuteman program (which also implies a limited amount of subscale testing) and also that there had to be a very considerable amount of optimization and advancement of the state-of-the-art in the Minuteman program. However, since it is indicated in other parts of this review that the statement that development can be completed on the NOVA engines with subscale engines and without advancement of the state-of-the-art is overly optimistic, it is concluded that the development program of NOVA engines will not be so significantly different from that of the Minuteman engines.

The number of engines which will be implied by this discussion probably can be reduced in the NOVA program first, by the conservatism of the design and test philosophy and second, by the fact that testing will be carried out at a slower rate, thereby allowing design modifications to be introduced and tested with less lead time problems. This means there will be less testing of obsolete designs which were cast or fabricated before concurrent testing and analysis required their modification.

There were a total of 69 tests of the first stage Minuteman engine before the PFRT program was completed.

Engines No. 1-30 (initial development of the PFRT design): There were no applicable or representative configurations. This sample consisted of 12 silo test engines, i.e., very short duration firings, and 18 engines having a mixture of heavy weight and/or experimental components.

There were 10 failures of the case-liner-insulation subsystem and three failures of the movable nozzle system in the 18 intended full duration firings.

Engines No. 31-42 (interim development of the PFRT design): This period saw the first engines containing applicable subsystems. Approximately half of these engines have representative propellant and case-liner-internal-insulation systems which could be evaluated; however, the nozzles were still undergoing intensive development. There were no case-liner-insulation failures but there were nine failures of the movable nozzle thrust vector control system.

Engines No. 43-69 (final development and verification of the PFRT design): of these 27 engines, seven were development engines for a later phase of the program, i.e., Wing I and therefore are not entirely applicable. This sample saw the first completely applicable configuration (test No. 44) in which all the subsystems were of the intended PFRT design. In this sample two failures of the applicable engines occurred. One was in the thrust vector control system when a nozzle jammed for a period of 12 seconds and another occurred when a pressure transducer (part of the flight instrumentation) failed, causing a small fire in the interstage compartment area.

This development time (starting with the first full-scale engine test) covered a period of approximately 18 months, i.e., at the average rate of one test firing per week.

If, for the purpose of estimating the number of engines in the NOVA program, the Minuteman engine silo firings are omitted and if the seven later development firings are omitted, then there were a total of 50 tests of full-scale units. The last 20 of these tests were tests of a supposedly established configuration but even so, two failures occurred. While many of these tests were significantly extending the state-of-the-art of the major subsystem of the engine, i.e., nozzle insulation and thrust vector control, together with testing the interaction of these components, this type of testing of the design will not be entirely absent on the NOVA engines and will require a significant number of test firings. In addition, further firings will be necessary for the manufacturing and quality control problems to exhibit themselves before entering the period of expected successful firings. This last phase will provide engineering confidence and also demonstrate reproducibility of performance. It is believed that taking all these considerations into account about 20 engines of each type will be needed in a truly conservative development program.

2.8.2.2 Reliability Growth

While the absolute failure rates exhibited by the three major subsystems of the Minuteman engines are not appropriate for system reliability prediction, it is pertinent to compare their relative failure rates and the rate of decrease of failure over an 18 month period. After an early failure, propellant ignition system experienced no further failures. The failure rate of the liner and insulation dropped from 33 per cent to 12.5 per cent to 8.5 per cent. The failure rate of the thrust vector control system dropped from 33 per cent to 25 per cent during the period that fixed nozzles were being tested and then down to 21.5 per cent when movable nozzles were being tested; of this last figure 40 per cent of the failures were due to failure of the kinematic mechanism. The conclusion drawn from this is that the liner and insulation are conservative in design in the NOVA engines, then this mode of failure should not appear. Ignition problems on the Stage I Minuteman engine have not been so apparent as on the upper stages, probably attributable to the rocket type rather than the pellet type design. The hinged nozzle thrust vector control system has shown a slower reduction in the failure rate than the other two subsystems; however, if secondary fluid injection thrust vector control is used on the NOVA engine it is believed that the failure pattern will be somewhat different. Movable nozzle development on subscale engines was not as rewarding as hoped for, consequently most of the development work has to be performed on full-scale development engines. However, with secondary liquid injection, it is considered that more independent testing of that subsystem can be performed separately from the full-scale NOVA engine. This in turn helps in reducing the number of full-scale engines for development firings.

2.8.3 Quality Control

The inability to realistically test a solid propellant rocket engine without consuming it is a major difference between solid and most liquid propellant rocket engines. As a consequence, quality control represents an area of extreme importance in this program. Close control over both manufacturing and assembly by clearly defined standard operating and inspection procedures should be established and maintained. In addition, all available and applicable nondestructive inspection techniques should be utilized to endeavor to establish acceptance and rejection criteria as a protection against failure of non-visual and nontestable parts and components. A very extensive and comprehensive event failure, and discrepancy reporting system, such as is used on the MINUTEMAN Program, must be implemented immediately after the program is initiated. This reporting system must not only apply to design failures and discrepancies but also be human errors and procedural and process inadequacies. This will help ensure that all sources of discrepancies or failures are minimized. Close control over all documentation must be maintained so that specifications, procedures, process controls, inspection and testing operations are effectual and kept current. Basic materials specifications should be established with close control over both the input variables of the processes as well as sampling, testing or inspection of the output. Independent tests and inspection should be made at both the vendor's outgoing inspection and the contractor's incoming inspection with data from both points being reported to the Systems Engineering Contractor for review.

2.8.4 Environmental Factors

The large physical size of the system will result in some potential problems associated with the following environmental factors. For instance, the high humidity, heat, fungus, sand and salt spray found in the suggested locations of fabrication and test may have deleterious effects on the components, especially since it probably will not be possible to completely protect an assembled system or even the major components such as a single engine. Consequently, seals, rings, liners, hydraulic fluids, internal and external insulation, real and synthetic rubber, etc., should be chosen for their superior performance and stability under such conditions. Where good data are not available, study projects should be initiated to establish the effect of the environmental factors on these materials.

3.0 FACILITIES AND GROUND SUPPORT

The major components of the launch vehicle are shown in Figure 3.0-1. Because of the large size of many of the components required to make up the vehicle, special facilities and ground support equipment will be needed to implement the program. The associated requirements have been examined and it appears feasible to provide such facilities and equipment. It is believed that the time allotted in the JPL program for their provision was underestimated.

3.1 PRODUCTION FACILITIES

New facilities will be required for production of the solid propellant grain, the engine cases, and the nozzles. However, the facility requirements are not unreasonable, and if their scheduled construction is timely, no difficulties are anticipated.

3.1.1 Continuous Propellant Processing Facility

Continuous propellant processing can be provided to support the program as presently visualised. Considerable development effort will be required to improve current techniques for storing, transporting, and feeding propellant ingredients into the process. Methods for mixing and de-aerating the propellant need to be scaled up; however, existing commercial equipment can be utilized. Effort is also needed in advancing the current analytical methods for process control. Particular attention should be given to rapid measurement of propellant quality in the continuous process by nondestructive means and developing methods for diverting unacceptable propellant from the main stream. STL concurs with the JPL proposal to size the propellant loading facilities on the basis of a class 9 material. This will allow possible future use of the facilities for propellants which are known to be in this category. Additional ammonium perchlorate capacity is required, but this presents no major problem.

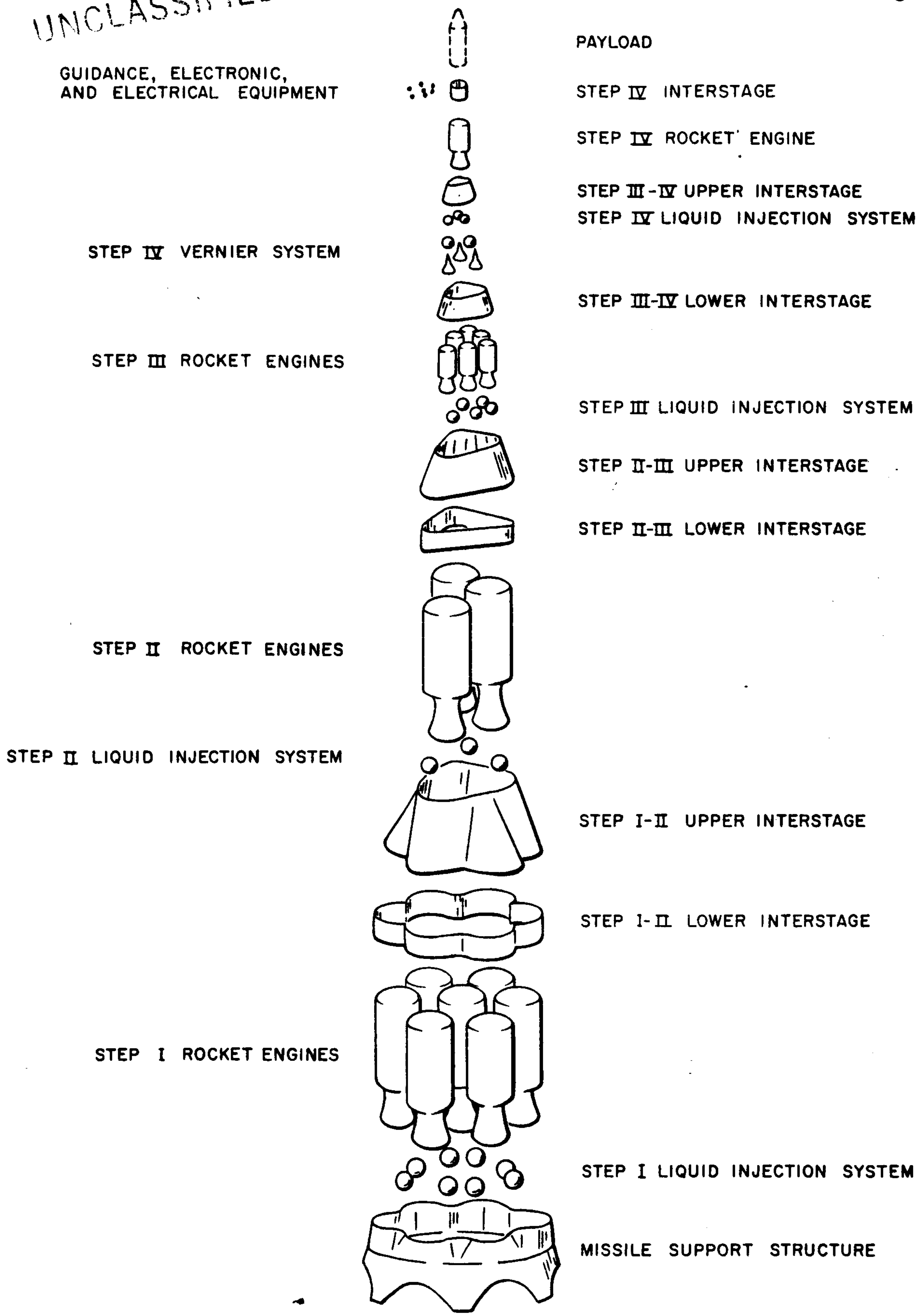

Figure 3.0-1. Major Components, Solid Propellant NOVA Vehicle.

3.1.2 Engine Case Facility

The facilities cost estimates in Reference 2 appear reasonable, but it is believed that the rate of production may require additional equipment or tooling. It appears that the shear forming equipment for the cylindrical segments would require significant advances in current state-of-the-art, and the development of this tooling would require considerable effort. However, it is believed entirely feasible even if costly.

Additional roll-ring forging capacity would be required to sustain the desired volume and to avoid possible delays in transportation from the north in winter, when, for example, navigation on the Great Lakes may be weather limited. This is appropriate to consider if the Ladish Co., at Cudahy, Wis., is a potential supplier of roll ring forgings. They are one of only a very few companies capable at this time of supplying these large forgings. If additional facilities are developed near the engine case fabrication facility, costs for the hardware could be expected to rise due to overhead and shakedown of a new facility. This matter should receive further consideration. As mentioned in Section 2.6 additional vacuum melt capacity is required for the production runs, but would probably not represent a tangible program cost. The heat treatment facility costs indicated in Reference 2 would be low by a factor of approximately two if entire engine cases were heat treated.

3.1.3 Nozzles

New high density graphite manufacturing capacity is required to produce rings 9 feet in diameter and 12 feet long for the "A" engine nozzle throats. Discussions with manufacturers reveal no major problems in providing this capability.

3.1.4 Vehicle Support and Interstage Structure

These structures are discussed in detail in Section 2.6. Since they are conventional airframe type structures, no new facilities are needed.

3.2 TRANSPORTATION AND HANDLING

The most practical transportation of very large components is via water. This influences the location of production, storage, assembly, and launch facilities adjacent to navigable water. Because of the size of the vehicle and structural components, it may not be economical to design the transportation and handling equipment so that resulting loads are below the flight loads. Any such instances would of course be minimized.

3.3 LAUNCH COMPLEX

An offshore launch complex has been suggested for NOVA operations. This concept has been examined to establish its suitability for the large all solid propellant vehicle system operations. Two alternative launch complex designs have been studied. Method I as presented in this report is a modification of the JPL system described in Reference 1. Method II represents a further revision. The general applicability of an offshore launch complex is believed to be established. Detailed studies are required to determine whether offshore launch complexes are needed and economical compared with other sites.

For the purpose of this critique, the launch complex has been defined as the pad, umbilical tower, alignment bench marks, breakwater and all equipment used solely in the complex. The equipment includes such items as the hard lines to the launch base and the support craft used at the complex but does not include the craft used for transportation from remote sites such as the engine processing facilities.

3.3.1 Launch Site Selection

This study assumes that an offshore launch site would be located in the vicinity of Cape Canaveral. While the general location appears feasible, it is not clear that this location or the use of an offshore installation provides the best launch site. The STL study did establish that the launch complex is a major program expense and is the pacing schedule item. Consequently, the necessity for a complete launch site evaluation cannot be overemphasized.

The launch complex studied is assumed to be located 6 to 12 miles east of Cape Canaveral where water depths vary from 40 to 100 feet at mean tide. Shoals exist in certain areas and could be considered as possible pad areas. For purposes of conservative estimating, depth of 100 feet at the launch complex was used. Further conservatism was introduced by the assumption of a sandy or loose bottom rather than a solid coral bottom.

3.3.2 Launch Complex, Method I

The modified JPL launch complex is presented in Figure 3.3-1.

A semi-circular breakwater is constructed on the offshore side of the launch pad. The pad is located at the center of a 1000 foot radius circle that is defined by six equally spaced bench marks, four of which are located on the breakwater. The remaining two are on the shore side of the pad and are erected on artificial islands mounted on concrete bridge piers. A section through the breakwater is a trapezoid 110 feet high with a 100 foot base and a 30 foot top. A major problem in the construction of a breakwater of this size off the Florida coast is the availability of ballast materials for its construction.

The pad and umbilical tower are also erected on permanent bridge piers. The launch pad base structure is in the form of a truncated cone 150 feet in diameter at the base and 100 feet in diameter at the top. The height is 50 feet with the top 50 feet below the water surface. Permanent steel fittings are provided on top of the pier to fasten a replaceable conical steel blast cap and to secure the legs of the truss structure forming the pad. The exact shape and depth of the blast cap would be determined by scale testing of launch pad models.

The launch pad itself consists of six truss tripods mounted on the bridge pier base. The apex of each tripod is located 25 feet above mean waterline and provides the vehicle support points which are spaced around the periphery of a 75 foot diameter circle. Each tripod is replaceable and is sub-assembled so that only a minimum number of basic connections are

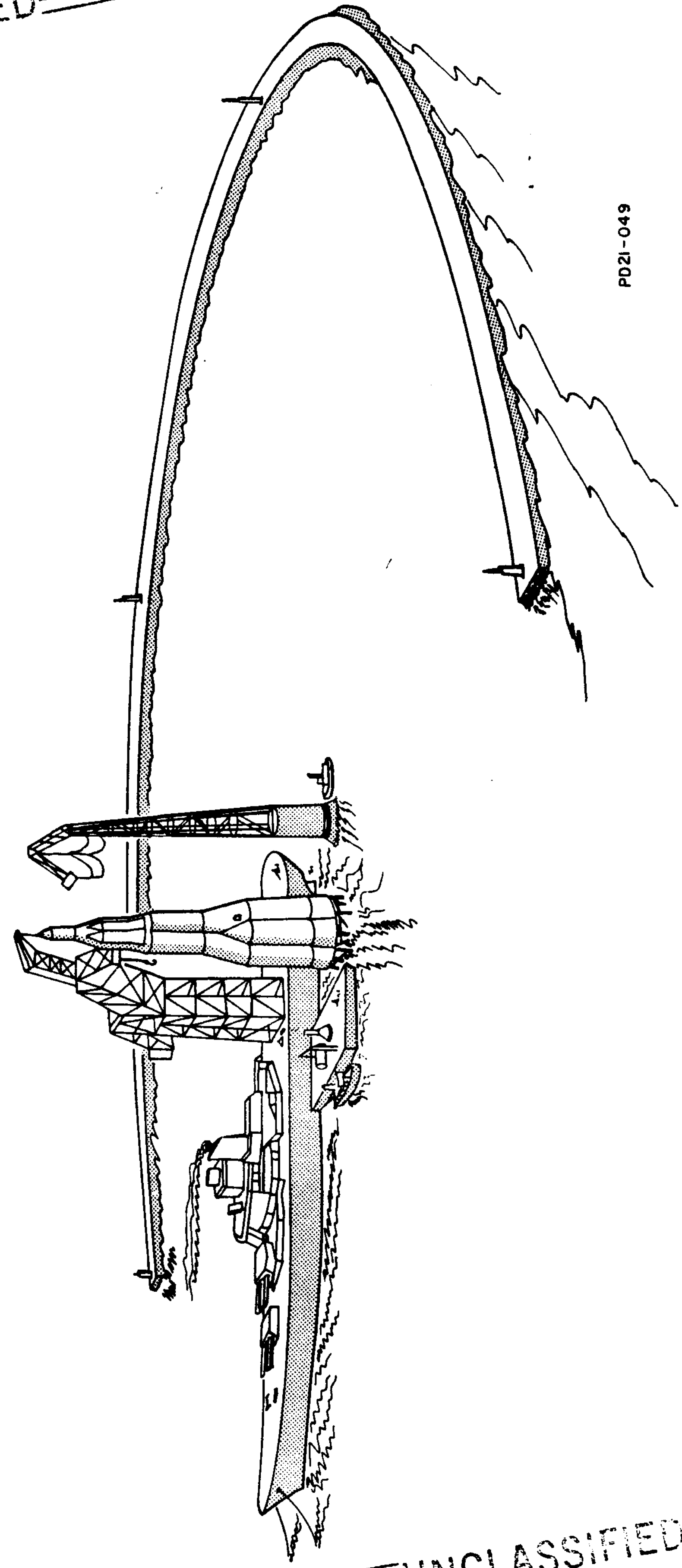

Figure 3.3-1. Launch Complex, Method I.

made to the pier below the surface of the water. Additional auxiliary structure is attached to the pier to support the center step I engine during initial assembly and to provide a "camel back" for mooring the crane ship. Work platforms, utilities, auxiliary moorings, and shark nets may be attached as sub-assemblies to the tripods. It has been assumed that the blast cap and base tripods may require replacement prior to each launch because of damage caused by the rocket blast. To facilitate final pad alignment, minor location adjustment must be built into the apex of each tripod.

A vertical full scale type A engine static test stand can be errected as a platform placed on tripods that are identical to those used for the vehicle launch pad.

The umbilical tower will also be placed approximately 100 feet from the launch pad. The lower section of the umbilical tower is considered to be permanent and will contain the umbilical service equipment such as payload and vernier propellant topping tanks, cryogenic temperature conditioning equipment, power supply, elevator, etc. The upper portion of the tower is considered to be replaceable after each launch and is designed as a sub-assembly so that replacement time at the launch complex will be minimized. The upper portion is a fixed vertical tower containing the elevator mechanism to the payload level. A dual-jointed, cantilever, retractable boom will serve as access to the payload and will be retracted to the vertical tower position during launch. Use of the tower for work crew emergency escape may be desirable.

A support and checkout ship and a floating crane complete the launch complex. The large capacity crane and its base are discussed below.

3.3.2.1 Floating Assembly Crane

A large capacity crane is required for this method of vehicle assembly. The crane requirements are as follows:

Weight to be Lifted	Height of Hook Above Water (feet)	Horizontal Distance (Cantilever) (feet)
1520 tons (3,040,000 lb) Step I A Engines	130	160
1520 tons (3,040,000 lb) Step II A Engines	250	130
261 tons (522,000 lb) Step III and IV B Engines	325	140
65 tons (130,000 lb) Spacecraft	400	125

These sizes suggest a crane incorporating two primary hooks: a 1600 ton hook at the 250 foot level and a 270 ton hook at the 400 foot level. It should be noted that a floating crane of this size and capacity is not currently available.

Availability of a ship for the floating base was determined. All three Midway class aircraft carriers are in active use, four Iowa class battleships are in storage, several Essex class aircraft carriers are in storage, and larger ships, barges, or catamarans could be built although with possible cost and time penalties. Since the crane support structure must be tied into the hull of the ship, a battleship would be a good crane base because it has existing very massive structure for gun turrets. Compared to the ex-battleship Kearsarge of 11,520 tons displacement which has a 250 ton capacity crane installed on its after deck, an Iowa class battleship of 63,000 tons displacement should be able to support a 1500 ton capacity crane.

Stability of the floating crane was thoroughly investigated and it was found that current crane ships have not presented any significant operational problems. The German built YC-171 floating crane of 350 ton capacity successfully utilizes an automatic counterweight positioning system to provide static stability.

Stability parameters were not immediately available for the Iowa (BB-61 through 64) class battleships, but the following information was obtained on the smaller Essex class aircraft carriers.

	Essex	Iowa
Full load displacement (tons)	44,750	70,600
Draft (feet)	29.3	38
Length overall (feet)	898	888
Beam (feet)	101	108
Center of gravity height above bottom of hull (feet)	35.4	
Metacentric height (MG) (feet)	10.2	
Full period of roll (seconds)	15.8	
External moment to heel (roll) ship one degree (foot tons)	7,740	
External moment (calculated) to heel ship ten degrees (foot tons)	77,300	

An unbalanced load of 446 tons at the 250 foot high and 130 foot out crane position would induce a heel angle of 10 degrees on an Essex class hull. This is less than the maximum stability roll angle which exceeds 30 degrees for this class of vessel. The rolling moment induced by a 125 mile per hour wind load would not exceed the above unbalanced loads. Consequently the floatation stability is considered satisfactory.

The effect of the crane floatation on precision of assembly can be estimated in terms of the performance of other large floating cranes. The YC-171 floating crane has for example, lifted 250 ton submarine hulls from the water to the dock without damage and has held a ship's bow while it was welded onto a damaged ship in a drydock. The proposed crane would have a much greater mass of hull and (sheltered by a breakwater) should be capable of the precision of installation required. The flexibility of the boom and cables, the slowness of load movement, and the large weight would combine to damp out unwanted motions. Additional handling gear could be added to the rocket engines during assembly and removed prior to launch.

An unofficial Navy estimate of the cost of duplicating the YC-171 craneship is 38 million dollars which may be compared to the modernizations to the Midway class carriers which cost 48 million dollars. A four times size YC-171 crane on a modified Iowa battle ship was estimated at 50 million dollars.

The ship also provides personnel living quarters for a full pad complement for around the clock operation if necessary. The normal assembly facility utilities such as electrical power, pneumatic, water, fire protection, etc., can be supplied to the launch pad from existing ship utilities. The floating crane can service two launch pads and is readily movable to prevent damage during the launch phase.

3.3.3 Launch Complex, Method II

The launch complex for this method is similar to that of Method I in that it is built offshore and is protected from the open sea by a breakwater. The launch pad is located above the water and is serviced by a travelling gantry instead of a floating crane. Figure 3.3-2 shows a possible configuration for the launch complex. Considerable study is needed to determine if one gantry can be utilized to service two launch pads. Further study is also needed to determine the effect of a catastrophic failure of the vehicle on the launch facilities.

3.3.3.1 Gantry

The entire complex for this method is based on the use of a gantry crane instead of a floating crane. This system has been studied since considerable experience has been gained in the use of gantry cranes in the assembly of boosters and space vehicles while no experience currently exists in the use of a floating crane for this purpose. The gantry envisioned

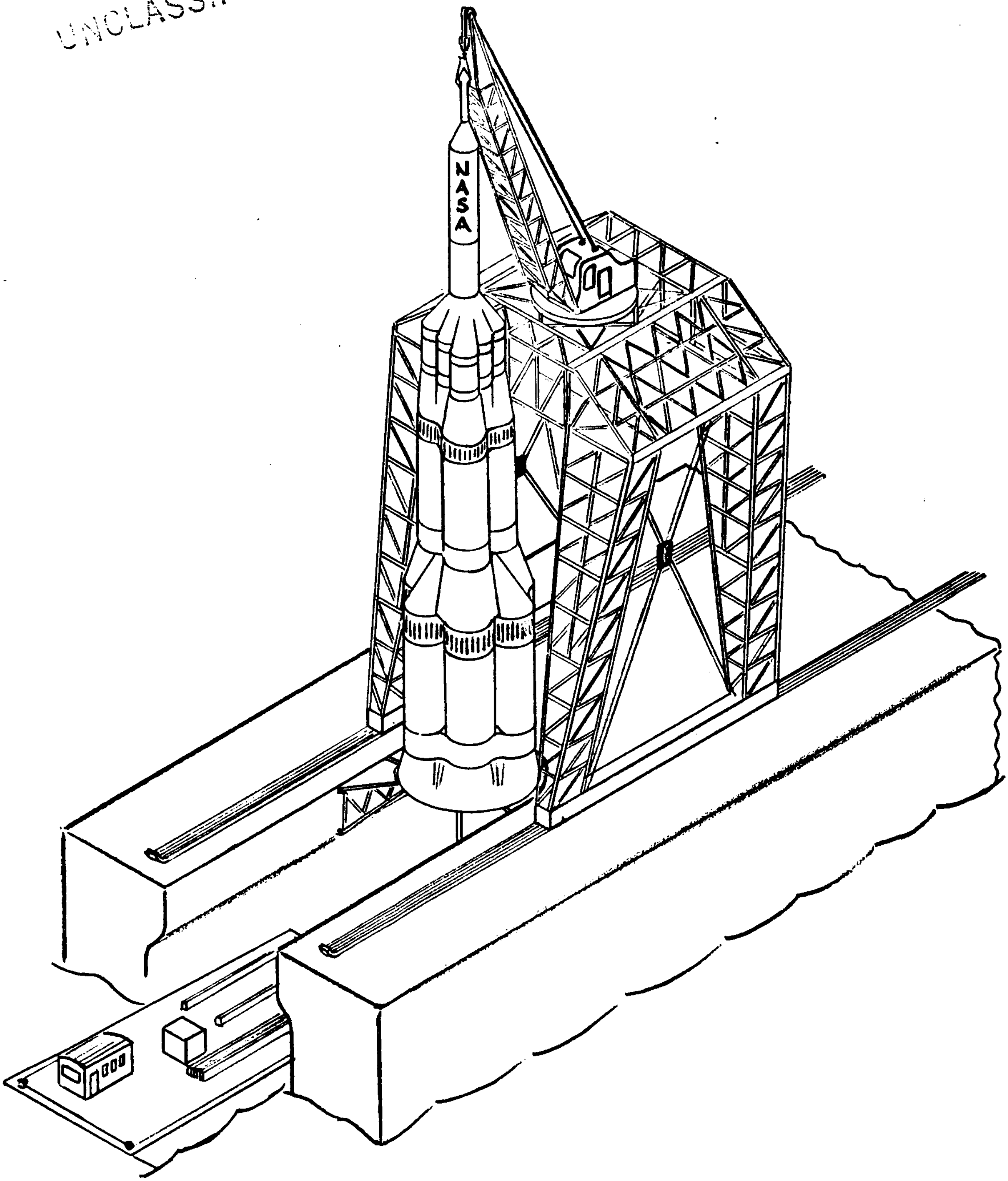

Figure 3.3-2. Launch Complex, Method II.

has two cranes each of a different capacity. The main crane, used for assembling the first two steps, has a 2500 ton capacity while a smaller crane mounted on top of the gantry and used for assembling the upper steps and spacecraft has a 500 ton capacity. Because of the size of the gantry, smaller hoists for handling tools and small pieces of equipment can be easily incorporated. The top of the gantry is approximately 250 feet above the launch pad, and the top crane extends to a height that easily clears the top of the vehicle.

3.4 VEHICLE ASSEMBLY AND CHECKOUT

The two different launch complexes (particularly the launch pads) discussed in Section 3.3 make possible two completely different assembly methods for the vehicle at the launch site. These two assembly methods are discussed below.

3.4.1 Assembly Method I

The assembly of the vehicle in Method I uses the launch site described in Section 3.3.2. The assembly sequence is shown in Figure 3.4-1 and is detailed in Section 3.5. A maximum amount of subassembly on the barges and crane ship is envisioned in order to reduce assembly time on the launch pad to a minimum. Installation of equipment in a lower step on the pad and simultaneous assembly of upper steps is considered feasible with a resultant saving in time.

A major problem with this method of vehicle assembly is the support of the step I rocket engines while they are being attached to the vehicle support structure. If the vehicle support structure is mounted to the launch pad first, and then individual step I rocket engines lowered into it, the step is not self supporting until it is completely assembled. Consequently, each engine needs to be supported by auxiliary members from the launch pad, in addition to its normal supports, until the step I cluster is completely assembled. This is also true if a portion of the vehicle support structure is lowered into place while attached to each engine.

~~CONFIDENTIAL~~ UNCLASSIFIED

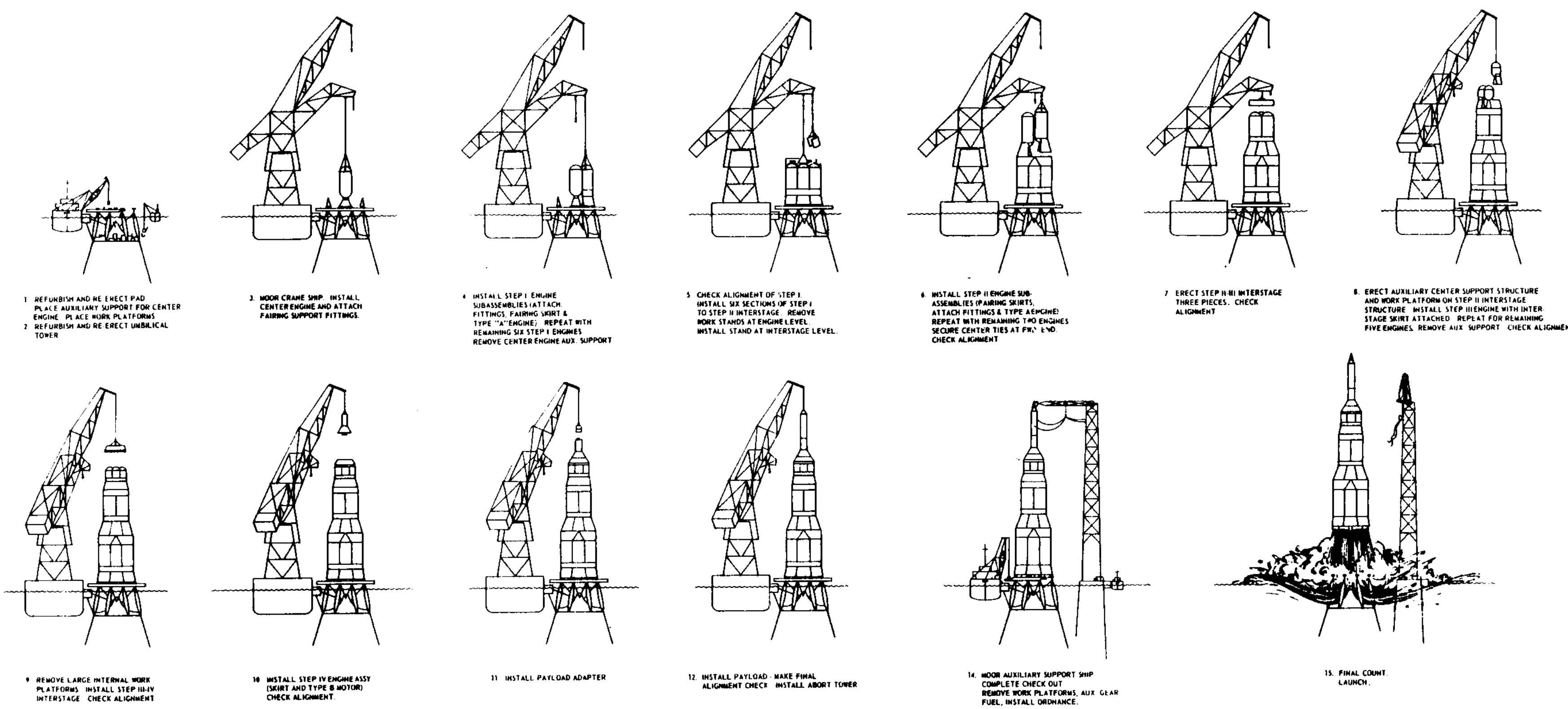

Figure 3.4-1. Assembly Sequence, Method

~~CONFIDENTIAL~~ UNCLASSIFIED

Ideally, it would be desirable to mount the center engine of the step I cluster in place on the launch pad first. However, since the loads from the center engine are carried through the outer engines in the cluster, an auxiliary launch pad support (which must be removed before firing) is required to hold the center engine. Further, the fact that the vehicle support struts attach to the launch pad at a water depth of 50 feet adds to the difficulty of the assembly procedure. This method of assembly requires further study to evaluate the detail problems.

3.4.2 Assembly Method II

This method of assembling the vehicle at the launch site uses the launch pad described in Section 3.3.3. The sequence of operations is shown in Figure 3.4-2 where the gantry is used in assembling the vehicle.

It is fully realized that complexity is added to the assembly operation if the step I engines are supported from below before they are connected together. Consequently, a fixture is used in the gantry to suspend them from above while they are being interconnected and the vehicle support structure is assembled in place. In a similar manner, the step II engines are assembled in a fixture in the gantry at the same time that the step I-II interstage is assembled on the top of the step I cluster. The assembly fixtures are easily removed from the launch area by use of the gantry which carries them to a storage area. The upper steps and the payload are assembled by use of the smaller capacity crane on top of the gantry.

During the assembly of the lower steps, work platforms are mounted on the gantry in a similar manner to those in use at present launch installations. For the upper steps and payload, work platforms would probably be mounted to the vehicle itself. The placement of much of the checkout equipment on the gantry would simplify check out procedures.

This method of vehicle assembly, wherein a gantry is employed, adapts itself ideally to a land based launch site should this be considered.

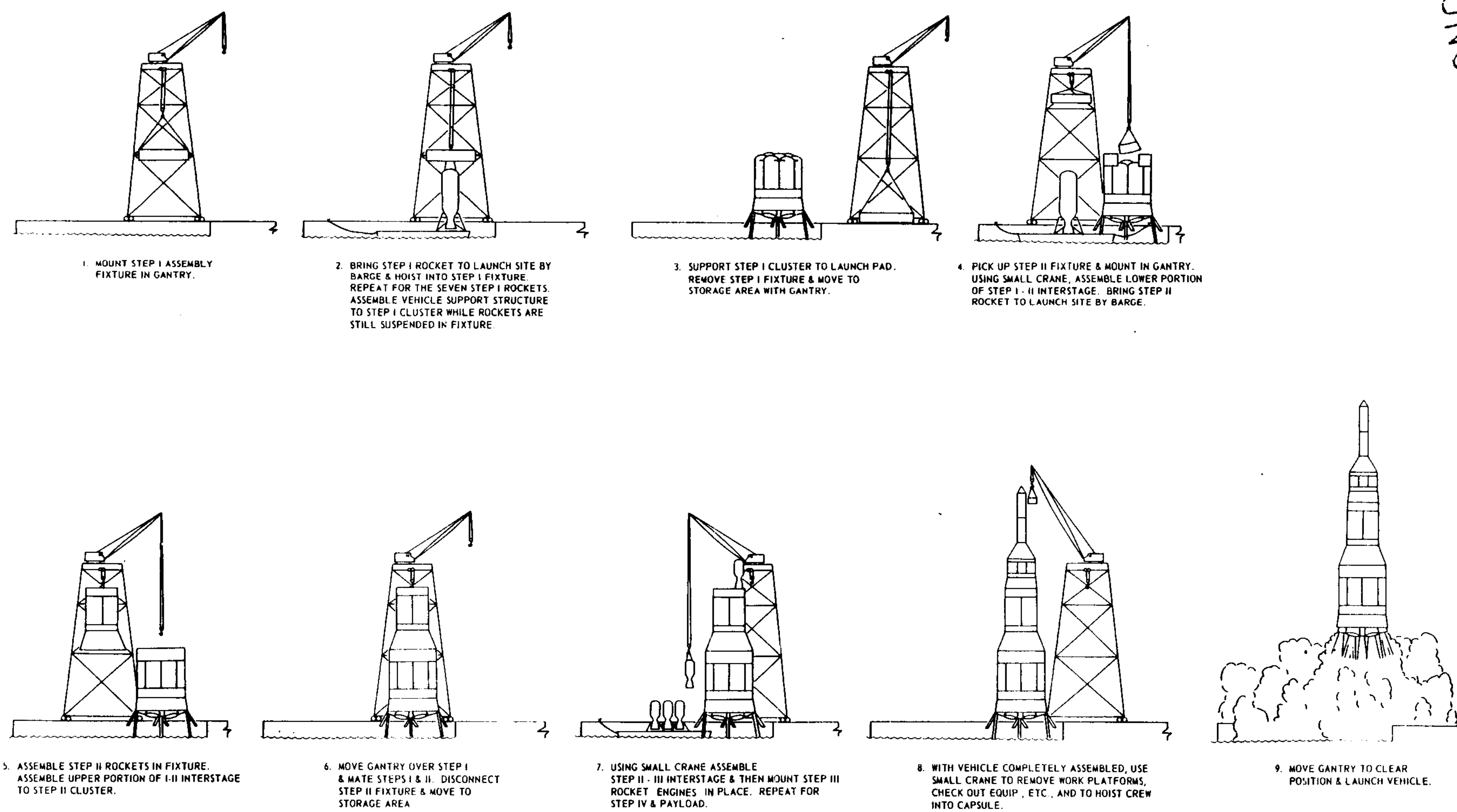

Figure 3.4-2. Assembly Sequence, Method II.

3.4.3 Electrical GSE

The electrical GSE for support of the solid NOVA launch vehicles is not a pacing item with respect to delivery of equipment or utilization at the launch site. No major technical problems are expected in the development of the equipment.

Functional and electrical compatibility tests of each step, as they are progressively combined on the launch pad, is proposed to ensure that the assembly, which is a major operation, proceeds smoothly.

3.5 LAUNCH OPERATION CYCLE

Vehicle assembly, checkout, and launch preparations were examined to insure that the vehicle could be assembled and checked out and to determine the effect of launch sequence and pacing schedule items on the proposed launch rate. Several assembly procedures were considered and two feasible methods were discussed (see Section 3.4). The first followed the general sequence and configuration suggested in Reference 1 and is illustrated in Figure 3.4-1. Table 3.5-I presents the detail steps and pacing schedule time estimates for this method. The schedule presented in Figure 3.5-1 shows this information graphically. The launch date estimated by JPL in Reference 1 is shown for comparison.

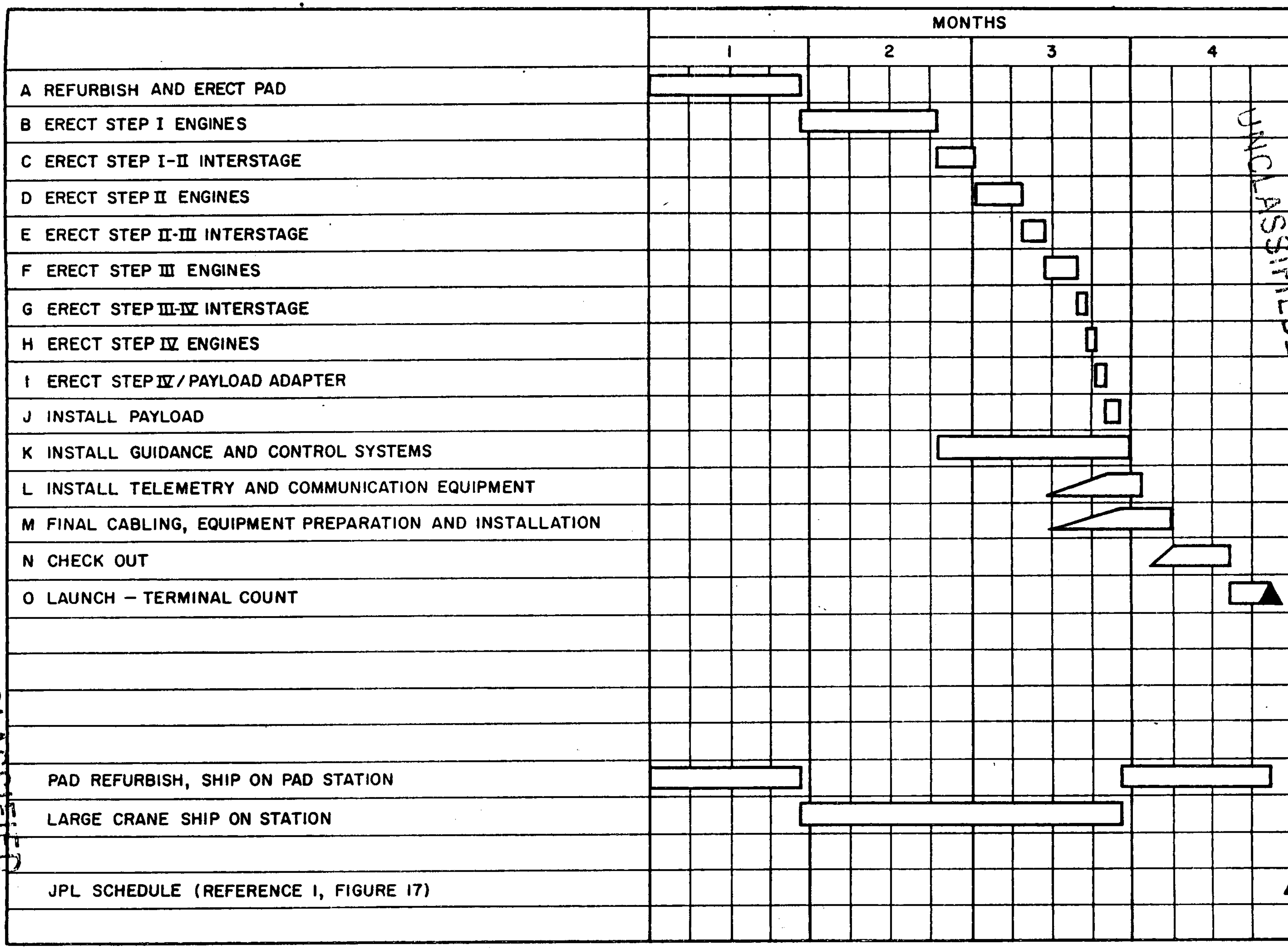

Figure 3.5-1. Launch Operations Schedule.

Table 3.5-I. Launch Operations

	Schedule Time (months)
A. <u>Refurbish and Re-erect Pad</u>	0.96
1. Check bench marks adjacent to pad (6 each)	
2. Inspect bridge piling (shark net required); inspect fittings and clear for crane mooring	
3. Erect camel back, using tugs and small service craft	
4. Moor large crane to base of pad against "camel back"; secure to adjacent permanent mooring	
5. Replace damaged portion of submerged steel pier cap	
6. Replace auxiliary support for center engine; install work platforms	
7. Remove main pad stress structure damaged by launch	
8. Replace main pad truss structure, 6 prefab tripods, 12 major connections	
9. Install work platforms on main pad truss	
10. Inspect umbilical tower	
11. Replace damaged equipment	
12. Check out physical alignment and correct	
a. Main pad	
b. Umbilical tower	
B. <u>Erection of Step I ("A" Engines 1 through 7)</u>	0.83
1. Moor "A" engine barge (center engine)	
2. Install bridle to top of engine	
3. Pick up with large crane	

Table 3.5-I. Launch Operations (Continued)

Schedule Time (months)

4. Install on auxiliary support structure

5. Attach rings with assembly fittings to top and bottom of engine and work platforms

6. Install vehicle support fairing fittings (2) on two pad support points adjacent to first outboard engine mounting position

7. Remove center engine barge

8. Moor outboard engine barge attach bridle, etc

9. Pick up engine

10. Move outboard engine to working area on crane ship; install center engine; attach fittings top and bottom

11. While still holding engine with crane, install base fairings to engine support ring and vehicle support fairing fittings

12. Move to pad; align and install

13. Remove crane and bridle

14. Repeat 6 thru 13 on engine position opposite to that already installed

15. Install vehicle support fitting (1) on next engine position

16. Remove empty engine barge

17. Moor next engine barge; attach bridle

18. Pick up

19. Move outboard "A" engine to work area in crane ship; attach fittings—top and bottom

Table 3.5-I. Launch Operations (Continued)

	Schedule Time (months)
20. While still holding engine with crane, install base install base fairing section to engine support ring and vehicle support fittings	
21. Move to pad and install	
22. Remove crane and bridle	
23. Repeat 15 thru 22 on engine position opposite to engine last installed	
24. Remove last barge	
25. Moor next engine barge attach bridle	
26. Pick up, move to working area	
27. While still holding engine with crane, install base fairing section to engine support ring and vehicle support fittings on adjacent engines	
28. Move to pad and install; remove bridle	
29. Repeat 24 thru 27 for final position opposite to last engine installed	
30. Check step I alignment	
C. Erection of Step I-II Interstage (6 Pieces) Already on Board Crane Ship	0.22
1. Pick up half cone	
2. Install on top of step I "A" engine	
3. Repeat 1 and 2	
4. Repeat 1 and 2	
5. Pick up corner interstage	
6. Install corner interstage section	

Table 3.5-I. Launch Operations (Continued)

	Schedule Time (months)
7. Repeat 5 and 6	
8. Repeat 5 and 6	
9. Check alignment	
10. Remove work stands at top of step I	
11. Install work stands at separation plane level	
D. <u>Erection of Step II (3-"A" Engines)</u>	0.30
0. Install work platforms on top of engines (small auxiliary crane)	
1. Moor step II—"A" engine barge—attach bridle	
2. Pick up engine	
3. Move to working area on large crane dock	
4. Pick up interstage fairing section on auxilliary crane; install on engine	
5. Check alignment of section and engine	
6. Move to top of step I interstage	
7. Install, remove cone and bridle	
8. Check alignment	
9. Repeat 1 thru 8	
10. Repeat 1 thru 8	
11. Secure center ties at top of step II	
12. Check total alignment	

Table 3.5-I. Launch Operations (Continued)

		Schedule Time (months)
E.	<u>Erection of Step II-III Interstage (3 Pieces) Already on Board Crane Ship</u>	0.11
	1. Pick up corner piece; attach bridle	
	2 Install on nose ring at step II engine	
	3. Same as 1 and 2	
	4. Same as 1 and 2	
	5. Check alignment and concentricity	
	6. Remove work stand at top of step II	
	7. Install work stand at separation plane level	
F.	<u>Erection of Step III Engines (6 Type "B")</u>	0.25
	1. Moor two type "B" engine barge (carry 3 each)	
	2. Remove engines and install interstage sections (6 engines)	
	3. Erect auxiliary assembly support structure and work platform on step III interstage structure	
	4. Install "B" engine with interstage section attached	
	5. Secure to step II interstage at bottom, and to auxiliary structure at top	
	6. Repeat 4 and 5 for opposite engine	
	7. Remove auxiliary support structure	
	8. Repeat 4 and 5 for last engine	
	9. Alignment check	

Table 3.5-I. Launch Operations (Continued)

	Schedule Time (months)
G. Erection of Step III to IV Interstage (1 Piece)	0.05
1. Remove large internal work platforms from II-III interstage region	
2. Pick up III-IV interstage and install on top of Step III; work platforms already in place	
3. Check alignment	
4. Remove step III "B" engine barges	
H. Erection of Step IV Engine	0.05
1. Moor step IV "B" engine barge	
2. Install skirt on "B" engine on board	
3. Hook up bridle and cone	
4. Pick up and install	
5. Check alignment	
I. Erection of Step IV to Payload Adapter Section Already on Board Crane Ship	0.05
1. Install work platforms (external)	
2. Install adapter section	
3. Alignment check	
J. Install Payload - (Structure only; no servicing)	0.15
1. Propellant tank	
2. Module (service module)	

Table 3. 5-I. Launch Operations (Continued)

	Schedule Time (months)
3. Module (manned)	
4. Alignment check	
K. Installation of Guidance and Control Systems	no pacing
1. Step I - concurrent with step II erect	
2. Step II - concurrent with step III erect	
3. Step III - concurrent with step IV	
4. Step IV - concurrent with payload	
5. Payload module	
6. Perform connections and checkout steps	
L. Install Telecommunications, etc.	0.34
1. Connections	
2. Checkout	
M. Final Cabling and Equipment	
1. Connections - including umbilical tower, etc.	
2. Checkout	
3. Remove propellant temperature conditioning equipment	
N. Final Checkout	0.46
Mock count - time liftoff time	
Remove all work platform and auxiliary equipment	

Table 3.5-I. Launch Operations (Continued)

	Schedule Time (months)
O. <u>Launch</u>	0.25
Tower stage - control fluid	
Propellant loading - upper stage (payload)	
Ordnance installation and checkout	
Propellant topping	
Final count	

4.0 REFERENCES

1. Technical Memorandum No. 33-52, "System Considerations for the Manned Lunar-Landing Program," Jet Propulsion Laboratory, Pasadena, California, August 3, 1961.

2. Technical Memorandum No. 33-52 (Addendum A), "A Solid-Propellant NOVA Injection Vehicle System," Jet Propulsion Laboratory, Pasadena, California, August 3, 1961.

3. "Project Apollo Spacecraft Development Statement of Work, Phase A," NASA Space Task Group, Langley Field, Virginia, 28 July 1961.

4. Final Report PFRT XM-55, TCC Document TW-773-5-61, Report No. VER-446, May 1961.

5. STL TR-59-0000-00746, "One Dimensional Flow of a Gar-Particle System," by J. R. Kliegel, Space Technology Laboratories, Inc., Los Angeles, California, 8 July 1959, Revised 28 August 1959.

6. "Launch Vehicle Dynamics," H. L. Runyan and A. C. Rainey, NASA-Industry Apollo Technical Conference, July 18-20, 1961, A Compilation of Papers Presented.

7. STL GM-TR-190, "On the Prediction of Acoustic Environments from Rockets," by V. Chobotov and A. Powell, Space Technology Laboratories, Inc., Los Angeles, California, 1960.

8. STL TM-60-0000-00095, "A Study of a Blender for a Highly Elastic Booster," Space Technology Laboratories, Inc., Los Angeles, California, 1960.

9. STL Report 9862.2-41, "Phase I Summary Report, Launch Vehicle Size and Cost Study," Space Technology Laboratories, Inc., Los Angeles, California, 15 June 1961.